

Alternative method for equipment condition monitoring on South African mines

GJ Cloete



orcid.org 0000-0002-0034-5880

Dissertation submitted in fulfilment of the requirements for the degree *Master of Engineering in Mechanical Engineering* at the North-West University

Supervisor:

Prof M Kleingeld

Graduation May 2018

Student number: 23378646

ABSTRACT

TITLE: Alternative method for equipment condition monitoring on South African mines

AUTHOR: GJ Cloete

SUPERVISOR: Prof M Kleingeld

KEYWORDS: Condition monitoring; Fault detection; Autoregressive model

The practicality of accurate condition monitoring and fault diagnostics depends on the type of parameter measured and the accuracy of the measurement. In the South African mining industry, it is common to find large electrical machines with limited logged parameters, which significantly decreases fault diagnostic capability.

In this study, a condition monitoring methodology that incorporates an autoregressive fault detection model is developed to improve condition-based maintenance strategies on South African mines. Autoregressive models have shown to be able to detect and predict equipment defects with available temperature parameters. A method to determine the condition of equipment is developed by establishing an autoregressive model on the modal parameters of both healthy and unhealthy machines. The method was validated by comparing results with the mine's maintenance reports.

The model was implemented in two case studies which include large three-phase induction motors. Case Study 1 presents a large disturbance in the temperature of a non-drive end bearing of a multistage centrifugal compressor that was detected by the model. Case Study 2 presents a gradually increasing motor winding temperature of a multistage centrifugal pump that was also successfully detected.

The method is a viable alternative to the mines due to the capability of automatically detecting faults even within the mines' alarm and trip limits. The model automatically adapts to the behaviour of the input parameters and monitors the mean and variance shifts. This allows the method to be interchangeable with different types of equipment. The method can continuously evaluate a system of multiple components and provide simple, actionable feedback if a fault is detected.

ACKNOWLEDGEMENTS

First and foremost, I would like to thank God for the knowledge and opportunity to have completed this dissertation.

I would like to express my gratitude towards the following people whom made a critical contribution towards the success of the study:

- My parents, Johan and Hendré Cloete, my sister and brother, Marique and Hennie for your love, support and encouragement throughout this dissertation.
- My friends and colleagues, Stéphan Taljaard and Neil Zietsman, for your valued inputs in this study and motivation throughout the study.
- Dr Willem Schoeman for your guidance, mentorship and patience.
- Enermanage (Pty) Ltd and its sister companies for financial support to complete this study.
- Prof. Eddie Matthews and Prof. Marius Kleingeld for the opportunity to complete this study.

CONTENTS

1. INTRODUCTION TO CONDITION MONITORING	2
1.1. INTRODUCTION.....	2
1.2. CONDITION MONITORING.....	2
1.3. SOUTH AFRICAN MINING INDUSTRY.....	6
1.4. CONDITION MONITORING APPROACH.....	11
1.5. CONCLUSION.....	13
2. CONDITION MONITORING OVERVIEW	16
2.1. INTRODUCTION.....	16
2.2. CONDITION MONITORING BACKGROUND.....	16
2.3. DATA EVALUATION AND ANALYSIS METHODOLOGY.....	23
2.4. CONDITION PREDICTION MODEL.....	27
2.5. CONCLUSION.....	46
3. METHOD DEVELOPMENT	48
3.1. INTRODUCTION.....	48
3.2. DATA ACQUISITION AND EVALUATION.....	48
3.3. DEVELOPMENT OF METHOD.....	53
3.4. MODEL VERIFICATION AND VALIDATION.....	67
3.5. CONCLUSION.....	70
4. EVALUATION OF THE ALTERNATIVE CONDITION MONITORING METHOD (CASE STUDIES) 73	
4.1. INTRODUCTION.....	73
4.2. CASE STUDY 1: DEWATERING SYSTEM.....	73
4.3. CASE STUDY 2: COMPRESSORS.....	78
4.4. CONCLUSION.....	83
5. CONCLUSION	85
5.1. INTRODUCTION.....	85
5.2. SUMMARY.....	85
5.3. RECOMMENDATIONS.....	86
APPENDIX A SYMPTOMS OR PARAMETERS THAT ARE RELEVANT TO PUMPS	95
APPENDIX B THE INDICATORS OF MACHINE AND COMPONENT DETERIORATION	96
APPENDIX C REGRESSION ANALYSIS	97
APPENDIX D VIBRATION INSTRUMENT SPECIFICATIONS	99
APPENDIX E MONTHLY FEEDBACK REPORT	108
APPENDIX F CASE STUDY 1: MAINTENANCE REPORT	111

LIST OF FIGURES

FIGURE 1-1 CENTRIFUGAL PUMPS FAILURE CAUSE DISTRIBUTION	5
FIGURE 1-2: PRINCIPLE CAUSES BEHIND MAJOR ACCIDENTS	6
FIGURE 1-3 DATA TRANSMISSION PATH INTO ALARM	8
FIGURE 1-4 ARCHITECTURE OF CONDITION-BASED MAINTENANCE	12
FIGURE 2-1 CAUSE-AND-EFFECT DIAGRAM OF A MAIN SHAFT FAILURE.....	16
FIGURE 2-2 MAINTENANCE BREAKDOWN.....	17
FIGURE 2-3 ASSET FAILURE CURVE	18
FIGURE 2-4 SCADA CONDITION MONITORING PANEL.....	21
FIGURE 2-5 ALARM AND TRIP LIMITS OF A COMPRESSOR	22
FIGURE 2-6 PERFORMANCE MONITORING AND CONDITION MONITORING.....	28
FIGURE 2-7 MONITORED PARAMETERS OF A MULTISTAGE CENTRIFUGAL PUMP	29
FIGURE 2-8 MONITORED PARAMETERS OF A MULTISTAGE CENTRIFUGAL COMPRESSOR	30
FIGURE 2-9 RATE OF FAILING OPERABILITY AS TIME PROGRESSES: FAST SPEED FAULT	35
FIGURE 2-10 RATE OF FAILING OPERABILITY AS TIME PROGRESSES: MEDIUM SPEED FAULT	36
FIGURE 2-11 RATE OF FAILING OPERABILITY AS TIME PROGRESSES: SLOW SPEED FAULT	36
FIGURE 2-12 INTEGRATED REAL-TIME STATISTICAL MONITORING SCHEME.....	38
FIGURE 2-13 BEARING TEMPERATURE EVOLUTION WITH THE TWO DAMAGE OCCURRENCES AND THE PERIOD USED TO DEVELOP THE MODEL	43
FIGURE 3-1 DEVELOPED VIBRATION SIGNALS OF A MULTISTAGE CENTRIFUGAL PUMP.....	48
FIGURE 3-2 RAW BEARING TEMPERATURE DATA FOR A MULTISTAGE CENTRIFUGAL PUMP	49
FIGURE 3-3 RUNNING STATUS CLASSIFIER	50
FIGURE 3-4 DETERMINING IDLE TEMPERATURE OF THE EQUIPMENT	51
FIGURE 3-5 TEMPERATURE OF A WIND TURBINE GENERATOR BEARING VS. AMBIENT TEMPERATURE AND ACTIVE POWER	52
FIGURE 3-6 COOLING RATE OF A MULTISTAGE CENTRIFUGAL PUMP	53
FIGURE 3-7 MULTISTAGE CENTRIFUGAL COMPRESSORS MEASURED PARAMETERS	54
FIGURE 3-8 MULTISTAGE CENTRIFUGAL PUMP MEASURED PARAMETERS.....	55

FIGURE 3-9 COMPRESSOR VIBRATION VERSUS POWER CONSUMPTION	56
FIGURE 3-10 CORRELATION BETWEEN PUMP EFFICIENCY AND VIBRATION	57
FIGURE 3-11 FLOWCHART FOR FAULT DETECTION AND CONDITION PREDICTION	58
FIGURE 3-12 A MODEL-BASED CONDITION PREDICTION SYSTEM	60
FIGURE 3-13 ACTUAL TEMPERATURE VERSUS AR(3) PREDICTED TEMPERATURE	62
FIGURE 3-14 RESIDUALS OF THE AR MODEL.....	62
FIGURE 3-15 RESIDUAL DISTURBANCES WITH CONTROL LIMITS	63
FIGURE 3-16 STATUS FILTERED, ACTUAL TEMPERATURE VERSUS AR(1) PREDICTED TEMPERATURE	65
FIGURE 3-17 STATUS FILTERED, RESIDUAL DISTURBANCES.....	66
FIGURE 3-18 NORMAL DISTRIBUTION OF FILTERED AND UNFILTERED DATA.....	67
FIGURE 3-19 LINEAR FUNCTION.....	68
FIGURE 3-20 RANDOM BETWEEN FUNCTION.....	68
FIGURE 3-21 SINE FUNCTION	68
FIGURE 3-22 DOUBLE SINE FUNCTION	68
FIGURE 3-23 LINEAR AND RANDOM.....	68
FIGURE 3-24 LINEAR, RANDOM WITH FAULT	68
FIGURE 4-1 CASE STUDY 1: NDE BEARING TEMPERATURE BEFORE MAINTENANCE	74
FIGURE 4-2 PERIOD USED TO DETERMINE THE AR(3) MODEL	75
FIGURE 4-3 AR(3) MODEL FITTED TO THE TEMPERATURE BEFORE THE MAINTENANCE PERIOD.	75
FIGURE 4-4 RESIDUALS BEFORE AND AFTER MAINTENANCE	76
FIGURE 4-5 CASE STUDY 1: TEMPERATURE RESIDUALS BEFORE AND AFTER MAINTENANCE.....	78
FIGURE 4-6 COMPRESSOR MOTOR BEARING AND WINDING TEMPERATURES	79
FIGURE 4-7 AR(1) MODEL RESULTS	80
FIGURE 4-8 RESIDUALS WITH CONTROL LIMITS.....	81
FIGURE 4-9 WEEKLY MEAN RESIDUAL.....	82
FIGURE A-1 SYMPTOMS OR PARAMETERS THAT ARE RELEVANT TO PUMPS.....	95
FIGURE B-1 THE INDICATIONS OF COMPONENT DETERIORATION.....	96
FIGURE C-1 MODELLED DATA STATISTICS.....	97

LIST OF TABLES

TABLE 1-1 THE BENEFITS OF CONDITION MONITORING	9
TABLE 2-1 DEVELOPING STRATEGIES FOR MAINTENANCE MANAGEMENT	20
TABLE 2-2 VIBRATION SEVERITY CHART	21
TABLE 2-3 EXAMPLE OF AVAILABLE CONDITION MONITORING SYSTEMS	22
TABLE 2-4 KEY MONITORED PARAMETERS OF DIFFERENT STUDIES	31
TABLE 2-5 FUNDAMENTAL TERMS AND UNITS IN PUMP PERFORMANCE	32
TABLE 2-6 FUNDAMENTAL TERMS AND UNITS IN COMPRESSOR PERFORMANCE.....	33
TABLE 2-7 DIFFERENT CONDITION MONITORING METHODS	34
TABLE 2-8 STATISTICAL VIBRATION CONDITION INDICATORS	39
TABLE 2-9 OPERATIONAL VALIDITY CLASSIFICATION	44
TABLE 3-1 ALARM AND TRIP LIMITS OF A CENTRIFUGAL PUMP	59
TABLE 3-2 AUTOREGRESSIVE MODEL RESULTS ON CONTINUOUS DATA	61
TABLE 3-3 AR(3) REGRESSION STATISTICS OF UNFILTERED TEMPERATURE RESIDUALS	63
TABLE 3-4 AUTOREGRESSIVE MODEL RESULTS ON DISCONTINUOUS DATA	65
TABLE 3-5 AR(1) REGRESSION STATISTICS OF STATUS FILTERED TEMPERATURE RESIDUALS	66
TABLE 3-6 REGRESSION STATISTICS OF SIMULATED SIGNALS	69
TABLE 4-1 AR(3) REGRESSION STATISTICS AR(3) MODEL	76
TABLE 4-2 RESIDUAL DISTRIBUTION COMPARISON BEFORE AND AFTER MAINTENANCE	77
TABLE 4-3 AUTOREGRESSIVE MODEL RESULTS	79
TABLE 4-4 REGRESSION STATISTICS OF AR(1) MODEL	80
TABLE 4-5 RESIDUAL DISTRIBUTION COMPARISON BEFORE AND AFTER SHUTDOWN	81
TABLE E-1 MONTHLY FEEDBACK REPORT	108

LIST OF ABBREVIATIONS

AIC	AKAIKE INFORMATION CRITERION
AR	AUTOREGRESSIVE
ARIMA	AUTOREGRESSIVE INTEGRATED MOVING AVERAGE
ARMA	AUTOREGRESSIVE MOVING AVERAGE

CBM	CONDITION-BASED MAINTENANCE
CUSUM	CUMULATIVE SUM
DE	DRIVE END
EO	ENERGY OPERATOR
ER	ENERGY RATIO
EV	EXPLAINED VARIANCE
EWMA	EXPONENTIALLY WEIGHTED MOVING AVERAGE
FFT	FAST FOURIER TRANSFORM
FMECA	FAILURE MODE EFFECT AND CRITICALITY ANALYSIS
IID	INDEPENDENTLY AND IDENTICALLY DISTRIBUTED
ISO	INTERNATIONAL ORGANISATION FOR STANDARDISATION
KDE	KERNEL DENSITY ESTIMATIONS
KPI	KEY PERFORMANCE INDICATOR
LCL	LOWER CONTROL LIMIT
LDR	LEVINSON-DURBIN RECURSION
MA	MOVING AVERAGE
MAE	MEAN ABSOLUTE ERROR
MLE	MAXIMUM LIKELIHOOD ESTIMATION
MSE	MEAN SQUARE ERROR
NC	NUMERICAL CONTROL
NDE	NON-DRIVE END
ODS	OPERATIONAL DEFLECTION SHAPE
PLC	PROGRAMMABLE LOGIC CONTROLLER
RCM	RELIABILITY CENTRED MAINTENANCE
RMS	ROOT MEAN SQUARE
RMSE	ROOT MEAN SQUARE ERROR
RSS	RESIDUAL SUM OF SQUARES
SCADA	SUPERVISORY CONTROL AND DATA ACQUISITION
SPC	STATISTICAL PROCESS CONTROL
UCL	UPPER CONTROL LIMIT



**ALTERNATIVE METHOD FOR EQUIPMENT
CONDITION MONITORING ON SOUTH AFRICAN MINES**

CHAPTER 1

INTRODUCTION TO CONDITION MONITORING

1. INTRODUCTION TO CONDITION MONITORING

1.1. INTRODUCTION

Chapter 1 provides background on condition monitoring and the relevant information regarding condition monitoring. It will serve as motivation for the study and it will briefly explain the approach taken to achieve the aims of the study.

Condition monitoring aids in the detection, diagnosis and prognosis of faults in industrial systems (Beebe, 2004). Potential economic and safety implications of early fault detection makes condition monitoring an appealing field of research (Fugate, Sohn & Farrar, 2001).

Process industries are looking to reduce machine downtime and maintenance costs (Wasif *et al.*, 2012). A reduction in machine downtime and maintenance costs can be achieved by implementing a condition monitoring strategy (Beebe, 2004). Previous studies conducted by Chindondondo, *et al.* (2014) and Shafiee, *et al.* (2015) have reported a maintenance cost reduction of 8% - 30% by implementing a condition-based maintenance (CBM) strategy.

This study will focus on large electric motor-driven machines used in deep-level mines in South Africa. Examples of these machines include compressors, dewatering pumps and ventilation fans. These machines have a direct influence on the production of a mine (Karakurt *et al.*, 2011; Wilson *et al.*, 1975).

A condition monitoring methodology for the equipment is developed in this study. The methodology contains a model that aids to detect changes in developed signals. The developed model is implemented and verified on available case studies.

1.2. CONDITION MONITORING

The process of monitoring the condition or state of machinery and processes is called condition monitoring. Condition monitoring is regarded as a type of maintenance inspection with the purpose to detect signs of degradation, diagnose cause of faults and predict when a fault may occur (Beebe, 2004). The aim of condition monitoring is to predict equipment and process failure before it occurs whereby the equipment availability is maximised and associated hazards are reduced.

1.2.1. MEASURED PARAMETERS

Different parameters are used to measure the condition of equipment. Real-time condition monitoring makes use of non-destructive test methods. The following test methods are typically used as condition indicators (Zhou *et al.*, 2007):

- Vibration monitoring
- Temperature monitoring
- Current monitoring
- Acoustic emission monitoring
- Sound pressure monitoring
- Laser displacement monitoring
- Chemical (oil) analysis
- Operational performance monitoring

Vibration and temperature are commonly logged parameters on large mining equipment. Usually, only a select few of these techniques are used to monitor the condition of the equipment. It is not always necessary to make use of all these techniques since the critical test methods are equipment specific.

Key performance parameters include power consumption, flow(s), pressure(s) and calculated efficiency. Typical condition monitoring parameters include temperature and vibration. The measured parameters along with their set alarms are usually displayed online on the supervisory control and data acquisition (SCADA) system for operators to monitor.

If these monitored parameters exceed manufacturer's/operator's set limits an alarm triggered to indicate that a fault is imminent or has occurred. The equipment usually has a fail-safe programmed into the programmable logic controller (PLC) that will automatically trip the equipment. The SCADA will inform the operator that the equipment has tripped and the fault can be reported remotely by the client's remote alarm monitoring system - if such a system exists.

1.2.2. CONDITION PREDICTION MODELS

In literature, different modelling techniques are implemented to detect and predict equipment health (Jardine *et al.*, 2006). These models make use of parameters divided into three main categories: waveform data analysis, value type data analysis and data analysis combining event data and condition monitoring data (Jardine *et al.*, 2007).

Three different domains are used to analyse a time series, namely: time-domain analysis, frequency-domain analysis and time-frequency analysis (Jardine *et al.*, 2006). This study will focus on the time-domain analysis of temperature and vibration profiles.

Condition prediction models analysing the time-domain parameters have been shown to successfully detect, predict and diagnose faults in industry (Baillie & Mathew, 1996). By predicting faults, the availability and reliability of machinery can be increased.

1.2.3. AVAILABILITY AND RELIABILITY

One of the main aims of maximising equipment availability is to increase production of a mine. The production of a mining company is usually listed as a key performance indicator (KPI) (Harmony Gold Mining Company Limited, 2017; Lonmin Plc, 2017). In the mining industry, one of the main KPIs is the cost per amount of material retrieved from the earth (intensity). A condition-based maintenance strategy can aid to increase the availability of production affecting equipment (Sitayeb *et al.*, 2011).

System availability, a fundamental measure for reliability is shown in Equation 1.1:

$$Availability = \frac{Mean\ time\ to\ failure(MTTF)}{Mean\ time\ to\ failure\ (MTTF) + Mean\ time\ to\ repair(MTTR)} \quad (1.1)$$

A machine with high availability is a machine that is only shut down for short periods of time due to maintenance or failure (Tavner, 2008). Availability is given as a percentage as calculated by using Equation 1.1. High availability is one of the main criteria for satisfactory performance (Davies, 1998).

Reliability of a machine is the measure of the consistency that the machine can operate without failure for a set time. It can statistically be defined as the probability that a machine will remain online producing as required for the desired period (Beebe, 2004).

Certain factors affect the reliability of the equipment. The design of the machine and the maintenance philosophy are the main contributors that affect the reliability of a machine (Beebe, 2004). The design of the machine includes the materials used, quality of the design and the quality of construction.

1.2.4. EQUIPMENT FAILURE

Equipment failures affects the reliability and availability. Bloch (1990) completed a root cause analysis on centrifugal pumps that experienced mechanical failure. The root cause analysis determined why the centrifugal pumps had failed. The failure cause distribution is shown in Figure 1-1.

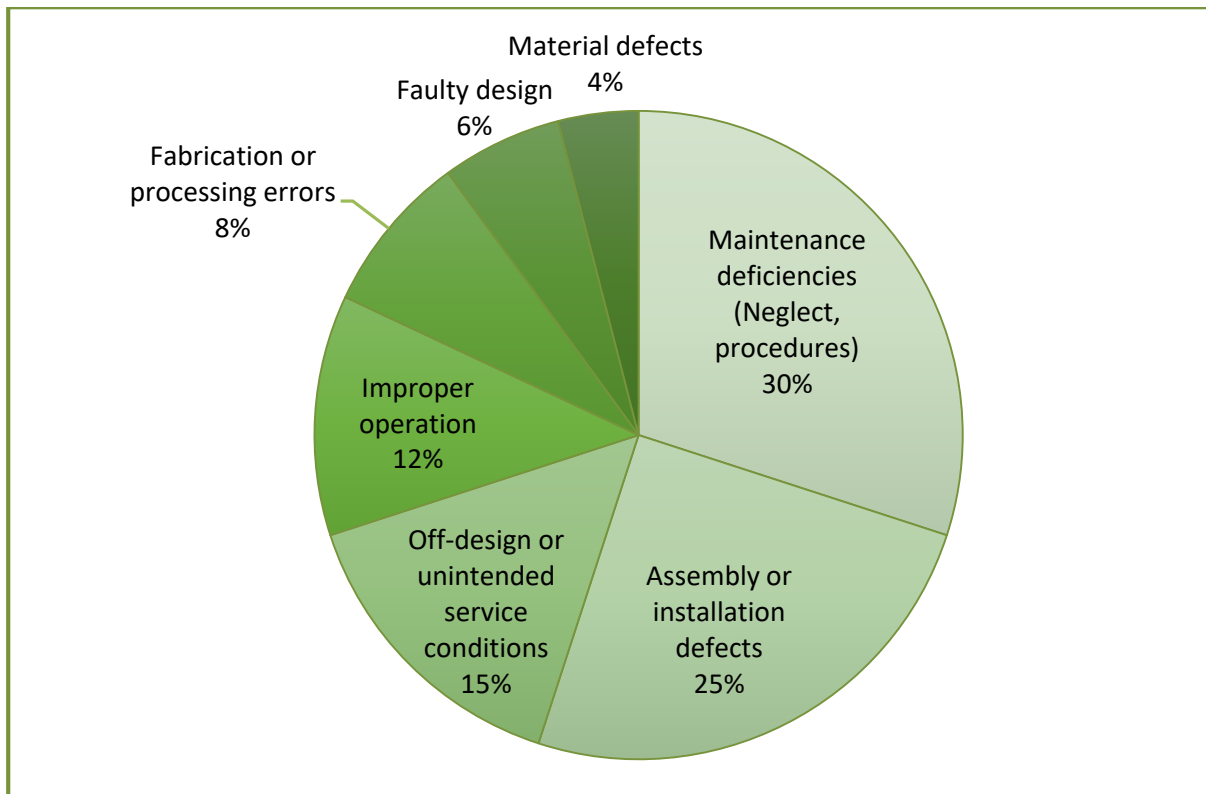


FIGURE 1-1 CENTRIFUGAL PUMPS FAILURE CAUSE DISTRIBUTION

Figure 1-1 shows that factors such as the materials used, the quality and design have an effect of the failure of pumps. Figure 1-1 also shows that the main source of pump failure is maintenance deficiencies. Maintenance deficiencies can be mitigated with a continuous condition monitoring strategy (Wasif *et al.*, 2012; Chindondondo *et al.*, 2014).

The maintenance philosophy contributes to the reliability of the machine after construction. The reliability of a machine is proportional to the cost of making the machine and will likely influence the maintenance cost. Beebe (2004) states that only 10% – 20% of machines reach their design life. Independent studies have shown that 15% – 20% of all equipment failures are age related (Amari & McLaughlin, 2006).

Condition monitoring aids in detecting early damage of machines. Damage to a machine can have potential economic and life-safety implications (Fugate *et al.*, 2001). The principle causes of major accidents are shown in Figure 1-2.

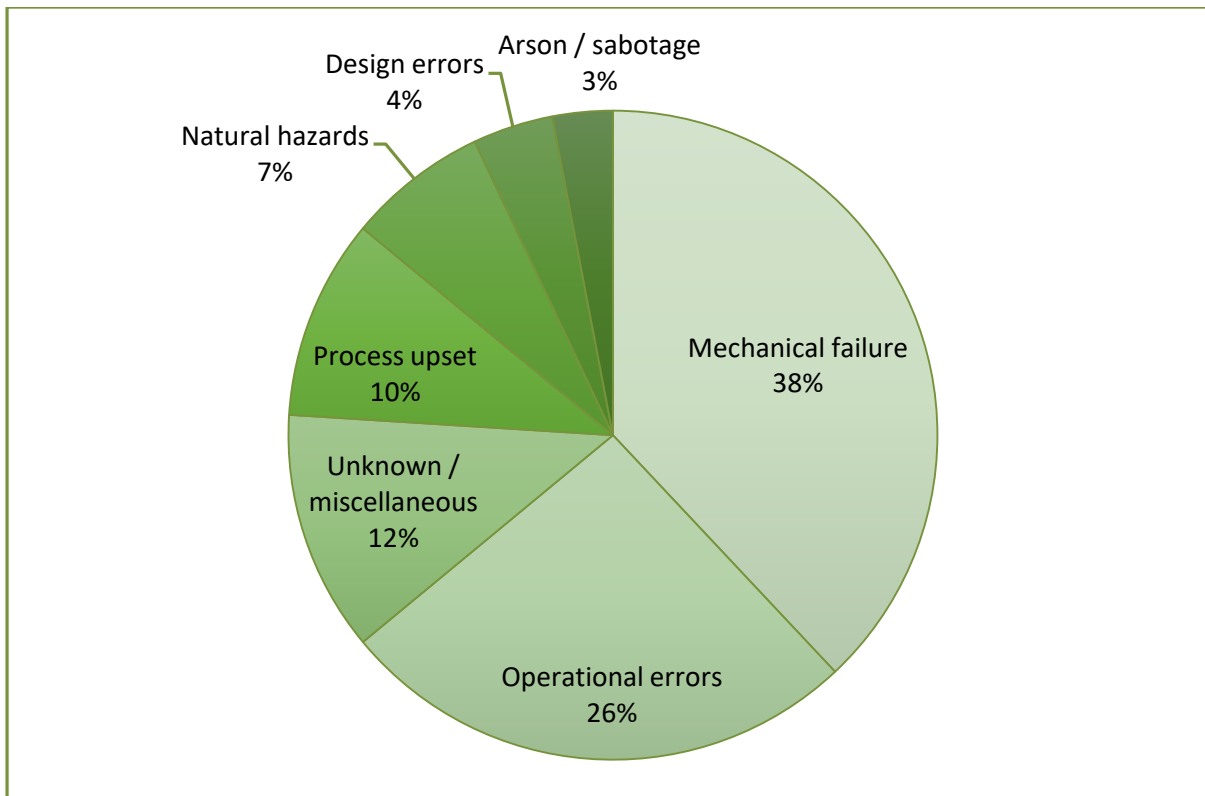


FIGURE 1-2: PRINCIPLE CAUSES BEHIND MAJOR ACCIDENTS
(DAVIES, 1998)

A survey completed by Davies (1998) reviewed 100 petrochemical plant accidents that took place between 1958 and 1987. Figure 1-2 indicates that 38% of all accidents occurred due to mechanical failure which stresses the importance of condition monitoring practices. In many of these cases, the accidents could have been prevented if the condition of the equipment was pro-actively monitored.

1.3. SOUTH AFRICAN MINING INDUSTRY

To fully understand condition monitoring the challenges specific to the South African industry will be assessed. Factors specific to South Africa, such as the economic climate, deep level mining and existing data handling infrastructure all influence current condition monitoring methodologies and strategies.

1.3.1. ECONOMIC CLIMATE

Mining companies are facing severe economic and financial challenges (Neingo & Tholana, 2016). South Africa was the leading gold producer until 2009 when China exceeded South Africa, and is still the leading producer to date. South Africa is currently the seventh top gold producer in the world behind China, Australia, Russia, United States of America, Canada and

Peru (Jasinski, 2017). South Africa produced an estimated 140 metric tons in 2016 which is a decrease from 145 metric tons in 2015 (Jasinski, 2017).

The monthly gold production index provides an indication of the extent that the production has fallen in South Africa from above 350 index points in January 1980 to less than 50 index points in January 2015 (Statistics South Africa, 2015). South Africa produced 87% less gold in January 2015 compared to January 1980 (Statistics South Africa, 2015).

The number of employees in the mining and quarrying industry are declining (Statistics South Africa, 2016). The average wages in the South African mining and quarrying industries are increasing at a rate higher than inflation (Statistics South Africa, 2016). Both the decrease of gold production and the wage increases stress the fact that the mining industry must adapt to the changing economic climate.

1.3.2. DEEP-LEVEL OPERATIONS

Monitoring and maintaining the condition of equipment in a South African underground mine is challenging due to the country's unique reef formations, as well as depths to reach the ore bodies (Johansson, 2010). This leads to many operational obstacles that can affect condition monitoring. Monitoring the condition of underground equipment is more difficult than equipment on the surface.

Underground conditions such as the temperature and humidity increase the difficulty of working underground. Virgin rock temperatures of 60°C are expected at 4000 m depths and are not uncommon in the deep gold mines of South Africa (Stephenson, 1983; Neingo & Tholana, 2016). In South African deep-level mines, it is common for a gold mine to be deeper than 3000 m below the surface.

These conditions can have a degrading effect on both the equipment and on the employees' performance thus increasing unplanned breakdowns and maintenance difficulty. To cool the working environment to a more bearable climate, gold mines utilise ventilation and refrigeration systems which are among the cost drivers (Neingo & Tholana, 2016).

Seismic activity can also have an impact on the availability and reliability of equipment. Seismicity mainly affects the production of the mine, but seldom affects the performance or condition of the large underground energy consumers such as pumps, fridge plants and other cooling auxiliaries (Neingo & Tholana, 2016).

1.3.3. DATA HANDLING

A mine is one large system that can be broken down into smaller subsystems to simplify data handling. This increases the difficulty of stable transmission of data to a central database. The cost to install or upgrade the infrastructure to transmit the data required for condition monitoring depends on the mine's existing infrastructure and long-term strategy. To make the study practical, the data collected by the mine's existing infrastructure will be used to determine the condition of the equipment.

To simplify the data collection methodology, it is divided into three main steps. The first step is the transmission of data between the PLC and SCADA system. The next step is to obtain the data from the SCADA and process the data remotely while ensuring data integrity. The third step is to report the results to the end user. The data obtained for this study is obtained remotely. The data transmission path is shown in Figure 1-3.

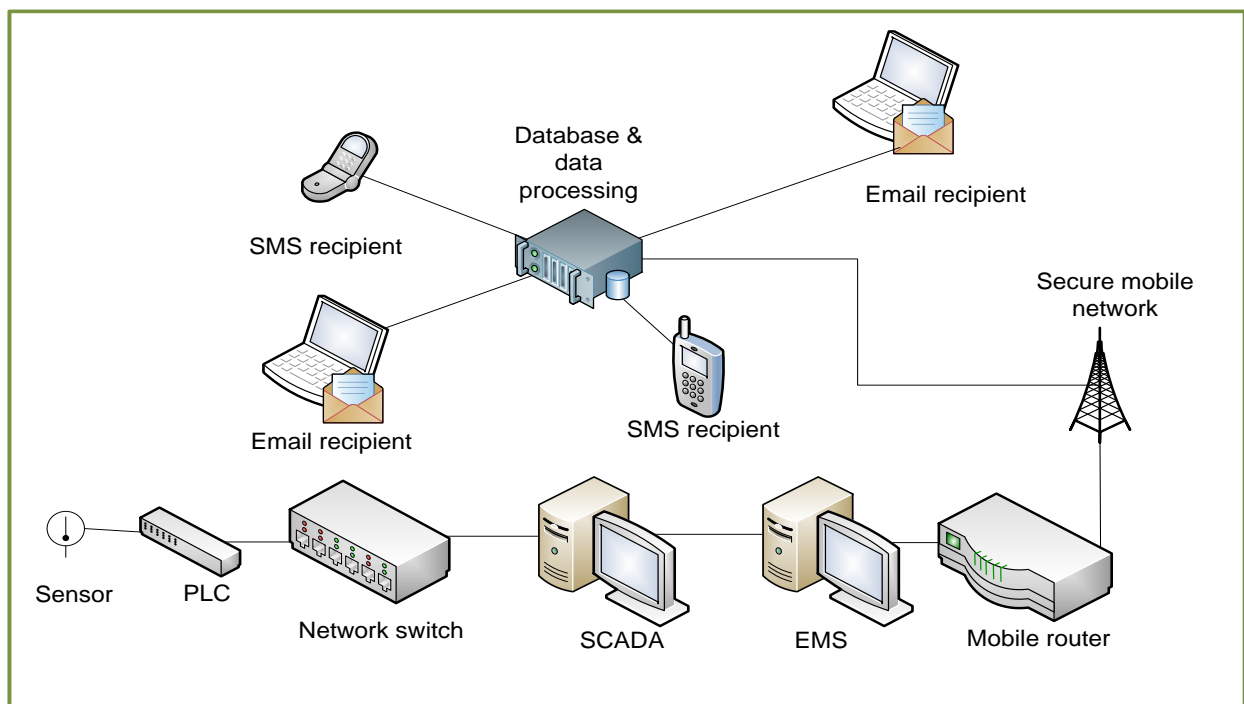


FIGURE 1-3 DATA TRANSMISSION PATH INTO ALARM

Using the data transmission path shown in Figure 1-3, the data is retrieved from the historian database in half hourly intervals to reduce data transmission cost. The transmitted data can include the following parameters, depending on what type of equipment is monitored:

- Active power output
- Reactive power

- Power factor
- Current and voltages
- Non-drive end (NDE) and drive end (DE) bearing temperatures of both the equipment and the motor
- Gearbox bearing temperatures (for gear-drive motors)
- NDE and DE vibration of the equipment and the motor
- Gearbox bearing vibration (for gear-drive motors)
- Motor winding temperatures
- Equipment specific performance parameters

Some South African mines have extensive logs of these parameters; up to millisecond intervals. Mines can improve its current fault detection abilities by implementing alternative and more effective detection and prognosis techniques.

1.3.4. IMPACT OF CONTINUOUS MONITORING IMPLEMENTATION

The benefits of implementing a continuous condition monitoring strategy include a reduction in the number of unplanned shutdowns, increased system availability, potential to pre-order spare parts, increased safety in plant operations, increased process efficiency and more effective process control.

By continuously monitoring and predicting the health of the process or equipment can decrease the number of unplanned shutdowns and mitigate production losses. If the condition of the system is declining and the responsible group is informed of the system's state, a pre-emptive strategy can be established to counter the risks.

If the group or responsible person is informed of a possible breakdown, the risk can pre-emptively be assessed and spare parts can be pre-ordered to reduce down time that would have been used to wait for parts to arrive.

A part of condition monitoring includes efficiency monitoring. One of the symptoms of a faulty electrical motor is the reduction of efficiency (Nandi *et al.*, 2005). If the equipment is powered by an electrical motor, the efficiency or performance of the machine is then also dependent on the condition of the electrical motor. This makes monitoring the performance a viable indicator of the condition of the equipment. There are many more benefits to condition monitoring Neale & Woodley (1975) summarised the benefits in Table 1-1.

TABLE 1-1 THE BENEFITS OF CONDITION MONITORING

(ADAPTED FROM NEALE & WOODLEY, 1975)

		Methods by which condition monitoring gives these advantages		
		Benefits		
			Lead time	Better machine knowledge
Safety	Reduces machinery related accidents, injuries and fatalities		Enables safe planned plant stops when instant shut down is not permissible.	Machine condition, as indicated by an alarm, is adequate if instant shut down is permitted.
	Output	Increased machine availability	Increased running time	Enables machine shut down for maintenance to be related to required production or service, and various consequential losses from unexpected shut downs to be avoided.
Reduced maintenance time			Enables machine to be shut down without destruction or major damage requiring a long repair time. Enables the maintenance team to be ready, with spare parts, to start work as soon as machine is shut down.	Reduces inspection time after shutdown and speeds up the start of correct remedial action.
Increased rate of nett output			Allows some types of machine to be run at increased load and/or speed. Can detect reductions in machine efficiency or increased energy consumption.	
Improved quality of product or service		Allows advanced planning to reduce the effect of impending breakdowns on the customer for the product or service and thereby enhances company reputation.	Can be used to reduce the amount of product or service produced at substandard quality levels.	

1.4. CONDITION MONITORING APPROACH

1.4.1. MAKING CONDITION MONITORING PRACTICAL

State of the art equipment produces tremendous amounts of data. Analysing this data can result in a large time and financial expense (Wiggelinkhuizen *et al.*, 2007; Yang *et al.*, 2014). Bauer *et al.* (1998) states that the measurement equipment in the mining environment must be robust because of the extreme conditions. To make condition monitoring practical, the method itself should be robust. It has to compensate for limited logged parameters and still result in an accurate fault detection estimate.

The monitoring method should be cost effective. By using the mine's current monitoring infrastructure, implementation cost can be minimal. If the infrastructure already includes condition monitoring functionality, the focus can be shifted to the data analysis.

To increase the practicality of the condition monitoring method, performance parameters can be monitored. Performance monitoring is more practical because the performance parameters are more commonly measured. Performance monitoring is essentially a type of condition monitoring. Running machinery or processes in an unhealthy condition can have an adverse effect on the performance of the equipment. An example of such an effect is that the deterioration in the condition of the machine causes an increase in energy usage (Beebe, 2004).

The condition monitoring model, in this study, will be developed using data from South African mines. The study will focus on large electric motor-driven machines since most machines on the mine and in the mining industry are powered electrically.

1.4.2. APPROACH TO CONDITION MONITORING

The aim of improving condition monitoring capabilities, is to improve the CBM. CBM process consists of many sub steps. The whole architecture of CBM is summarised into seven steps (Prakash Kumar & Srivastava, 2014). This study focusses on signal processing condition monitoring health assessment and prognostics step presented in Figure 1-4.

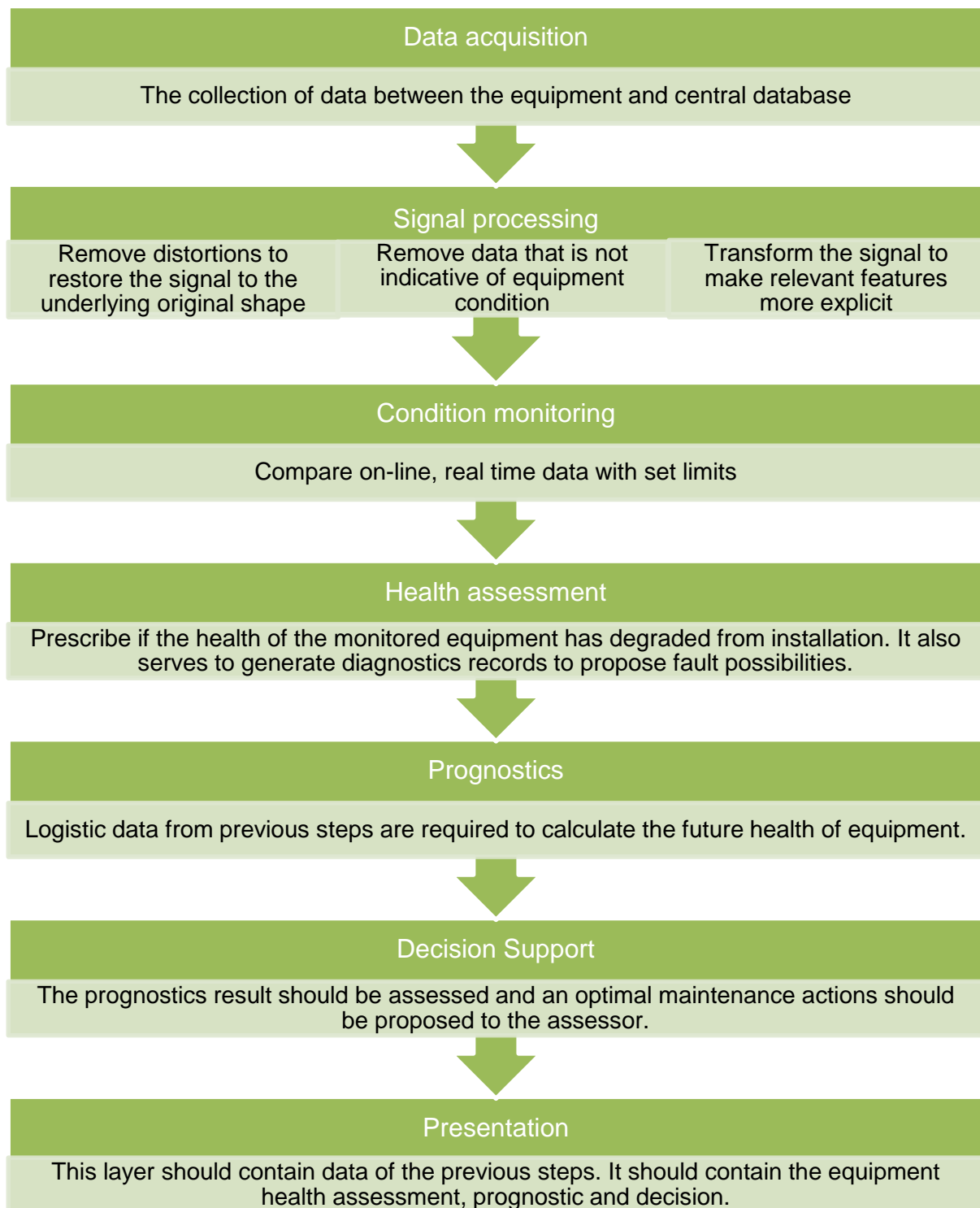


FIGURE 1-4 ARCHITECTURE OF CONDITION-BASED MAINTENANCE
(PRAKASH KUMAR & SRIVASTAVA, 2014)

A limiting step of this study is the data acquisition, therefore the focus shifts to the signal processing to improve condition monitoring, health assessment and prognostics steps of the equipment. The approach of this study will focus on reducing the difficulty of implementing a condition monitoring strategy.

1.5. CONCLUSION

Condition monitoring is an appealing field of research because of its benefits (Fugate *et al.*, 2001). A list of problems concerning condition monitoring in the South African mining industry is presented in Section 1.5.1. The aims of the study are given in Section 1.5.2.

1.5.1. PROBLEM STATEMENT

Many industries depend on a remote monitoring system built into the SCADA to indicate the condition of equipment. This method only triggers alarms when failures occur. This results in large failure-related cost such as production losses, consequential damage to other equipment, catastrophic failure replacement cost, unplanned maintenance overtime cost, etc. (Beebe, 2004; Wasif *et al.*, 2012).

South African mines only measure limited condition defining parameters. Gouws (2007) states that the connection of sensors for the purpose of condition monitoring is not always possible. Therefore, the need for a practical condition monitoring method increases that can assist with detection and prognosis using available data.

Previous studies propose many complex solutions for condition monitoring. These solutions require a large amount of representative data for fault prognosis or diagnosis. In practice, a large amount of data is rarely available or accessible.

Financial constraints limit many South African mining companies to effectively implement a condition monitoring system. Infrastructure to acquire and manage large amounts of data is imperative for the precise monitoring of equipment condition. An upgrade to the existing infrastructure can be required if the current infrastructure is not adequate to execute the specific maintenance strategy.

A low sample rate of 30 minutes is available, which has been considered too low for accurate fault detection (Yang *et al.*, 2014). Thus, a need for a condition monitoring method that is practical, robust and accurate for the low sample rates exists.

1.5.2. AIM OF THE STUDY

- Develop a method to improve condition-based maintenance strategies on South African mines.
- Develop and validate an alternative method that continuously predicts faults using readily available, measured parameters.

- Develop a method to continuously predict the condition of equipment and display information in a practical and usable format.

1.5.3. OVERVIEW OF THESIS

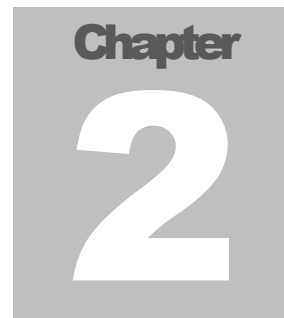
Chapter 1 sets the overview of the study. Elements concerning condition monitoring are explained and a list of advantages concerning condition monitoring are given. It also includes the steps taken to reach the aims of the study. The problem statement is presented along with the aims of the study.

Chapter 2 presents the literature on the topic of condition monitoring. To fully comprehend the state of the art the literature includes international studies and studies completed in South Africa. The literature search provides the basic concepts of condition monitoring. It compares how condition monitoring techniques are implemented in other industries and which parameters are required to make use of these techniques. The parameters are assessed individually to ensure that the measured parameters will give an accurate estimation of equipment condition.

Chapter 3 explains the development of the model. From the findings in Chapter 2, the technique is chosen to determine the condition of the equipment. The model is developed, trained and fine-tuned to suite the specific parameter and equipment. The method is compared to alternative techniques and critically evaluated.

Chapter 4 shows how the available condition monitoring data from different mines and equipment is used to test the autoregressive model in two separate case studies. The results are given and discussed in this chapter.

Chapter 5 reports the findings of the study. A summary of the study is given and a conclusion is drawn. The final condition monitoring methodology is reported. Recommendations for further studies are presented.



**ALTERNATIVE METHOD FOR EQUIPMENT
CONDITION MONITORING ON SOUTH AFRICAN MINES**

CHAPTER 2

CONDITION MONITORING OVERVIEW

2. CONDITION MONITORING OVERVIEW

2.1. INTRODUCTION

To fully comprehend condition monitoring methods, a literature review is done in Chapter 2. The literature study first provides the basic concepts of condition monitoring. Different condition monitoring techniques are presented and evaluated. The implementation of a condition monitoring technique is discussed. The common condition indicating parameters are listed and discussed. Different methods of how data is pre-processed and analysed is explained in this chapter.

2.2. CONDITION MONITORING BACKGROUND

Condition monitoring focuses on detecting the failure while a root cause analysis focuses on the underlying root causes of the fault (Tavner, 2008). Figure 2-1 shows the difference between the failure sequence and root cause analysis. Figure 2-1 is constructed using an example failure; the failure of a main shaft on a rotating electrical machine.

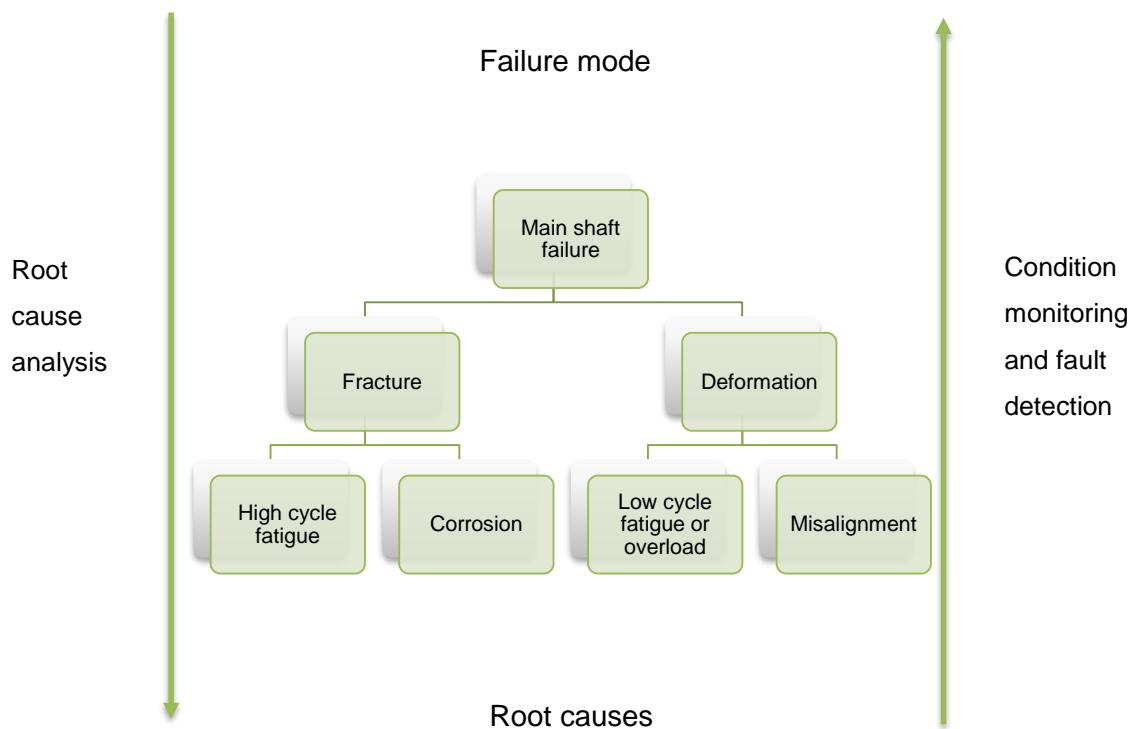


FIGURE 2-1 CAUSE-AND-EFFECT DIAGRAM OF A MAIN SHAFT FAILURE (TAVNER, 2008)

According to Vas (Cited by Nandi *et al.*, 2005), the most prevalent faults in rotating electrical machines are:

- bearing;
- stator or armature faults;
- the broken rotor bar and end ring faults of induction machines;
- and the eccentricity-related faults.

These faults are detected by monitoring various parameters. Beebe (2004) gives a table of symptoms or parameters that are relevant to pumps in Appendix A. Neale & Woodley (1975) summarised indications of machine or component deterioration in Appendix B.

By identifying outliers or a change in the behaviour of these parameters can give an indication of the equipment condition (Beebe, 2004). If such a change is detected or predicted, it allows maintenance to be scheduled or other action to be taken to prevent failure.

2.2.1. MAINTENANCE PHILOSOPHIES

Two important types of maintenance include corrective maintenance and preventive maintenance. According to European standards, Standard EN 13306, these maintenance types can be broken down as shown in Figure 2-2.

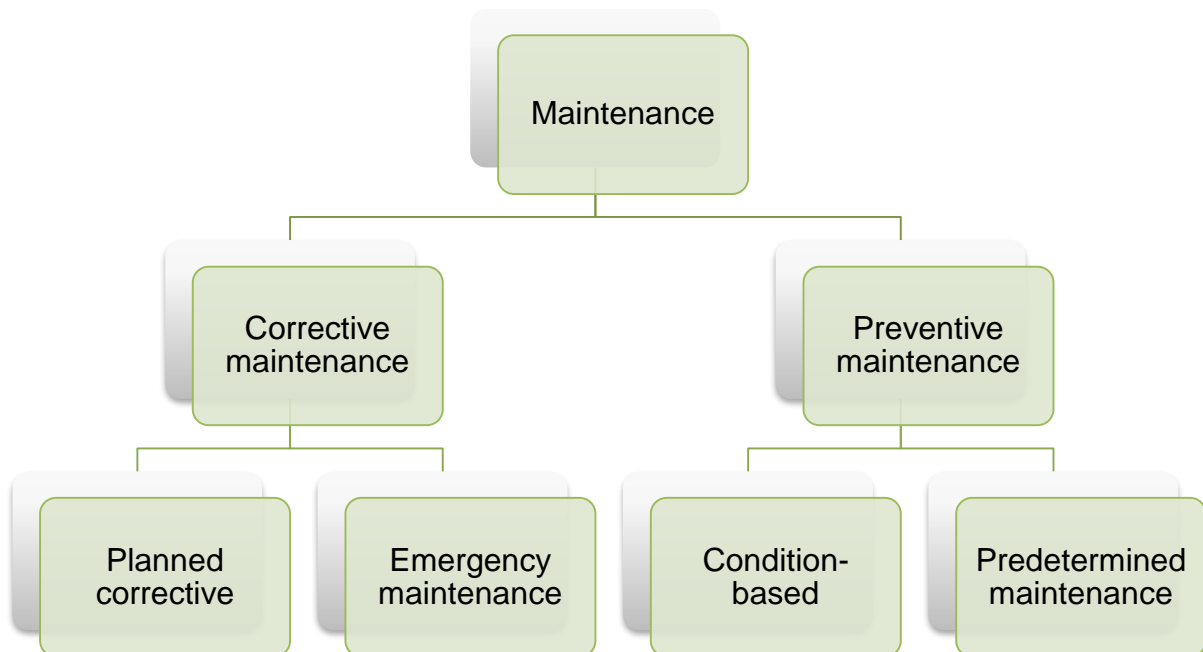


FIGURE 2-2 MAINTENANCE BREAKDOWN

Figure 2-2 illustrates that corrective maintenance includes planned corrective maintenance and emergency maintenance. The figure also illustrates that preventative maintenance includes CBM and predetermined maintenance. Moubray (1997) introduced a P-F curve as illustrated in Figure 2-3 (Wessels, 2003).

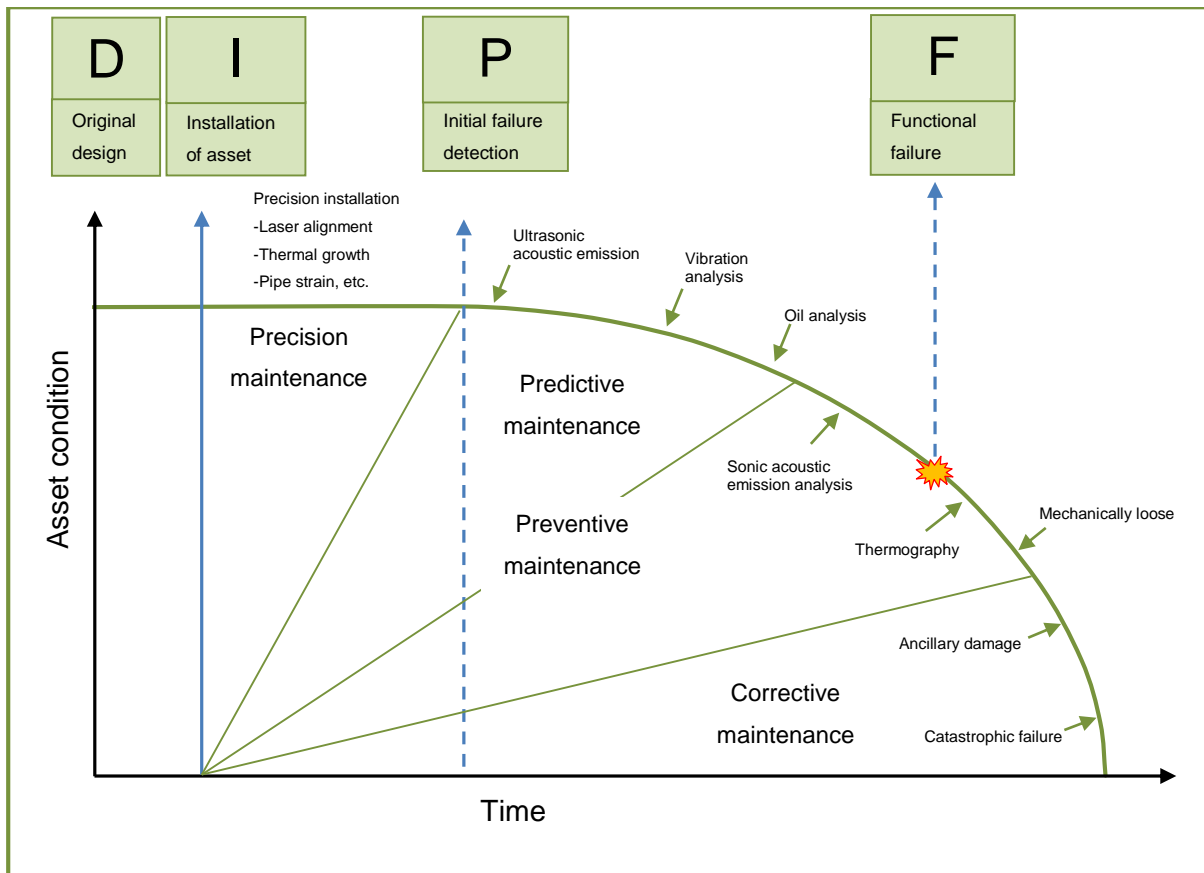


FIGURE 2-3 ASSET FAILURE CURVE
(Adapted from Etchson, 2017)

Figure 2-3 presents an asset failure curve, or in this case, a DIPF curve. Other variations include PF, IPF curves (Munio, 2017). The illustration provides context for the different maintenance types. The vertical axis (y) represents the asset condition and the horizontal axis (x) represents time.

The curve in Figure 2-3 shows that the asset gradually deteriorates throughout time from point I, the date of installation. P on the curve, shows the point in the process at which it is first possible to detect a fault. If a fault remains undetected or unmitigated, the rate of deterioration accelerates until a functional failure occurs at point F (Munio, 2017).

Failure symptoms and condition detection techniques are added to the curve to indicate the asset condition. Figure 2-3 also displays the different types of maintenance and in what regions they occur. The maintenance types after point P on the graph is explained, namely corrective maintenance and preventive maintenance which include predictive maintenance as described below.

2.2.1.1. CORRECTIVE MAINTENANCE

Corrective maintenance is also known as reactive maintenance, breakdown maintenance, operate to failure or run-to-failure (Beebe, 2004). This type of maintenance is performed after a breakdown or when a fault is detected. Early in a machine's lifetime, a minimal number of incidents of failure is expected (Sullivan *et al.*, 2010). Beebe (2004) states that corrective maintenance can sometimes be cost effective if the maintainability of the equipment is unproblematic.

2.2.1.2. PREVENTIVE MAINTENANCE

If a condition monitoring strategy detects a fault before it occurs, maintenance can preemptively be scheduled to repair the fault. This process is called predictive maintenance. Preventive maintenance includes predictive maintenance. Preventive maintenance is the actions performed on a machine that can detect, prevent or mitigate the degradation of the machine with the aim to extend the machine's lifetime (Beebe, 2004).

A real-time, online, condition monitoring system aids in preventive and predictive maintenance strategies. Predicting a potential fault then allows for convenient repair scheduling (Beebe, 2004).

2.2.1.3. MAINTENANCE STRATEGY COMPARISON

Studies have shown that corrective maintenance is the predominant mode of maintenance in the mining industry (Mkernai, 2011; Sullivan *et al.*, 2010). More than 55% of maintenance resources and activities of an average facility are spent on corrective maintenance, 31% is spent on preventive maintenance, 12% is spent on predictive maintenance and 2% is spent on other methods (Sullivan *et al.*, 2010). In addition to the predicted savings, preventive maintenance will effectively extend the life of the equipment (Beebe, 2004; Sullivan *et al.*, 2010).

Louit & Knights (2001) state that implementing an adequate maintenance philosophy can result in reduced hidden costs, reduced unplanned and emergency work at a small cost of more planning, and higher preventive and planned maintenance expenses. A large part of the hidden costs and unplanned and emergency work are converted into cost savings (Louit & Knights, 2001).

To understand how the different types of maintenance are performed, Costinas & Comanescu (2004) compiled a table that explains the different techniques used to successfully implement the maintenance plan. Table 2-1 is adapted to accommodate the mining industry's monitoring systems and not only the monitoring of substations as was used in their study.

TABLE 2-1 DEVELOPING STRATEGIES FOR MAINTENANCE MANAGEMENT
(ADAPTED FROM COSTINAS & COMANESCU, 2004)

	Maintenance strategy	Required techniques / tools
<i>Corrective maintenance</i>	Replacement or repair is performed only if a failure occurred.	The spare parts and equipment themselves.
<i>Preventive maintenance</i>	Time based maintenance, recommendation from manufacturer and experience with same type of equipment; it has been practiced as the usual maintenance strategy in electrical power systems for many years.	Waveform analysis: data sheets; periodic component replacement.
<i>Predictive maintenance</i>	In accordance with condition and importance; concept of availability & reliability and reliability centred maintenance (RCM); power supply monitoring.	Waveform analysis: vibration monitoring; spectrographic oil analysis; thermographic analysis; infrared thermography; ultrasonic inspection; use of computers for analysis and trending.
<i>Proactive maintenance</i>	Proactive approach can be suited for equipment associated with the organisation's significant environmental aspects.	Monitoring and correction of failure root cause; root cause analysis; failure mode effect and criticality analysis (FMECA).

Mkemai (2011) compared the time spent on corrective maintenance and preventive maintenance of load haul dump machines in mines in Sweden. He found that corrective maintenance seems to dominate the maintenance activities in a mining environment. The study also showed that the time spent on corrective maintenance strategies increased if the machinery aged.

2.2.2. INDUSTRY APPROACH, STANDARDS AND STRATEGIES

Many condition monitoring systems are available for implementation in South Africa (Siemens South Africa, 2009; Crystal Instruments, 2017a; Rockwell Automation, 2017a; SKF, 2017). An example of such a system is given in Figure 2-4.

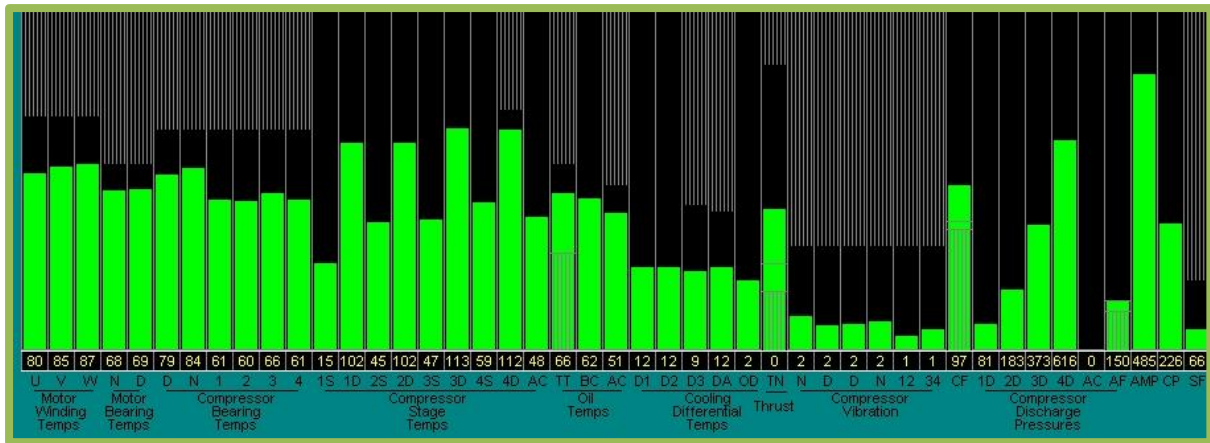


FIGURE 2-4 SCADA CONDITION MONITORING PANEL

Figure 2-4 shows a condition monitoring panel displayed on a mine’s SCADA interface. This specific example illustrates all the measured, condition-determining parameters of a multistage centrifugal compressor. The grey areas of each bar in the figure displays the trip limits. The SCADA system is developed by Rockwell Automation, but the condition monitoring of the equipment is handled by Siemens.

To monitor the parameters, the International Organisation for Standardisation’s (ISO) 10816-3 guideline is convenient to use for the process alarm and trip limits. Table 2-2 illustrates a recommended vibration velocity severity chart. According to Table 2-2, the vibration severity depends on the rated power and the foundation type of the motor. Machinery running with shaft speeds of more than 600 rpm should be analysed with a frequency of 10-1000 Hz (ISO 10816-3, 2009). Machinery running at speeds of more than 200 rpm should be analysed with a frequency of 2-1000 Hz (ISO 10816-3, 2009).

TABLE 2-2 VIBRATION SEVERITY CHART
(ISO 10816-3)

Machinery groups 2 and 4 Machinery groups 1 and 3

Velocity mm/sec RMS	Rated Power			
	Group 2: 15 kW – 300 kW		Group 1: 300 kW – 50 MW	
11.0	Red	Red	Red	Red
7.1	Red	Red	Red	Orange
4.5	Red	Orange	Orange	Yellow
3.5	Orange	Yellow	Yellow	Yellow
2.8	Orange	Yellow	Yellow	Green
2.3	Yellow	Green	Green	Green
1.4	Yellow	Green	Green	Green
0.7	Green	Green	Green	Green
0.0	Green	Green	Green	Green
Foundation type	Rigid	Flexible	Rigid	Flexible

Referring to Table 2-2, the red cells indicates severe condition, and the green cells indicate an acceptable operating condition. The foundation type of the equipment depends on how the machine is mounted to the floor. The mine operates with a compressor vibration trip limit of 6 mm/s and an alarm limit of 4 mm as shown in Figure 2-5.

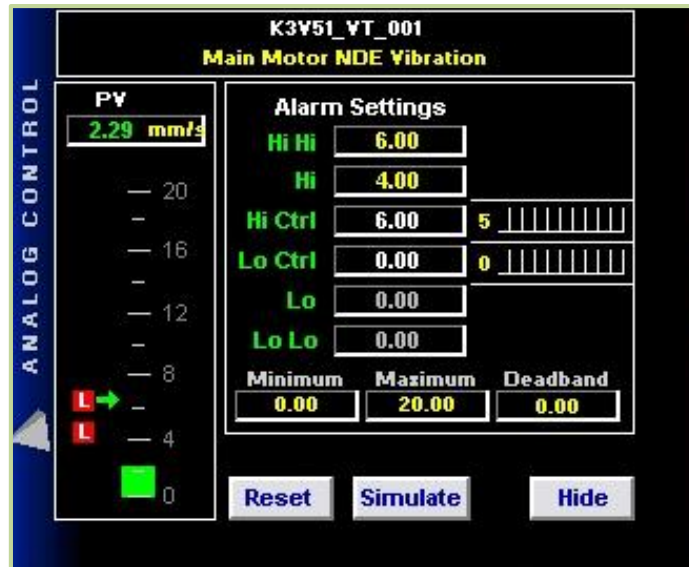


FIGURE 2-5 ALARM AND TRIP LIMITS OF A COMPRESSOR

The parameter data shown in the SCADA screenshots, Figure 2-4 and Figure 2-5, are logged in a database that can be analysed internally or by specialist third party companies. A list of available online monitoring systems in South Africa is compiled in Table 2-3.

TABLE 2-3 EXAMPLE OF AVAILABLE CONDITION MONITORING SYSTEMS

Supplier	Monitoring system	Analysis type	Online analysis	Source
Crystal instruments	Engineering Data Management: Post Analyser	Waveform analysis and value analysis: Fast Fourier transform (FFT) spectral analysis; octave and acoustic analysis; order tracking; orbit plot; sine reduction; basic signal conditioning	Yes	(Crystal Instruments, 2017b)
Siemens	Simatic Maintenance Station	Waveform analysis and value analysis which include oil analysis	Yes/No	(Siemens South Africa, 2009)

Rockwell Automation	Emonitor Condition Monitoring Software	Waveform analysis and value analysis: Trend projection; FFT spectral analysis; automated diagnosis	Yes	(Rockwell Automation, 2017b)
SKF	Surveyor NetEP	Waveform analysis and value analysis	Yes	(SKF, 2017)
TAS Online	Remote monitoring	Value analysis	Yes	(TAS Online, 2017)
WearCheck	N/A	Waveform analysis, value analysis and physical inspection: Operational deflection shape, transient analysis, resonances tests	No	(WearCheck, 2017)

Table 2-3 provides a list of available condition monitoring systems that is available for use in South Africa. The list only includes a small number of the available suppliers. The analysis technique is also included in Table 2-3 to show how the condition of the equipment is determined. The systems report on the current state of the equipment and give suggestions to what should be corrected.

2.3. DATA EVALUATION AND ANALYSIS METHODOLOGY

Raw data has to be pre-processed to ensure that the critical, representative data is analysed (Baillie & Mathew, 1996). Four main parts should be contained in a condition monitoring system, namely: the sensor, data acquisition, fault detection and diagnosis (Grimmelius, 1999; Tavner, 2008). This section will discuss the different sensors, how the data is stored and available data analysis methods.

2.3.1. SENSORS

Vibration, shock and acceleration is measured using different types of accelerometers. Direct techniques include accelerometers of the following types (Brodgesell *et al.*, 2003):

- A. Seismic (Inertial)
- B. Piezoelectric
- C. Piezoresistive and strain gauges
- D. Electromechanical sensors
- E. Capacitive and electrostatic

- F. Velocity sensors
- G. Noncontact proximity sensors
- H. Mechanical switches
- I. Optical sensors

The typical range of vibration frequency, in Hz, for the different accelerometer types are given below (Brodgesell *et al.*, 2003):

- A. DC to 50 Hz
- B. From 1 to 15 000 Hz; special designs can go up to 30 000 Hz
- C. From 0 to about 1000 Hz
- D. Between 10 and 1000 Hz
- F. 0 to 3500 Hz
- H. 0 to 5000 Hz

Most rotary equipment vibrates at frequencies of between 1 and 20 000 Hz (Brodgesell *et al.*, 2003). Overall vibration levels are monitored in analogous RMS detectors (Večeř *et al.*, 2005). If the analogous vibration levels exceed the set trip limits, the machinery will trip. Special exceptions occur where a higher vibration set limit is set during the start-up of machinery. Specifics of a vibration sensor that is commonly used in the mining industry is attached in Appendix D.

Many different classes of temperature sensors are available (Rall *et al.*, 2003). The different classes have specific temperature ranges, accuracy and cost involved (Rall *et al.*, 2003). The selection of a suitable sensor depends on the specific application (Rall *et al.*, 2003). Temperature measurements are usually sampled at low sample rates (Ashlock & Warren, 2015).

2.3.2. FILTERING

To ensure that the data is representative, it must be filtered. Filters reject unwanted noise within a certain frequency range (Rall *et al.*, 2003; Ashlock & Warren, 2015). Filters are used to prevent aliasing from high-frequency signals (Rall *et al.*, 2003; Ashlock & Warren, 2015). The aim of a filter is to obtain a better signal-to-noise ratio (Večeř *et al.*, 2005). Low-pass filters are commonly used to eliminate high-frequency noise and 60 Hz power line noise.

Since temperature measurements are usually sampled at slow rates, it makes the measurements susceptible to high-frequency noise (Ashlock & Warren, 2015). Filtering the temperature signals increase the accuracy of the measurement.

Regardless of the type of measured parameter, the data has to be evaluated. Examining the quality of the data is a critical step to mitigate fault detection errors. The aim of the data evaluation step is to ensure that the data is at a high level of quality before it is processed and assumed to be accurate. Guenel *et al.* (2013) states that the evaluation of multiple sensor data is often a major problem due to complex interdependencies between measured sensor data and the actual system condition.

2.3.3. DATA ANALYSIS

Computation is required to analyse quantitative data for fault detection (Han & Song, 2003). Some high-frequency vibration monitoring systems analyse complete Fourier spectra (Jardine *et al.*, 2006). The analysis of resulting condition indicators are computed and considered in the decision making process to trip the machine (Večeř *et al.*, 2005). In this study, the high-frequency signals are not available, so other data analysis methods are considered in this subsection.

2.3.3.1. CONTROL CHARTS

Control charts are one of the primary techniques used in statistical process control (SPC) and are typically used to monitor the mean shift of statistical distributions (Kullaa, 2003). Control charts indicate significant changes in a system operation thus it can be applied to detect changes in equipment condition.

A control chart is a useful data analysis tool used to display the individual data points together with the mean and standard deviation of the dataset. Typical statistical calculations include the mean, standard deviation and frequency distribution. The mean is essentially the average of the filtered data. The standard deviation, or accuracy, measures the distribution of data point on either side of the mean. The control chart provides information about the consistency of the responses to help better understand the data.

A Shewhart \bar{X} control chart is used to monitor the mean of a quality characteristic of process variables. This control chart illustrates the basic trend of a process variable. It is simple to set up and easy for operators to understand.

Page (1954) proposed a cumulative sum (CUSUM) control chart which is another method to detect a shift in process mean. Studies have shown that the CUSUM chart is more efficient in detecting small and moderate shifts in the process mean than the \bar{X} control chart (Reynolds *et al.*, 1990; Zhang *et al.*, 2004). The CUSUM chart is updated using fixed-length sampling

intervals. Reynolds *et al.* (1990) suggested a CUSUM scheme which is updated using varied time intervals.

Exponentially weighted moving average (EWMA) is another statistic to monitor the mean shift of a quality characteristic. EWMA chart, just like the CUSUM chart, is commonly used for relatively small shift detection (Zhang *et al.*, 2004).

S and R charts are suitable for variance shift detection (Zhang *et al.*, 2004). To detect mean and variance shifts concurrently \bar{X} and S (or R) charts can be plotted on a joint graph. Another more recent approach, control chart is the weighted loss CUSUM chart. The aim of this chart is to detect both mean and variance shifts in one chart (Zhang *et al.*, 2004).

A study performed by Reynolds & Lu (1997) states that using traditional control chart methodology on auto-correlated processes can result in a biased estimate for process parameters. The study evaluates various types of EWMA control charts that were fitted to original observations or on residuals from a fitted time series model. The study showed that moderate levels of autocorrelation can have a significant effect on the performance of control charts. When autocorrelation is present, traditional control chart methodology should not be applied without modification (Reynolds & Lu, 1997).

Reynolds & Lu (1997) recommends that charts using residuals from a fitted time series model are not better unless the level of autocorrelation is high. So, for the condition monitoring method used in this study, it is critical that the residuals of the fitted time series model have a high level of autocorrelation.

2.3.3.2. MEAN AND VARIANCE SHIFT ANALYSIS STUDIES

Jun & Suh (1999) monitored the mean shift of time-domain averaged vibration signals for tool breakage detection. The tool was used to detect breakage for numerical control (NC) milling operations. They made use of Shewart \bar{X} , EWMA and adaptive control charts to detect breakage.

Kullaa (2003) made use of univariate and multivariate \bar{X} , CUSUM and EWMA charts to monitor the condition of the Z24 Bridge in Switzerland. The study monitored the mean shift of modal parameters such as stiffness, mass, damping, and boundary conditions.

Wang & Wong (2002) proposed a technique to detect faults in the vibration signals of helicopter transmission gears. The technique first establishes an autoregressive (AR) model on healthy gears. The AR model is then used as a linear prediction error filter to predict the

future-state signal from the gear. The condition of the gear is diagnosed by characterising the error signal between the filtered and unfiltered signals. This technique was validated using numerical simulation and experimental data.

Wang & Wong (2002) have shown that the AR modelling method is capable to detect a gear tooth crack earlier and with a higher level of confidence than with the traditional residual kurtosis method.

Fugate *et al.* (2001) also fitted an AR model to a healthy concrete bridge's vibration signal. The residuals errors were seen as damage-sensitive features. Fugate *et al.* (2001) applied the residuals to \bar{X} and S charts to monitor the mean and variance shifts.

Multiple parameters indicate the condition of gearboxes, so Baydar *et al.* (2002) proposed a multivariate statistical analysis to detect faults in helical gears. Q and T^2 statistics were adopted as the condition indicators. The study also predicted growing faults in the gearbox by monitoring the confidence regions based on kernel density estimations (KDE).

2.4. CONDITION PREDICTION MODEL

Condition prediction models use state or condition indicating parameters to estimate the condition of equipment. The condition indicating parameters or state observers helps to measure the condition of equipment that can not necessarily be seen or be measured directly.

2.4.1. KEY MONITORED PARAMETERS

The condition of machinery and processes affects certain parameters, such as vibration, temperature, acoustic emissions, etc. As mentioned in Section 2.4.1, the vibration, temperature and equipment specific performance parameters are the most commonly logged parameters.

Equipment monitoring can be divided into two groups, namely condition monitoring and performance monitoring. According to Yates (2002), the performance monitoring is the monitoring of performance parameters that determines the efficiency of the equipment and condition monitoring reduces the risk of failure. The operating functions and benefits of the two groups are summarised in Figure 2-6.

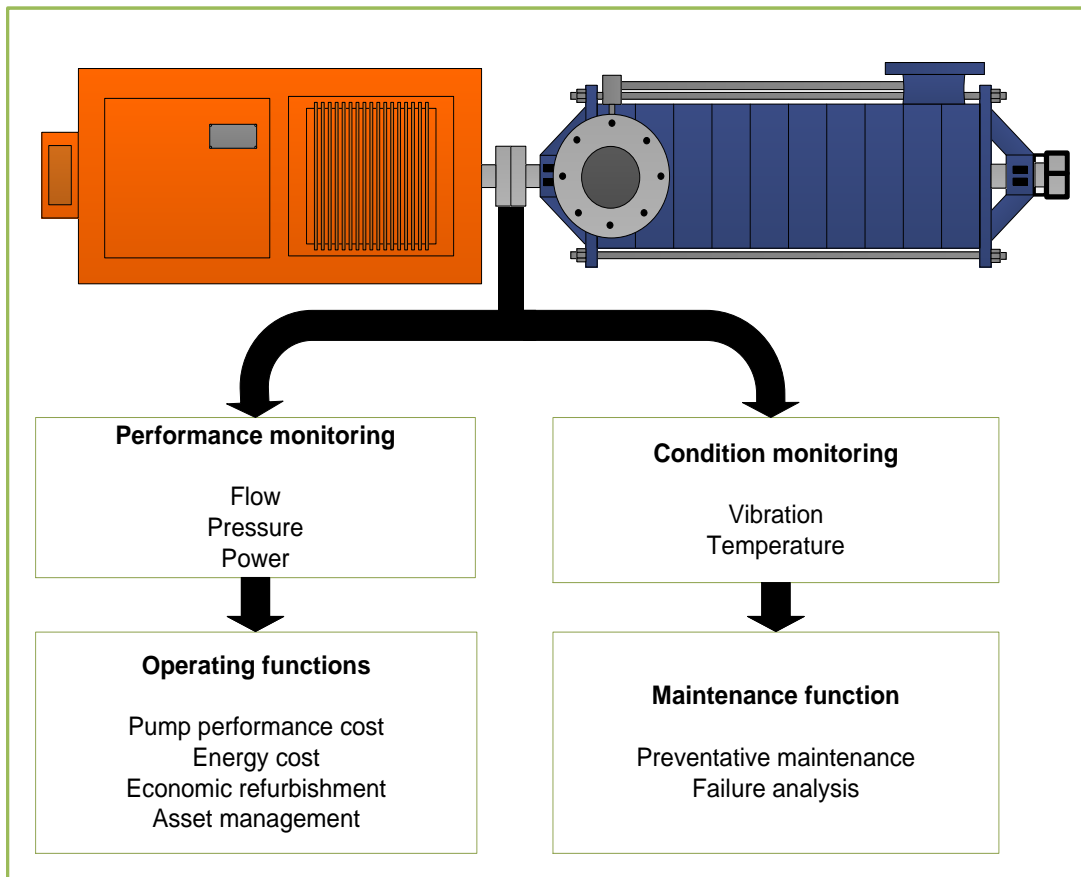


FIGURE 2-6 PERFORMANCE MONITORING AND CONDITION MONITORING
(YATES, 2002)

An example of the measured parameters of a multistage centrifugal pump and a multistage centrifugal compressor are given in Figure 2-7 and Figure 2-8 respectively. The parameters shown in both figures are typical monitored parameters on compressors and pumps. The figures were constructed using available parameters from different sources from South African mines and only the common measured parameters are shown. The cooling systems of the compressors are excluded from the drawings.

Mines make use of multistage centrifugal pumps that are essentially multiple pumps in series to obtain a desired performance (Beebe, 2004). The pumps are used in dewatering systems of underground mines, or to lower the water level in open pit mines. Deep mining operations have dams and pumping stations situated at different depths.

The pumping station typically contains at least two or more pumps, of which at least one serves as a backup. The pumping capacity of the pumps should be more than the inlet flow to avoid flooding. Figure 2-7 gives an illustration of the typical monitored parameters of a multistage centrifugal pump.

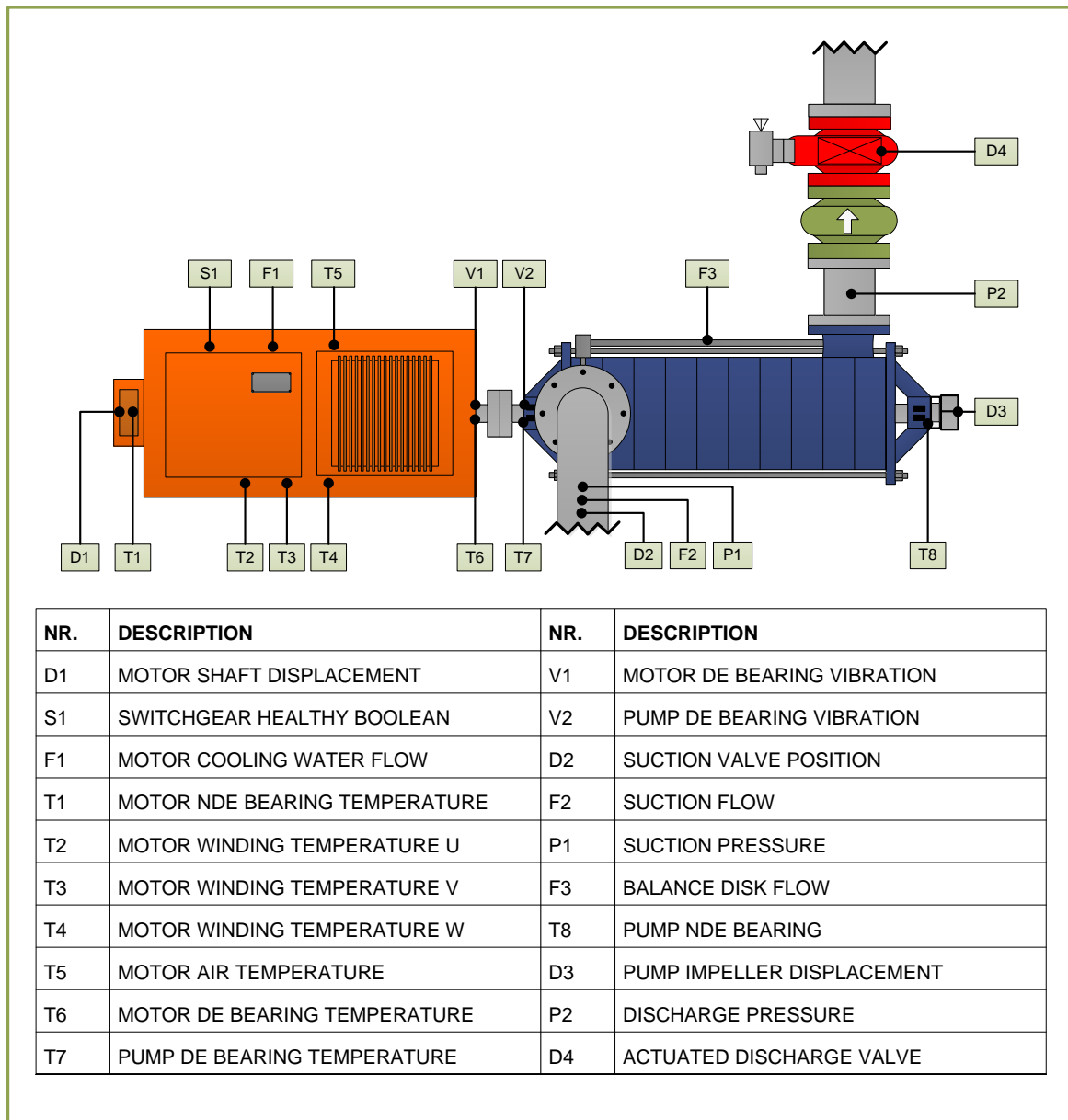


FIGURE 2-7 MONITORED PARAMETERS OF A MULTISTAGE CENTRIFUGAL PUMP
(Adapted from Oberholzer, 2014)

Figure 2-7 illustrates the typical condition monitoring parameters of a multistage centrifugal pump. The illustration includes both the electrical motor and pump components. The list of measured parameters in the illustration is compiled from different sources in literature.

The compressors deliver compressed atmospheric air to underground consumers. Examples of the underground compressed air consumers include rock drills, refuge bays and loading boxes. Some mines do not use pneumatic equipment but power the equipment hydraulically. Pressurised air, in deep-level mines, is required by law for the sole purpose of supplying air to underground refuge bays.

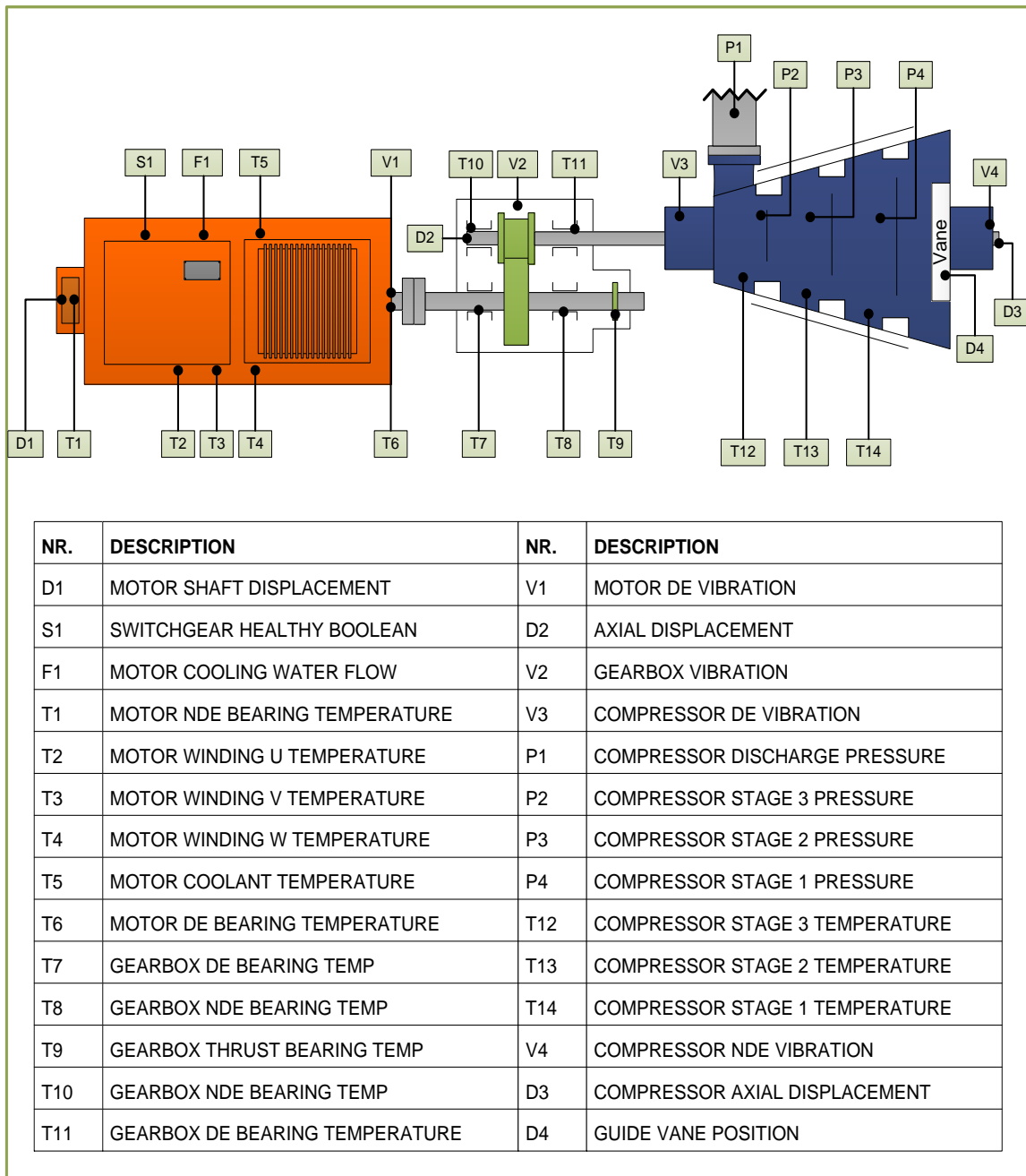


FIGURE 2-8 MONITORED PARAMETERS OF A MULTISTAGE CENTRIFUGAL COMPRESSOR

Figure 2-8 illustrates the typical condition monitoring parameters of a multistage centrifugal compressor. The illustration includes the electrical motor, gearbox and compressor. The list of measured parameters in the illustration is compiled from different sources in literature.

2.4.1.1. CONDITION MONITORING PARAMETERS

Parameters such as temperature and vibration are considered as condition monitoring parameters (Yates, 2002). Willier (1971) as referenced by Murray (1989), developed an equation (Equation 2.1) that uses a rise in temperature across a pump to determine the pump's

efficiency. This means that temperature can be considered a performance parameter because it is a measure of the energy losses on the machine (Murray, 1989).

TABLE 2-4 KEY MONITORED PARAMETERS OF DIFFERENT STUDIES

Component	Technique	Modelled parameters	Reference	Resolution
<i>Wind turbine generator</i>	Non-linear state estimation technique	Temperature	(Guo <i>et al.</i> , 2012)	10 min (2 min verification)
<i>Electrical power transformers</i>	Artificial neural networks	Vibration	(Booth & McDonald, 1998)	10 minutes
High sample rates				
<i>Helicopter transmission gears</i>	Autoregressive modelling	Gearbox vibration	(Wang & Wong, 2002)	High
<i>Experimental test rig gearbox</i>	Meshing resonance and spectral kurtosis methods	Gearbox vibration	(Wang <i>et al.</i> , 2017)	Various (High)
<i>Experimental test rig</i>	Autoregressive modelling	Bearing vibration	(Baillie & Mathew, 1996)	High
Other condition monitoring techniques				
<i>Mine excavators:</i>	Failure mode, effects and criticality analysis	Electric motors, bearing system and hydraulic system	(Mkemei, 2011)	Non-random

Table 2-4 shows the key monitored parameters of different studies. Table 2-4 also includes the sample resolution used in the specific study. And divides the studies accordingly. A FMECA on mine excavators is also added to the list.

2.4.1.2. PERFORMANCE MONITORING PARAMETERS

Murray (1989) states that monitoring a pump's efficiency is complementary to other condition monitoring techniques such as vibration and lubrication oil monitoring. An advantage of performance parameters is that it is commonly logged on mining equipment, usually intended to be used specifically for performance monitoring. Performance parameters, for example, the flow, discharge pressure and power consumption of a pump, can be used to calculate the efficiency of the pump. Table 2-5 gives the fundamental terms and units used in pump performance monitoring with the SI units in bold.

TABLE 2-5 FUNDAMENTAL TERMS AND UNITS IN PUMP PERFORMANCE
(BEEBE, 2004)

Quantity	Other terms used	Symbol	Units
<i>Flow</i>	Volumetric flowrate, capacity, discharge, quantity	<i>Q</i>	$\frac{m^3}{s}, \frac{L}{s}, \frac{m^3}{h}, \frac{ML}{d}$ Sometimes $\frac{kg}{s}$
<i>Head</i>	Total head, total dynamic head, generated pressure, generated head	<i>H</i>	m, kPa
<i>Power</i>	Power absorbed	<i>P</i>	W, kW
<i>Efficiency</i>		η	%

There are two different ways to calculate the efficiency of a multistage centrifugal pump, namely the conventional method and the thermodynamic (or thermometric) method (Murray, 1989; Beebe, 2004). The conventional method uses measured flow, head and power to calculate the efficiency. The thermodynamic method requires measuring the temperature and pressure rise across the machine. The temperature increase across a machine is a measure to determine the energy losses in the machine, while the pressure increase determines the useful work (Murray, 1989; Beebe, 2004). The thermodynamic method of calculating the efficiency is given by Equation 2.1.

$$\eta = \frac{1}{1 - \beta T + \frac{\rho c_p \Delta T}{\Delta P}} \quad (2.1)$$

Where:

- η is the efficiency of the pump
- c_p is the specific heat capacity of the fluid
- ΔT is the measured temperature increase across the machine
- ΔP is the measured pressure increase across the machine
- T is the absolute temperature
- β is the coefficient of cubical expansion of the liquid

For compressors, the monitored performance and condition indicating parameters are similar to those of pumps. The fundamental terms and units to determine the performance of a compressor is given in Table 2-6.

TABLE 2-6 FUNDAMENTAL TERMS AND UNITS IN COMPRESSOR PERFORMANCE

Quantity	Other terms used	Symbol	Units
Flow	Volumetric flowrate, discharge, quantity, mass flowrate	Q	$\frac{Nm^3}{s}, \frac{Nm^3}{h}, \frac{Std m^3}{h}$ $\frac{kg}{s}$
Power	Power consumption	P	W, kW
Pressure	Discharge pressure, delivery pressure, aftercooler pressure	p	Pa, kPa, bar
Temperature	Suction temperature, stage suction temperature, discharge temperature, aftercooler temperature		$K, ^\circ C$
Position	Guide vane position / blow off valve position		%
Efficiency		η	%

For compressors, the monitored parameters are similar to those of the pumps. The fundamental terms and units to determine the performance of a compressor is given by Table 2-6.

Table 2-6 provides a list of the parameters monitored to determine the performance of a compressor. The overall efficiency of a centrifugal compressor varies between 70% and 85% (Campbell *et al.*, 1992). To determine the thermodynamic efficiency, η , for an individual multistage centrifugal compressor, the following data is required:

- Flow (Normalised or standardised)
- Power consumption
- Suction, stage suction and discharge temperatures of usually three to four stages on a centrifugal compressor
- Aftercooler temperature and pressure
- Pressures between stages
- Guide vane position
- Blow off valve position

Apart from the performance parameters, a list of other condition monitoring methods are tabulated in Table 2-7. The list is adapted from Zhou *et al.*, (2007). Table 2-7 shows the advantages and disadvantages of the specified monitoring scheme.

TABLE 2-7 DIFFERENT CONDITION MONITORING METHODS

Monitoring schemes	Major advantages	Major disadvantages
<i>Vibration monitoring</i>	Reliable; standardised (ISO standards available)	Expensive; intrusive, subject to sensor failures
<i>Chemical analysis</i>	Physically monitoring the equipment	Limited to closed loop oil supply; specialist knowledge required
<i>Temperature measurement</i>	Standard available in some industries (IEEE standards available)	Embedded temperature detector required; other factors may cause same temperature rise
<i>Acoustic emission (ultrasonic frequency)</i>	High signal-to-noise ratio	Acoustic emission sensor required; specialist knowledge required
<i>Sound measurement</i>	Easy to measure	Background noise must be shielded
<i>Laser displacement measurement</i>	Alternative to vibration monitoring scheme	Laser sensor required; difficult to implement
<i>Stator current monitoring</i>	Inexpensive; easy to implement	Sometimes low signal-to-noise ratio; still in development stage

2.4.1.3. SAMPLE INTERVALS

Representative input data intervals are required to accurately develop a model and monitor the disturbances in the system. The model will only be able to detect a disturbance if the input data gives an indication of a potential disturbance. For example, if one is to monitor equipment temperature in a daily interval at 24H00 every day, the only the seasonal sinusoidal temperature profile can be observed. If the temperature is measured hourly, the daily sinusoidal profiles as well as the yearly profile can be observed. Similarly, a fault may only be observed by monitoring a certain interval. Thus, it is imperative to monitor the correct intervals.

Figure 2-9 to Figure 2-11 illustrates the effect of failure by plotting a normal distribution of the probability of a fault to occur vs. the reliability of a machine.

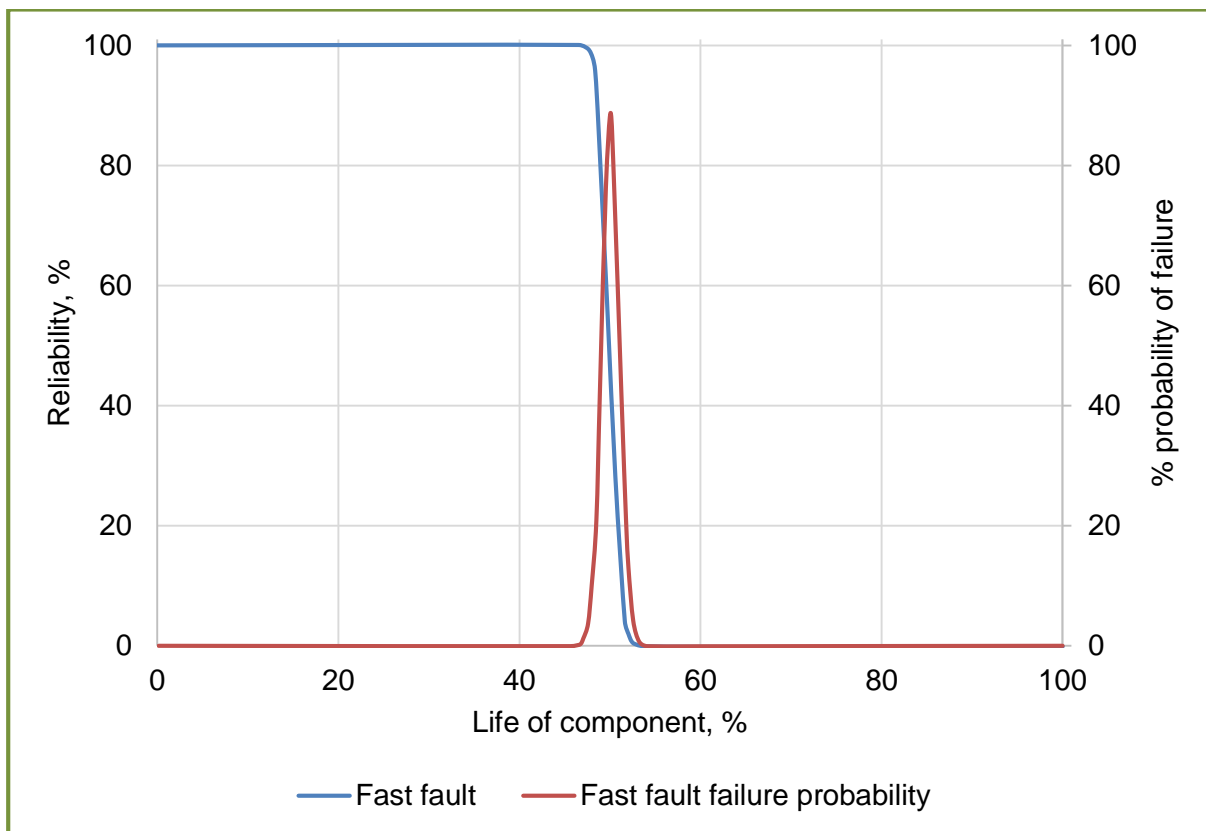


FIGURE 2-9 RATE OF FAILING OPERABILITY AS TIME PROGRESSES: FAST SPEED FAULT (TAVNER, 2008)

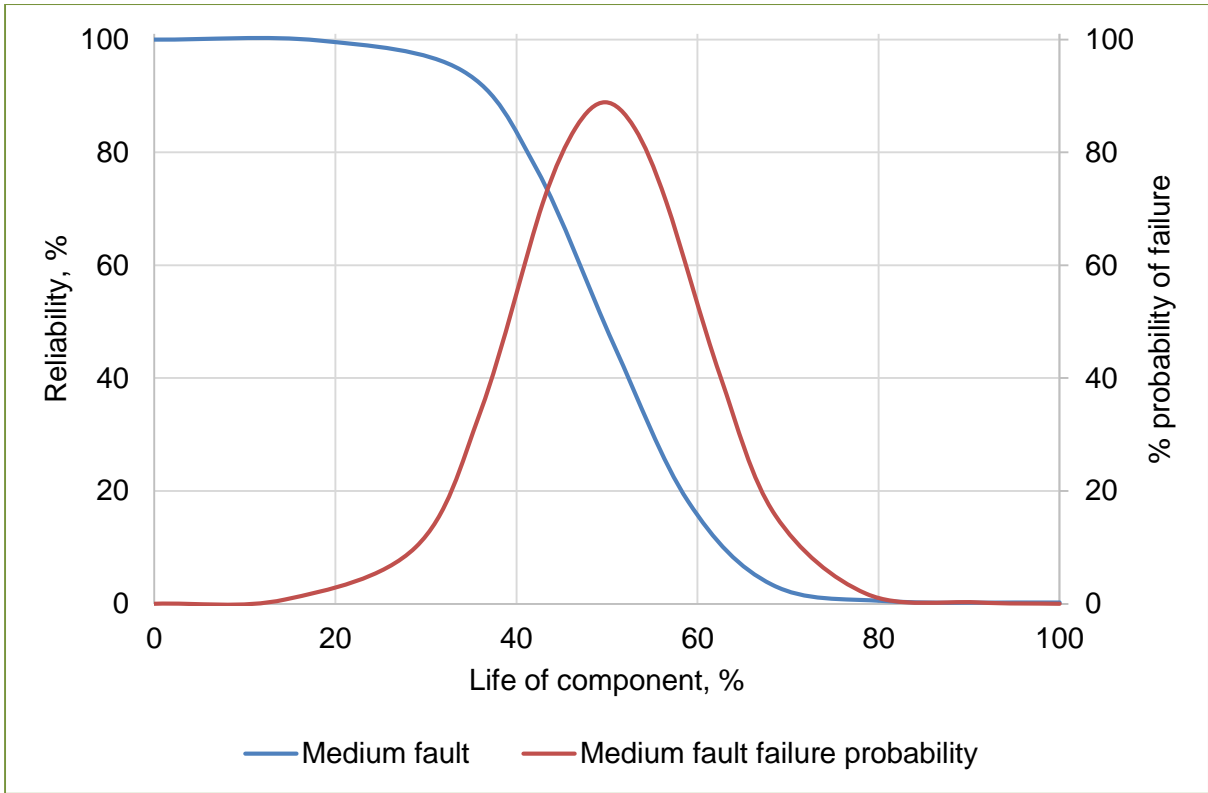


FIGURE 2-10 RATE OF FAILING OPERABILITY AS TIME PROGRESSES: MEDIUM SPEED FAULT (TAVNER, 2008)

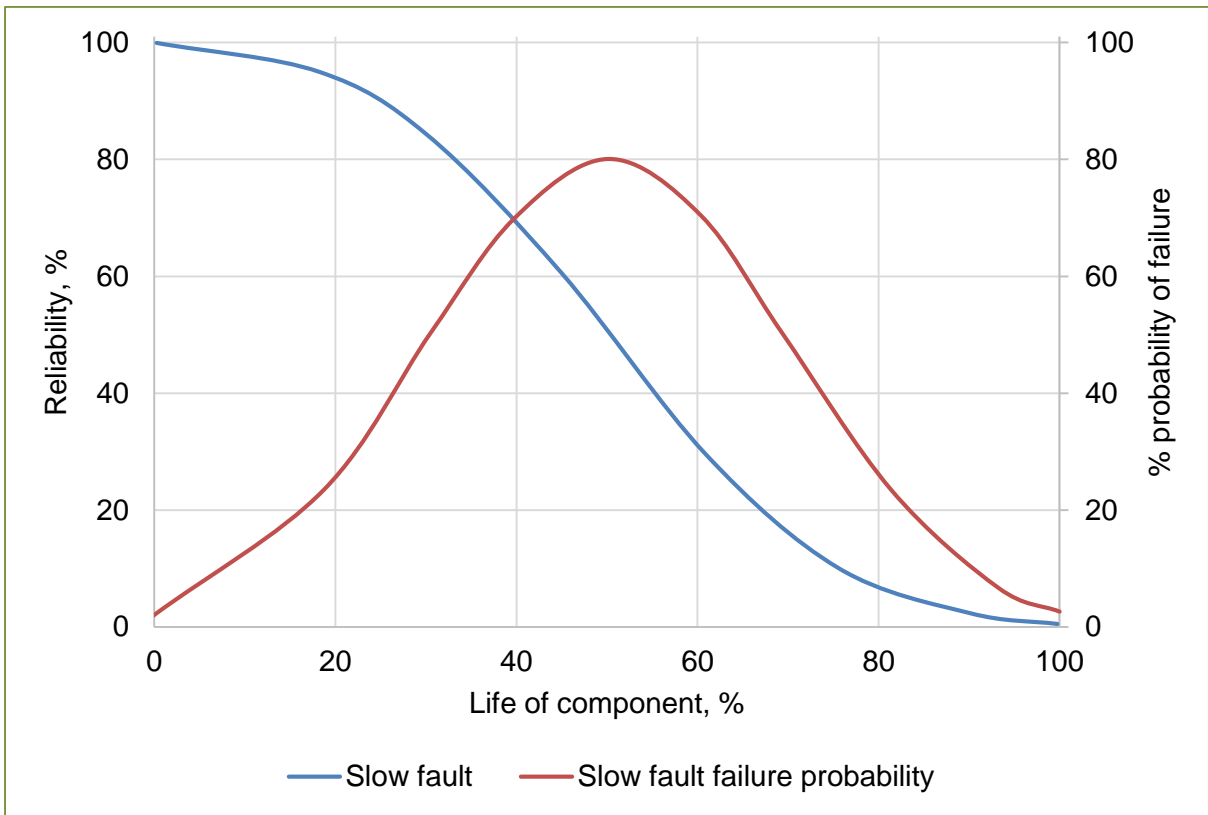


FIGURE 2-11 RATE OF FAILING OPERABILITY AS TIME PROGRESSES: SLOW SPEED FAULT (TAVNER, 2008)

Figure 2-9 through to Figure 2-11 shows the progression from a reliable to non-reliable operation at different fault progression rates: fast fault (Figure 2-9), medium fault (Figure 2-10) and a slow fault (Figure 2-11). Figure 2-9 shows a rapid progression from reliable to non-reliable at the 50% point. The probability of failure rises sharply at this point. The area under the normal distribution curve is equal to one, because there is 100% probability of failure throughout the life of a machine. The same graphing methodology is repeated for the medium and slow fault.

The different rates of failure should be considered while developing a model to detect equipment faults. Analysing a set interval that does not represent the fault yields inaccurate results (Večeř *et al.*, 2005; Yang *et al.*, 2013). Therefore, the model should at least take the interval of the measured parameter into consideration. If possible, the model should be tested with different intervals, relevant to the parameter type.

Inspection intervals parameters are vital to detect phased deterioration of equipment (Sherwin & Al-Najjar, 1999). Beebe (2004) states that the monitoring of vibration in monthly, quarterly and yearly intervals is unusual. Sherwin & Al-Najjar (1999) developed practical models for optimum condition monitoring inspection intervals using Markov models. Data sample intervals of 10 minutes have been considered too low for accurate fault diagnosis when conventional condition monitoring techniques are used (Večeř *et al.*, 2005; Yang *et al.*, 2013).

2.4.2. EXISTING METHODS

Different condition monitoring techniques exist with specific inherent attributes and requirements. These techniques range from basic statistical analysis of the data to in-depth model-based condition monitoring methods.

2.4.2.1. STATISTICAL MODELS AND INDICATORS

Guo *et al.* (1998) proposed an integrated real-time statistical monitoring scheme shown in Figure 2-12. This strategy is implemented in the semiconductor fabrication process, but the methodology of the strategy follows a generic structure that can be applied to other systems as well. The scheme requires tool data and process data as process variable inputs. Tool data includes different statistical indicators.

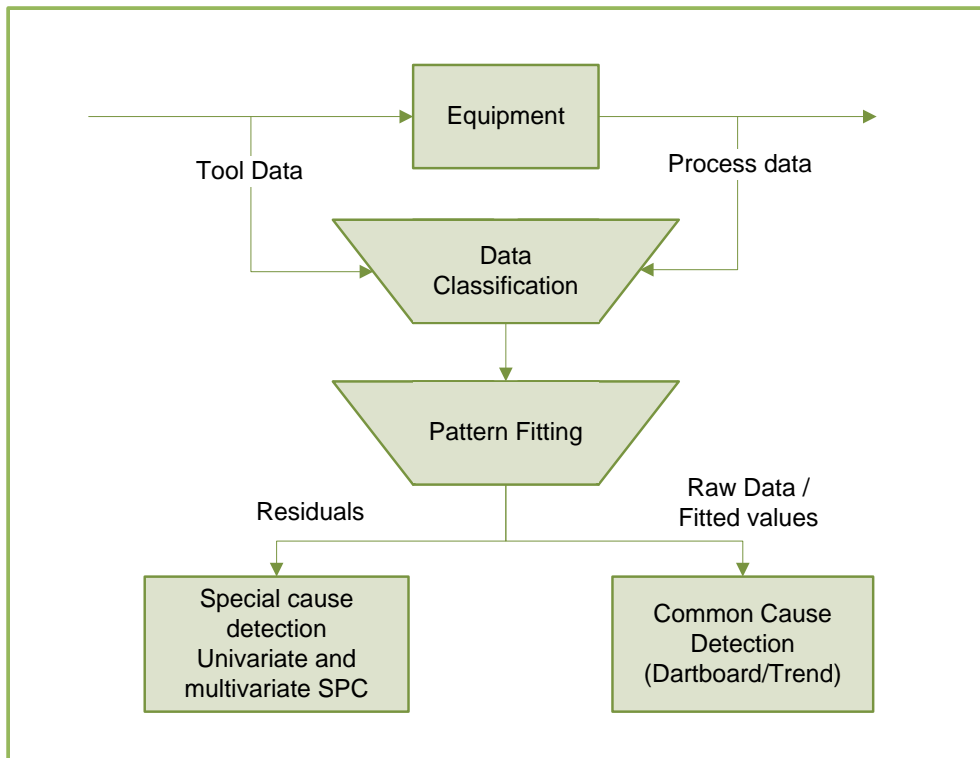


FIGURE 2-12 INTEGRATED REAL-TIME STATISTICAL MONITORING SCHEME
(ADATTED FROM GUO *ET AL.*, 1998)

Referring to Figure 2-12, Guo *et al.* (1998) gives an illustration of how a statistical monitoring scheme works. The illustration shows that process data and tool data is required for data classification. After the data has been classified, patterns are fitted to the data. Using the fitted patterns, two methodologies are followed to analyse the equipment condition namely special cause detection and common cause detection.

Special cause detection includes univariate and multivariate SPC methods to determine the condition of equipment. The univariate and multivariate SPC methods analyse the residuals of the fitted pattern to determine the state of the process. Common cause detection evaluates the raw or fitted values, and includes the standard trip and alarm level decisions.

Guo *et al.* (1998) proposed a feature factor; a method to determine the condition of a process using multiple monitored parameters. The feature factor is a scalar factor between one and zero which normalises and reflects the state of the parameter (Guo *et al.*, 1998).

Večeř *et al.* (2005) compiled a list of statistical time-domain features used to analyse developed vibration signals. These vibration statistical indicators are calculated before it is sent to the data historian.

TABLE 2-8 STATISTICAL VIBRATION CONDITION INDICATORS
VEČER ET AL. (2005)

Indicator	Calculation	Parameters
Root mean square value (RMS)	$v_{rms} = \sqrt{\frac{1}{T} \int_{T_i}^{T_f} v^2(t) dt}$	v_{rms} is the RMS value of the velocity of the vibration signal T is the integration time v is the velocity of the moving object
Delta RMS	$v_{\Delta rms} = \Delta v_{rms}$	$v_{\Delta rms}$ is the delta RMS
Peak value	$v_p = \text{Maximum of dataset}$	v_p is the maximum value of the signal in the dataset
Crest factor	$CF = \frac{S_{peak-peak}}{S_{rms}}$	CF is the crest factor $S_{peak-peak}$ is the peak to peak value of the signal S_{rms} is the RMS value of the vibration signal
Energy operator (EO)	$EO = \frac{N^2 \cdot \sum_{i=1}^N (x_i - \Delta \bar{x})^4}{\left(\sum_{i=1}^N ((\Delta x_i - \Delta \bar{x})^2)\right)^2}$	EO is the energy operator $\Delta \bar{x}$ is the mean value of signal Δx $\Delta x_i = s_{i+1}^2 - s_i^2$ N is the number of points in the dataset
Kurtosis	$Kurt = \frac{N \cdot \sum_{i=1}^N (s_i - \bar{s})^4}{\left(\sum_{i=1}^N ((s_i - \bar{s})^2)\right)^2}$	$Kurt$ is Kurtosis N is the number of points in in the history of signal s s_i is the i -th point in the time history of signal s
Energy ratio (ER)	$ER = \frac{\sigma(d)}{\sigma(r)}$	ER is the energy ratio $\sigma(d)$ is the standard deviation of the difference signal $\sigma(r)$ is the standard deviation of the regular signal

Table 2-8 shows the statistical condition indicators used when vibration is analysed. The same indicators can be applied to temperature. Gouws (2007) presents the time-domain features listed in Table 2-8 that can be applied to all other parameters. The EO and ER are not included Gouw's list (2007).

2.4.2.2. UNIVARIATE TIME SERIES MODELS

As explained in Section 1.2.2, the study will focus on analysing time series data. There are three main groups of univariate time-series models which are widely present in literature, namely, AR, moving average (MA) and autoregressive moving average (ARMA) processes. Another group is a non-stationary model, an autoregressive integrated moving average (ARIMA).

Autoregressive models are used to approximate underlying parameter behaviour (Zhang *et al.*, 2004). An example of an AR model is given in Equation 2-2:

$$y(t) = a_0 + \sum_{k=1}^p a_k x(t-k) + \varepsilon \quad (2.2)$$

Where:

- $y(t)$ is the observed parameter, e.g., temperature and vibration
- p is the order of the equation
- k is the time delay
- ε is the Gaussian white noise with zero mean and standard deviation σ

There are a few different methods available to determine the model coefficients, a_k , $k = 0, \dots, p$. The Yule-Walker is one method used to determine the type of method and requires solving using the Levinson-Durbin recursion (LDR) (Wang & Wong, 2002). Selecting the appropriate order of p is essential for a good model fit, because a large p over-fits the data and a small p under-fits the data.

An approach to determine the model order is the Akaike Information Criterion (AIC) (Zhang *et al.*, 2004). The optimal model order can be obtained by minimising the AIC below:

$$AIC(k) = \log(\sigma_k^2) + 2k \quad (2.3)$$

In the LDR, the error powers ($p_k = \sigma_k^2$) are for all AR models. This means Equation 2-3 is rewritten as Equation 2.4 below:

$$AIC(k) = \log(p_k) + 2k \quad (2.4)$$

The first term will decrease with an increase in the order (k), while the second term will restrict an increasing order. The predicted signal can then be calculated with Equation 2-5:

$$\hat{y}(t) = a_0 + \sum_{k=1}^p a_k y(t - k) \quad (2.5)$$

The difference between the actual and the model is calculated using the Equation 2.6:

$$e(t) = y(t) - \hat{y}(t) \quad (2.6)$$

$e(t)$ is the calculated residual that will follow an independent and identically distributed (IID) normal distribution. An estimated probability density function of the residual distribution can be plotted and be analysed. If the condition of the equipment changes, the change will result in a changed residual distribution, which will reflect in a change in variance or mean shift.

Schlechtingen & Santos (2010) found that AR models yield accurate results for modelling temperature of bearings in wind turbines. The large mass of the motor casing around the bearings cause bearing temperature to have a high autocorrelation (Schlechtingen & Santos, 2010).

Wang & Wong (2002) states that an AR(p) (AR model with the order p) model built on a stationary process will be able to predict stationary processes that are of the same family. Thus, a model will be used to make accurate predictions for any processes that are not related.

2.4.2.3. AUTOREGRESSIVE RESIDUAL ANALYSIS

AR models are used to model stochastic data to detect changes and predict future values based on a weighted sum of past values (Wang & Wong, 2002; Zhang *et al.*, 2004). The difference between the AR model's prediction and the actual value is defined as the AR residual. AR residual analysis is a method used to analyse the natural disturbance of equipment (Guo *et al.*, 1998).

Baillie & Mathew (1996) compared three different AR modelling techniques namely, back-propagation neural networks, radial basis functions and traditional linear AR models. The back-propagation neural network and radial basis functions are non-linear and the Box Jenkins model is linear. Baillie & Mathew (1996) fitted the models to a time series vibration of a rolling element bearing for various signal lengths. The study found that the back-propagation neural network outperformed both the radial basis functions and the linear regressive AR model.

Artificial neural networks (ANNs) are considered an attractive option for diagnostics as these networks offers excellent pattern recognition and classification abilities (Marais *et al.*, 2015). Baillie & Mathew (1996) consider ANNs to be more complex than linear models.

Statistical methods and ANNs are becoming commonly used to detect patterns that can aid in fault diagnosis and prognosis (Baillie & Mathew, 1996). Schlechtingen & Santos (2010) did a comparative analysis of neural network and regression based, or AR, condition monitoring approaches for wind turbine fault detection. The study applied three different developed models to five measured faults and anomalies. The wind turbine's monitoring system includes the following developed signals:

- Power output
- Generator bearing temperature
- Generator stator temperature
- Generator slip ring temperature
- Shaft speed
- Gearbox oil sump temperature
- Gearbox bearing temperature
- Nacelle temperature

Two catastrophic generator bearing failures occurred on a 2 MW offshore wind turbine. The anomalies were detected on the bearing temperature parameter. Both failures occurred on the same machine and both occurrences required a bearing replacement. Figure 2-13 shows the monitored bearing temperature. The two catastrophic bearing damages and the period used to train the ANN are illustrated in Figure 2-13.

Bansal *et al.* (2005) used neural networks in a predictive maintenance system. The study found that the accuracy of the predictive maintenance system is a direct function of the validity of the simulated data used to train the neural network. The neural network required a large amount of data to be trained (Bansal *et al.*, 2005). This is a disadvantage for data infrastructure that cannot handle such an amount of data to train the model.

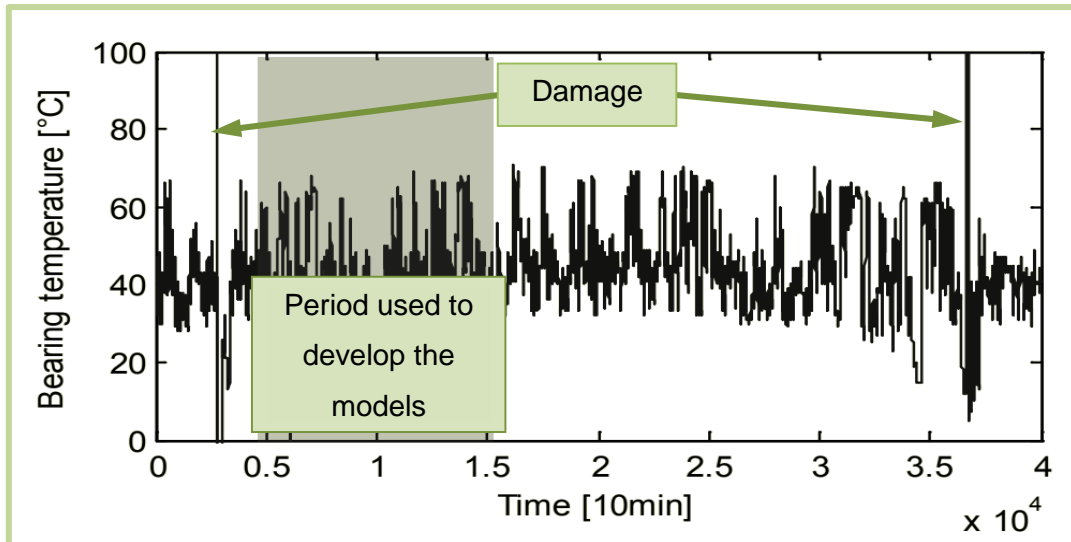


FIGURE 2-13 BEARING TEMPERATURE EVOLUTION WITH THE TWO DAMAGE OCCURRENCES AND THE PERIOD USED TO DEVELOP THE MODEL
(SCHLECHTINGEN & SANTOS, 2010)

2.4.3. VERIFICATION AND VALIDATION

To validate the aforementioned models, analysing the statistics have been shown to be an effective technique (Kleijnen, 1999; Sargent, 2012). Sargent (2012) defined a list of 17 techniques used to validate simulation models. Examples of the proposed techniques that is used in this study include: comparison to other models, historical data validation, parameter variability-sensitivity analysis, internal validity and predictive validation. A combination of these techniques is generally used to verify and validate subsequent models and the overall model (Sargent, 2012).

Five of the techniques that Sargent (2012) defined can be implemented for the verification and validation process to accommodate the available data and model used in this study. These techniques are: animation, historical data validation, parameter variability-sensitivity analysis and internal validity. The techniques are briefly described below:

Animation: Graphically display the model's operational behaviour. Kleijnen (1999) describes animation as the face validity of the statistical analysis. Face validity is the capability of an individual to determine if the model's input and output relationship is reasonable. In this case, the developed model and the actual values can be shown on a control chart. Sargent (2012) classifies face validity as a separate validation technique. The animation of a real-time control chart will ease the face validation.

Historical data validation: The model is applied to available historical data and is tested to the behaviour of the system. In this case, to test if the model can predict faults that were experienced in practice.

Parameter variability - sensitivity analysis: This technique involves the changing of the values of the input and internal parameters of the model to determine the effect on the model's behaviour. The observed behaviours of varying the parameters should be the same in both the model and real system.

Internal validity: Replicating results of the chosen stochastic model and analysing the stochastic variability of the results. A large variability spread may cause the model's results to be questionable.

Predictive validation: Using the model to predict the system's behaviour and comparing the model's forecast to the actual system behaviour can give an indication of the model's accuracy.

The above-mentioned techniques are used in Chapter 3 to determine the operational validity of the model. Operational validation is the process of determining whether the model's output is accurate enough for the intended purpose.

Two approaches can be followed to assess the operational validity of the model, namely a subjective approach or an objective approach. Sargent (2012) classifies the two approaches into an observable and non-observable systems in Table 2-9.

TABLE 2-9 OPERATIONAL VALIDITY CLASSIFICATION

Decision approach	Observable system	Non-observable system
<i>Subjective approach</i>	<ul style="list-style-type: none"> • Comparison using graphical displays • Explore model behaviour 	<ul style="list-style-type: none"> • Explore model behaviour • Comparison to other models
<i>Objective approach</i>	<ul style="list-style-type: none"> • Comparison using statistical tests and procedures. 	<ul style="list-style-type: none"> • Comparison to other models using statistical tests

Referring to Table 2-9, an observable system means that it is possible to collect data on the operational behaviour of the problem entity. 'Comparison' means the comparison to either the model and the system output or another model or statistical tests and procedures. 'Explore

model behaviour' means to analyse the output behaviour of the model using a sensitivity analysis.

To determine accuracy of the AR model, the model's prediction is statistically compared to the actual value. Common statistical measures are used indicate the model's accuracy include (Devore & Farnum, 2005):

- Residuals or explained variance (EV)
- Root mean square error (RMSE)
- Mean absolute error (MAE)
- Residual sum of square (RSS)
- Coefficient of multiple determination (R^2)

The calculation methodology of the above-mentioned statistical evaluation parameters is provided in Appendix C. Another statistic used the p-value, or observed significance level, which aids to determine the significance of a variable in a model. The null hypothesis, H_0 , is the hypothesis that the modelled data is a representation of the actual data. If the desired significance level, α , is the probability of a type I error to occur then the following applies:

- Reject H_0 if p-value $\leq \alpha$
- Do not reject H_0 if p-value $> \alpha$

Thus, a smaller p-value indicates a more statistically significant model. Statistically a condition monitoring system can give two types of errors, type I error and type II error. A type I error occurs if a fault is triggered under healthy conditions and a type II error occurs if a healthy condition is reported when a fault exists. If one of these errors occur, the integrity of the condition prediction system is questioned.

Another statistic proposed by Yang *et al.* (2013), the condition monitoring criterion, c , is calculated using Equation 2.7.

$$c = \frac{\int_{x_{min}}^{x_{max}} \sum_{j=0}^k |(a_j - b_j)x^j| dx}{x_{max} - x_{min}} \quad (2.7)$$

Where:

- a_j and b_j represent the coefficients of the models derived respectively from present and historic data.
- x_{max} and x_{min} are respectively the maximum and the minimum values of x .

From Equation 2.7 it can be inferred that $c \approx 0$ when the equipment is healthy while $c > 0$ if there is fault. The more serious the fault the larger the value of c tends to be.

Yang, *et al.* (2013) states that the significance of the fault-related features (temperature, vibration, etc.) is dependent on the load of the equipment. By using the evaluation criterion, c , the issue has been mitigated by the integral calculation. Defining the threshold for c is imperative to good fault detection (Yang *et al.*, 2013).

2.5. CONCLUSION

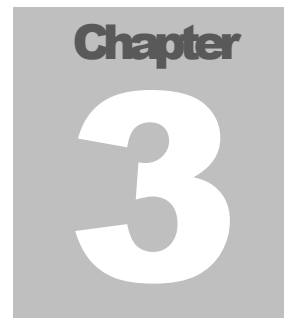
Minimal literature concerning the implementation or methodology of a condition monitoring of equipment in the South African mining industry is available. The South African mines from the two case studies have the necessary infrastructure to implement a preventative maintenance strategy, or already have a preventative maintenance strategy in place. The data is not readily processed to automatically detect changes and have to be pre-processed.

AR residual analysis detects the natural disturbance of process (Guo *et al.*, 1998). This analysis method has been shown to be effective to predict faults in helicopter transmission gears and to detect unusual vibrations in bridges. Wang & Wong (2002) states that an AR(p) (AR model with the order p) model built on a stationary process will be able to predict stationary processes that are of the same family. Hence it can be used to develop a generic baseline to accommodate different machines and sizes.

The AIC is an estimator used to determine the best fit models. The best fit model is determined by calculating the AIC for different model orders and by choosing the smallest result. The AIC makes use of the MLE statistical method.

Only a few studies considered low sample rates as input parameter to the model. Low sample rates of 10 minutes are considered. A low sample rate of 10 minutes is considered too low for accurate fault detection (Večeř, Kreidl & Šmíd, 2005; Yang *et al.*, 2014). These studies did not evaluate changes over a longer period.

Analysing statistics has been shown to be an effective technique to validate a model (Kleijnen, 1999; Sargent, 2012). Five techniques are chosen for the validation, namely: Animation (face validation), sensitivity analysis, historical data validation, internal validity and predictive validation. An objective approach will be followed by using statistical test procedures.



**ALTERNATIVE METHOD FOR EQUIPMENT
CONDITION MONITORING ON SOUTH AFRICAN MINES**

CHAPTER 3

MODEL DEVELOPMENT

3. METHOD DEVELOPMENT

3.1. INTRODUCTION

The methodology and reasoning behind the method development is presented in Chapter 3. The data acquisition and evaluation is explained in Section 3.2. A method to analyse equipment’s idling, or resting, temperature is proposed. The model choice and AR residual analysis methodology is explained in Section 3.3. The model verification and validation is discussed in Section 3.4.

3.2. DATA ACQUISITION AND EVALUATION

Pre-processing of data includes the classification into three different states: operational, idling and erroneous data. The classification allows for more accurate data analysis of the available data. The acquisition and evaluation of the data will be explained using example case studies.

3.2.1. OVERVIEW

As an example case study, a typical data sample of a 1.8 MW centrifugal pump is used to evaluate the quality of the data. Figure 3-1 and Figure 3-2 shows the half hourly averaged vibration and temperature of the multistage centrifugal pump.

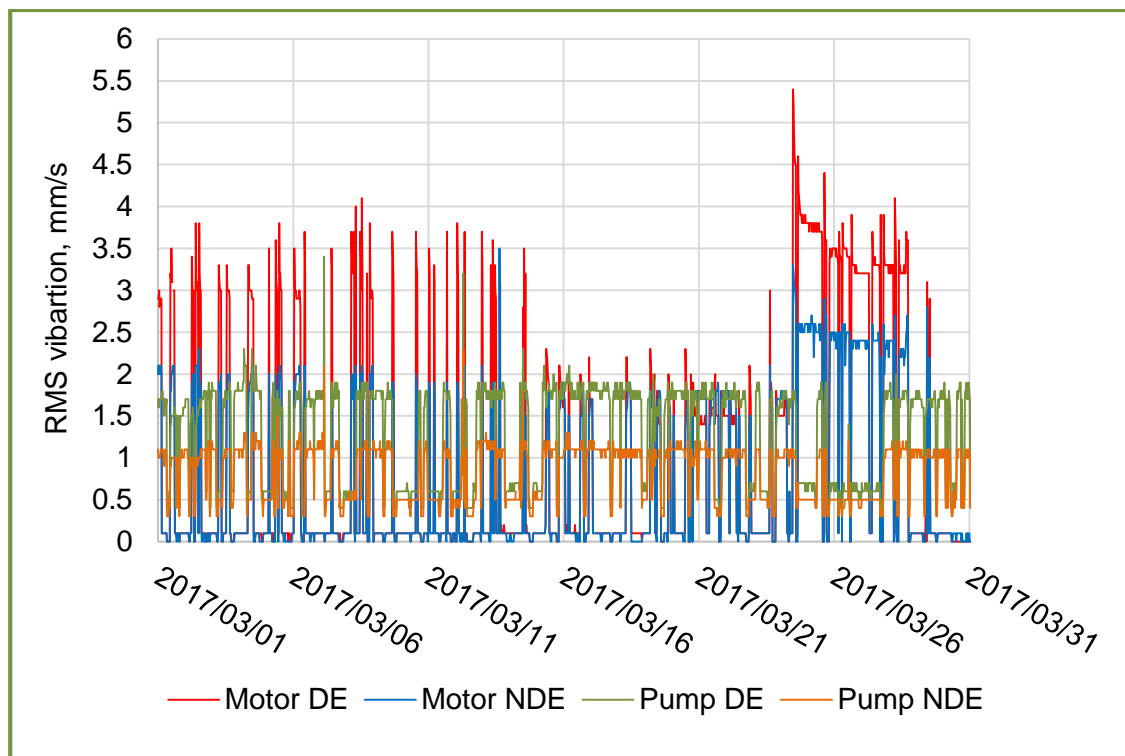


FIGURE 3-1 DEVELOPED VIBRATION SIGNALS OF A MULTISTAGE CENTRIFUGAL PUMP

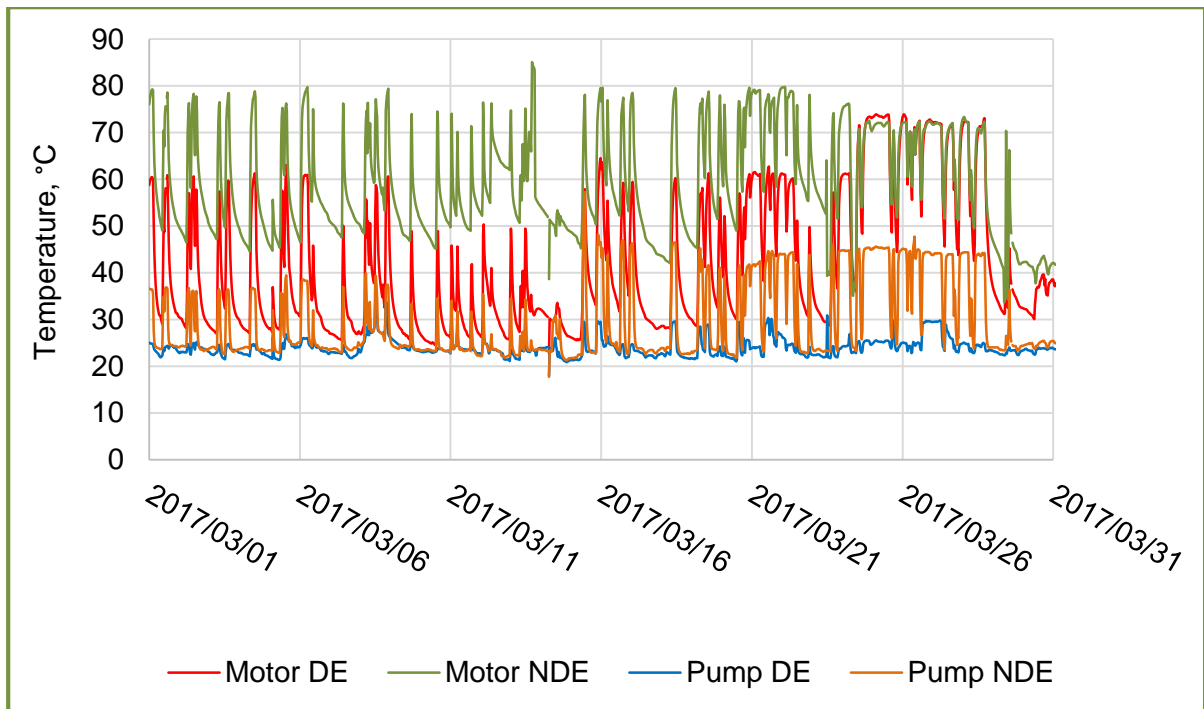


FIGURE 3-2 RAW BEARING TEMPERATURE DATA FOR A MULTISTAGE CENTRIFUGAL PUMP

Figure 3-1 and Figure 3-2 shows the half hourly RMS vibration and temperature respectively. From both figures, vibration and temperature spikes are observed. The pump is switched off during Eskom's peak demand periods to reduce the cost of electricity, which is the cause of the spikes.

3.2.2. ACQUISITION AND EVALUATION

Data acquisition is a basic requirement of condition monitoring. The lack of data can be a hindrance to monitor the condition of equipment and processes. Large amounts of data have to be analysed over different time intervals for accurate fault detection and condition monitoring. The data capturing methodology described in Section 1.3.3, which states that the data is only available in half hourly intervals.

SCADA historians can store data to an accuracy of 1 ms (Schneider Electric Software, 2016). All historian databases in this study use the delta storage method which stores the data values only if a change occurs. For this study, the data is retrieved from the historian using the cyclic retrieval mode which only retrieves data values that occur at a specific time interval (Schneider Electric Software, 2016).

The half hourly data for this study is retrieved from the historian using the cyclic method described by Schneider Electric Software (2016). In short, cyclic retrieval is the retrieval of stored data based on the specific cycle resolution of the stored data. The retrieved data may

not correspond to the actual stored data but is an adequate representation for the retrieval interval.

Half hourly data extraction intervals make the acquisition of the data practical with the disadvantage of losing detail information. An advantage of using larger sample intervals is that data that is available in smaller intervals can be processed to larger intervals. By doing so, the data processing using the larger intervals can be standardised and will be easy to implement on different types of equipment. The data acquisition interval constraint is unfavourable for the purpose of immediate fault detection, so the aim of the model is to detect changes in the shortest time possible.

For the example case study, 0.3% of the data has been lost. The lost data is excluded in the model fitting procedure. Data loss can have an effect on the AR model output and order selection. The model order is determined by minimising the AIC. The calculation of the AIC is described in Section 2.4.2.2. Since the AR model is dependent on the previous time step value, the prediction of the future value will be affected.

To ensure the data is representative, it is classified into three modes: operational, idling and disregarded data. The equipment's operating status is required for the classification procedure. The operation status classifier is illustrated in Figure 3-3.

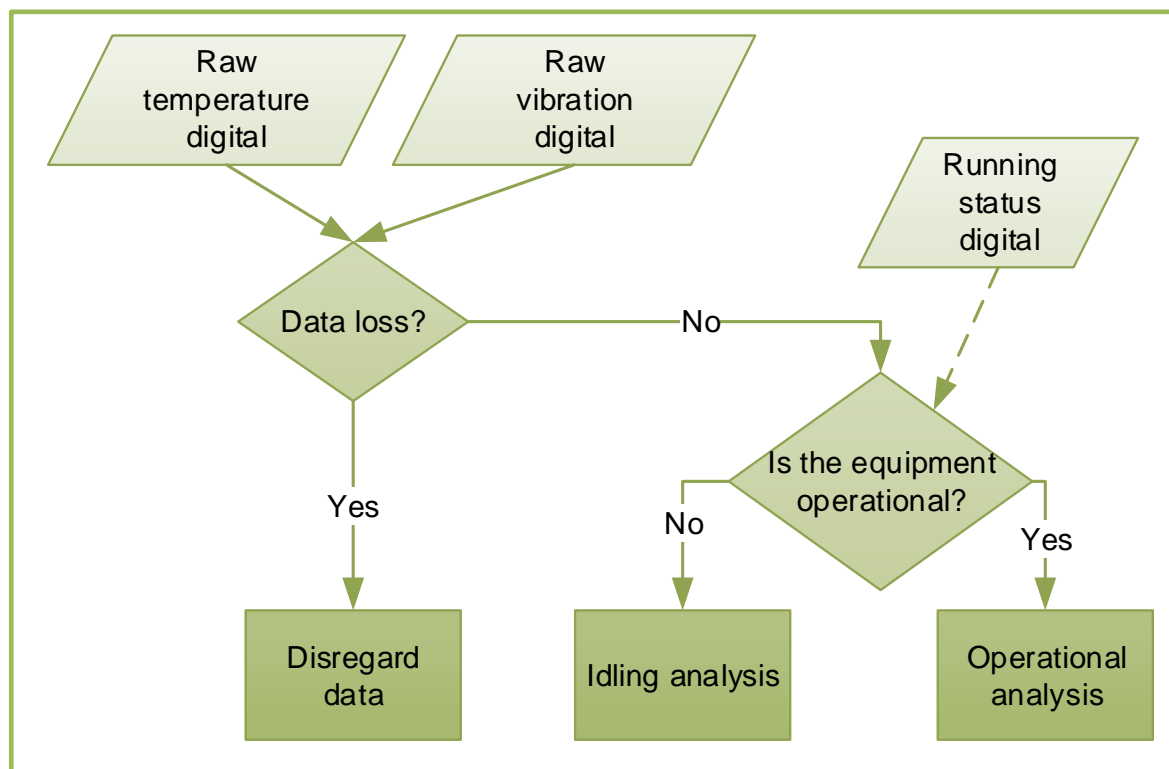


FIGURE 3-3 RUNNING STATUS CLASSIFIER

Referring to Figure 3-3, the classifier splits the data into operational and idling modes and disregards the lost data. The running status is retrieved from the historian database using the cyclic retrieval mode, resulting in a returned value between or equal to one or zero. If the value falls between zero and one, the data is disregarded. Using the proposed running status classifier, it is expected that the number of type I errors is reduced.

3.2.3. IDLING ANALYSIS

Analysing the idling temperature and vibration of the machine can give information of the specific temperatures and vibrations while the equipment is in idle mode or not in working order. In underground operations, the temperatures of air surrounding the pumps in the same pump station can vary significantly if the ventilation is insufficient. This means that the normal operating conditions vary for each specific pump and should be taken into consideration in the fault detection step.

The temperature, after the rate of cooling is equal to or less than a specified amount, can give an indication of the ambient temperature. The method to estimate the ambient air temperature will only be feasible if there is no external cooling source. The method is illustrated in Figure 3-4.

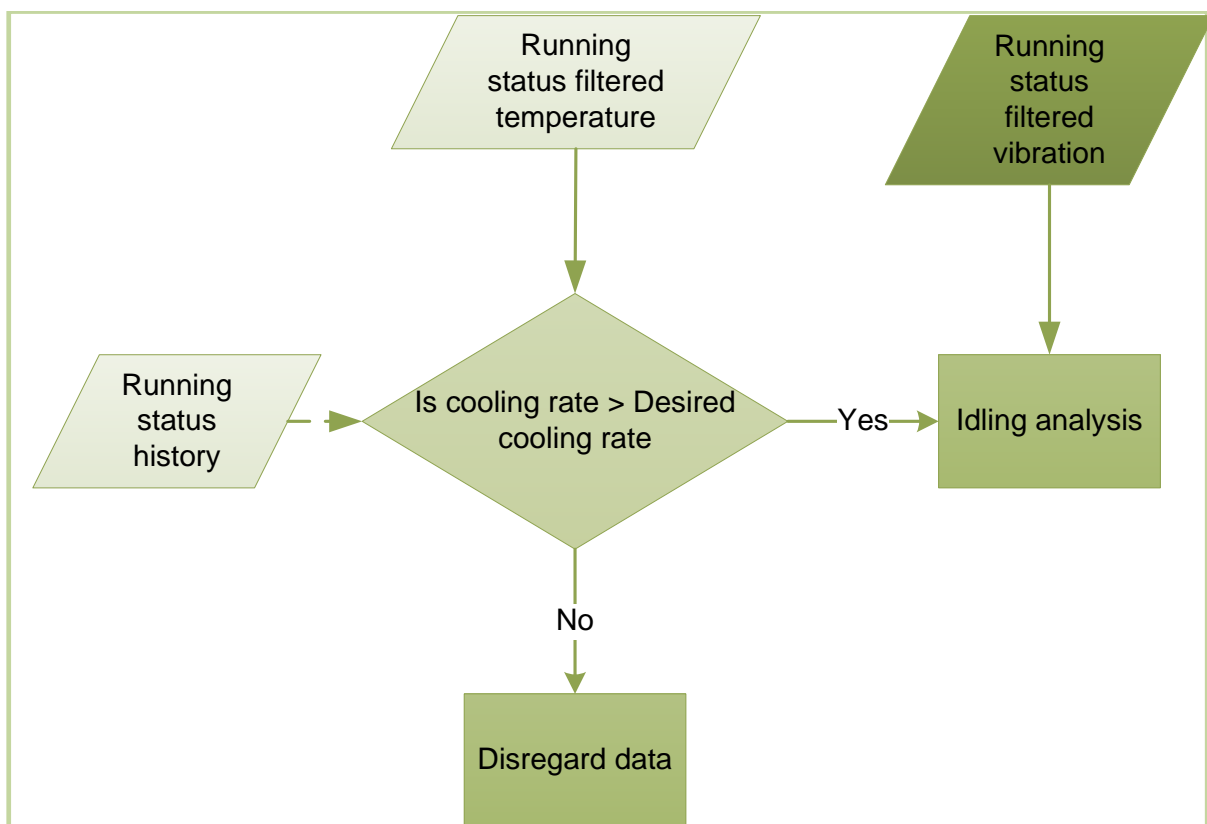


FIGURE 3-4 DETERMINING IDLE TEMPERATURE OF THE EQUIPMENT

By specifying a desired cooling rate, the temperature data can either be ignored or be analysed in the idling analysis. This classification process will only be significant for temperature analysis. The idling analysis will reveal information of the ambient condition of the equipment. It will be useful in underground mines to passively determine if the ventilation or cooling mechanisms are sufficient.

Figure 3-5 shows the relationship of a bearing temperature of a wind turbine generator bearing to the ambient temperature and active power (Wiggelinkhuizen *et al.*, 2007).

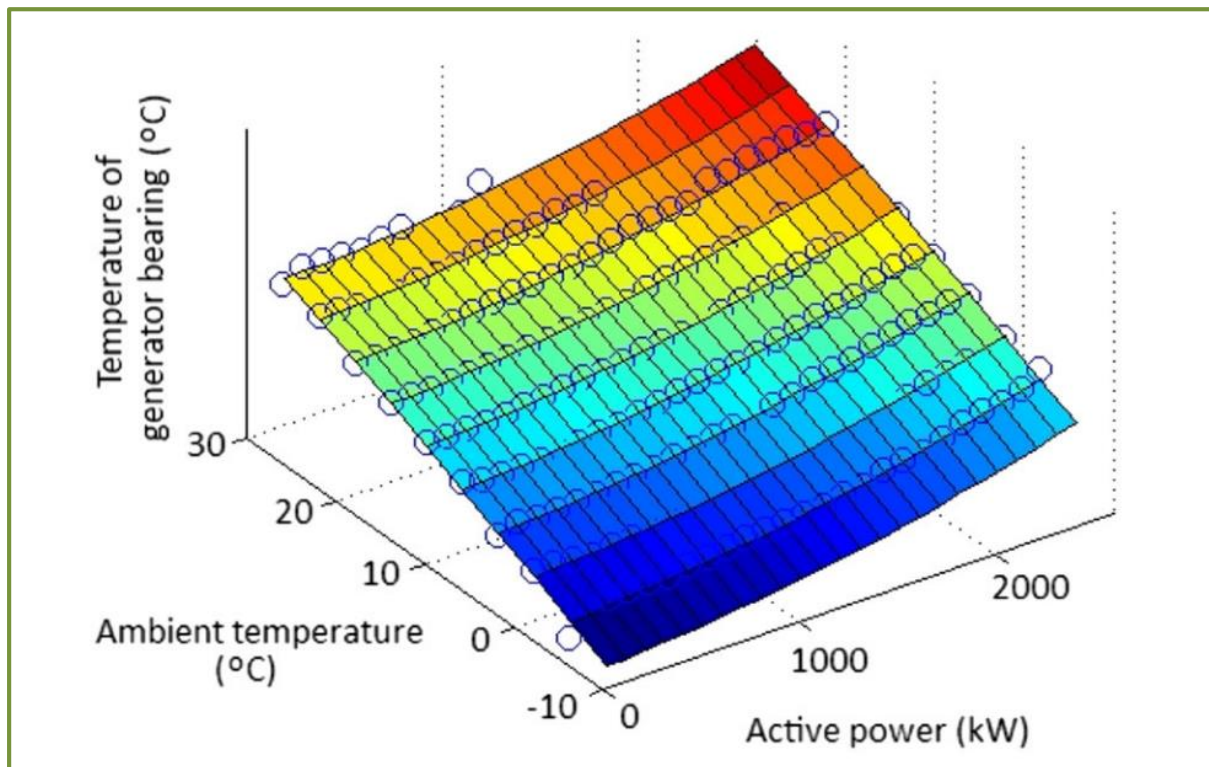


FIGURE 3-5 TEMPERATURE OF A WIND TURBINE GENERATOR BEARING VS. AMBIENT TEMPERATURE AND ACTIVE POWER (WIGGELINKHUIZEN *ET AL.*, 2007)

Figure 3-5 shows that the ambient temperature and power output affects the temperature of a wind turbine generator bearing. Hence, if the ambient temperature is monitored, a more accurate prediction of the losses to heat losses can be estimated. If the ambient conditions are not monitored, the temperature of an idling machine can be used to estimate the idling temperature. An example of the temperature of a machine that is not running is presented in Figure 3-6. Figure 3-6 shows NDE bearing temperatures of a centrifugal pump after has been stopped.

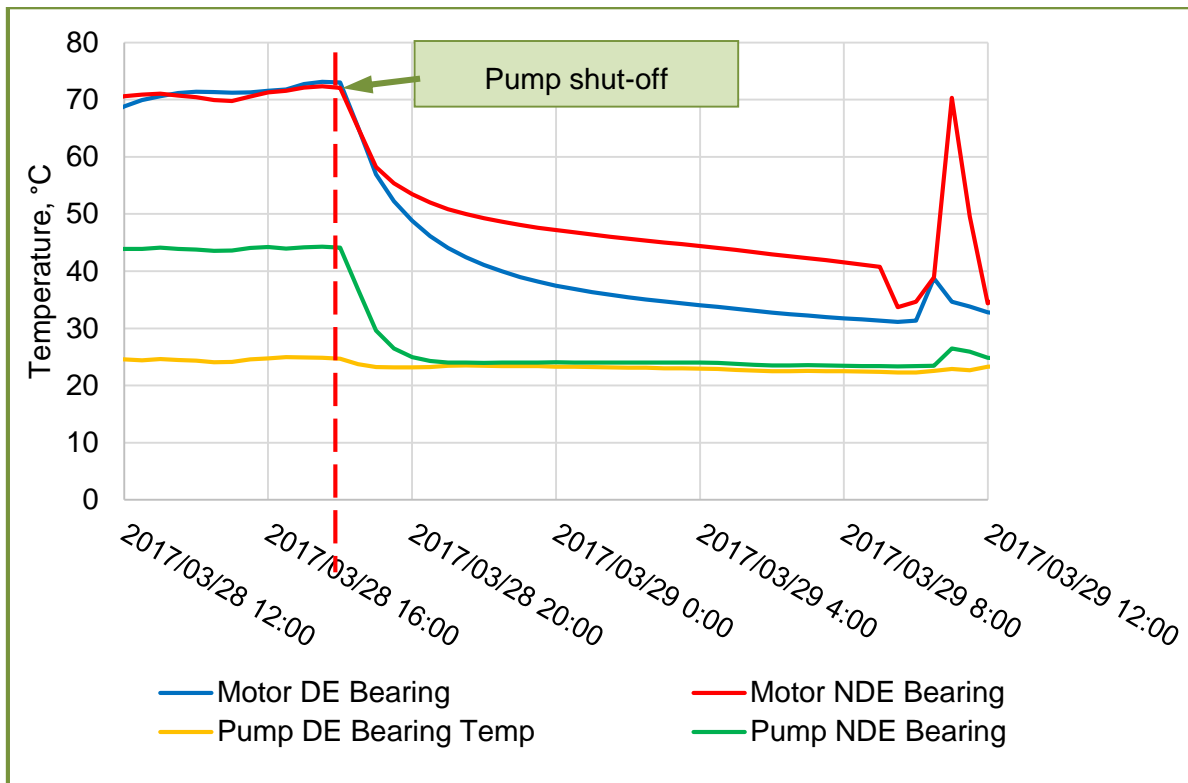


FIGURE 3-6 COOLING RATE OF A MULTISTAGE CENTRIFUGAL PUMP

Figure 3-6 illustrates the declining temperature of the pump and motor when the pump is switched off at 18:00 on 28 March 2017. The motor is only cooled by ambient air if the pump is switched off. The minimum temperature of all the data points is 22.3 °C, thus, it can be assumed that the ambient air temperature for the measured period is lower than 22.3 °C for this specific pump. Using this information, the specific pump alarm limit can be adjusted accordingly to accommodate abnormal ambient temperatures.

3.3. DEVELOPMENT OF METHOD

3.3.1. DESIGN REQUIREMENTS

The method has certain criteria that needs to be adhered to in order to ensure practicality and accuracy as mentioned in the problem statement described in Section 1.5.1. The design requirements are given below and will allow the implementation of the model to be practical and cost effective. The method should:

- Operate automatically
- Analyse multiple systems
- Make use of existing infrastructure
- Continuously evaluate the system
- Provides simple feedback that leads to swift actions being taken

In order to reach these design requirements, the key parameters are evaluated to ensure an accurate and practical method is implemented.

3.3.2. KEY PARAMETER SELECTION

According to Zhang *et al.* (2004) the selection of parameters sensitive to the condition of the equipment is critical for condition diagnosis and prognosis. Only the core parameters will be used to develop the method to keep the method as simple and generic as possible while keeping it applicable to different machines. A list of monitored parameters is given in Figure 3-7 and Figure 3-8.

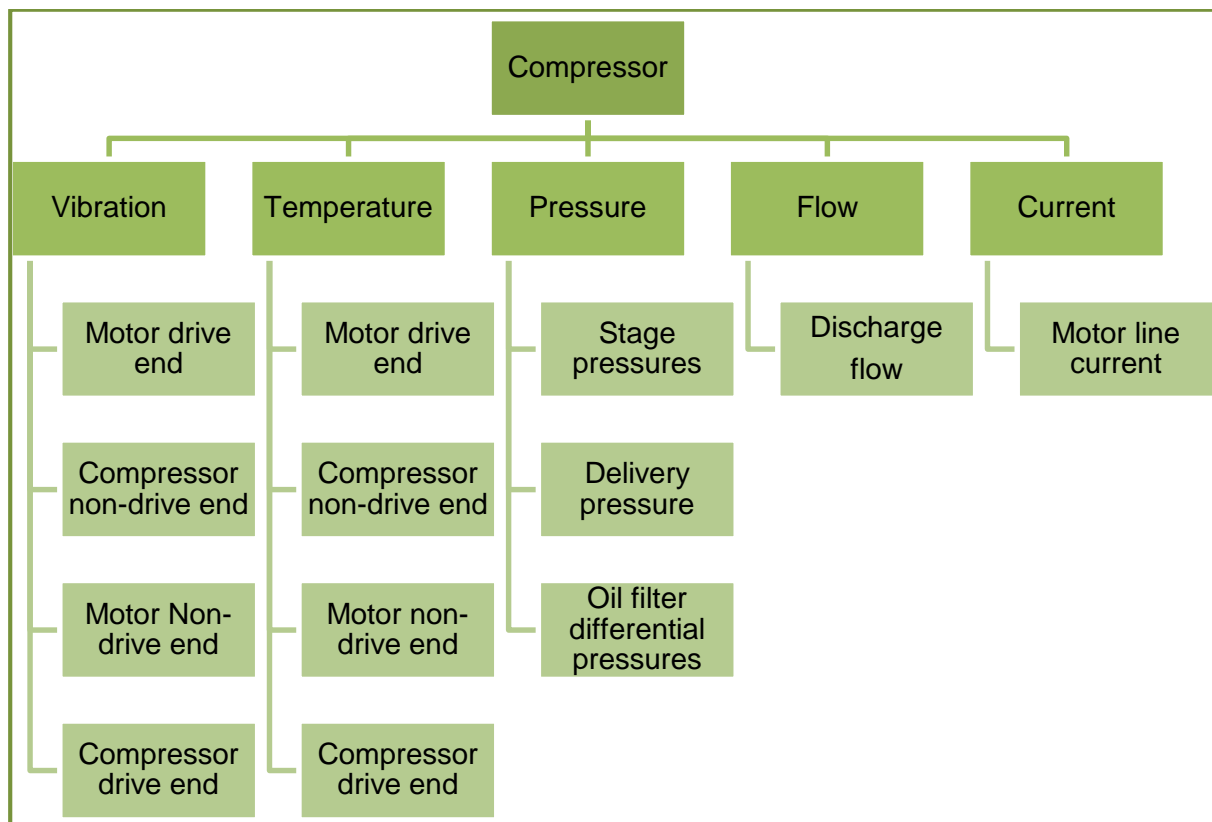


FIGURE 3-7 MULTISTAGE CENTRIFUGAL COMPRESSORS MEASURED PARAMETERS

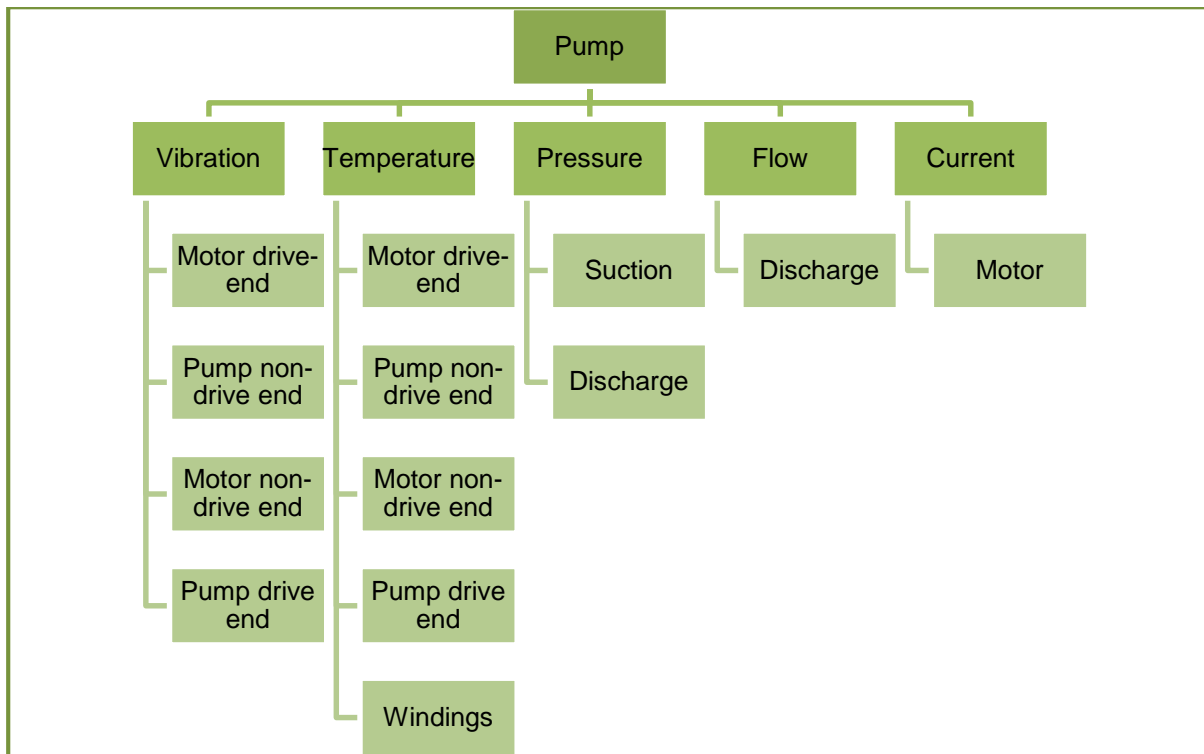


FIGURE 3-8 MULTISTAGE CENTRIFUGAL PUMP MEASURED PARAMETERS

Figure 3-7 and Figure 3-8 shows the available parameters that are monitored of the equipment in the case study. In this study, the parameters used include temperature, vibration and performance parameters. The selection of the AR model input parameters are discussed in Sections 3.3.2.1 to 3.3.2.3.

3.3.2.1. TEMPERATURE

Temperature logs are not required at such a high sample rate as vibration because the heat transfer rate is slow in comparison to the rate of vibration energy change. Temperature has been shown to have high autocorrelation with machines that have large mass that surrounds the measured component (Schlechtingen & Santos, 2010), hereby motivating the use of temperature as a key parameter for AR modelling.

3.3.2.2. VIBRATION

Vibration is usually analysed at high frequencies. A maximum RMS vibration value is available in a half hourly resolution for this study. Many studies use vibration analysis methods to determine the condition of rotating machinery. These analysis methods use high sample rates which is not available in this study and therefore those techniques cannot be used (Jardine *et al.*, 2006; Krauel & Weishäupl, 2016).

Krauel & Weishäupl (2016) states that Fourier transformations are used to describe oscillating behaviour and can easily give erroneous results if the sample rates are too low. Yang *et al.*

(2014) also considers a sample rate of ten minutes too low for accurate fault diagnosis on a similar rotating machine.

3.3.2.3. PERFORMANCE PARAMETERS

Performance parameters also give an indication of the condition of the equipment and how it can also be used as an input parameter to the monitoring method (Murray, 1989; Yates, 2002; Beebe, 2004). The efficiency of compressors and pumps can be calculated using the parameters listed from the illustrations in Figure 3-7 and Figure 3-8.

To determine if there is a correlation of the performance between the condition and performance indicators the vibration of the machine is plotted versus the power consumption in Figure 3-9. The compressor in the example is one compressor in a series of five compressors that has a common discharge manifold. The measured performance parameters include the guide vane position, power and the manifold's flow, and pressure which are available.

The guide vane position and compressor combination is constant. The outlet manifold pressure varied between 240 and 376 kPa. In this case, the performance parameter is chosen to be power. The vibration of the compressor motor is plotted versus the power consumption in Figure 3-9.

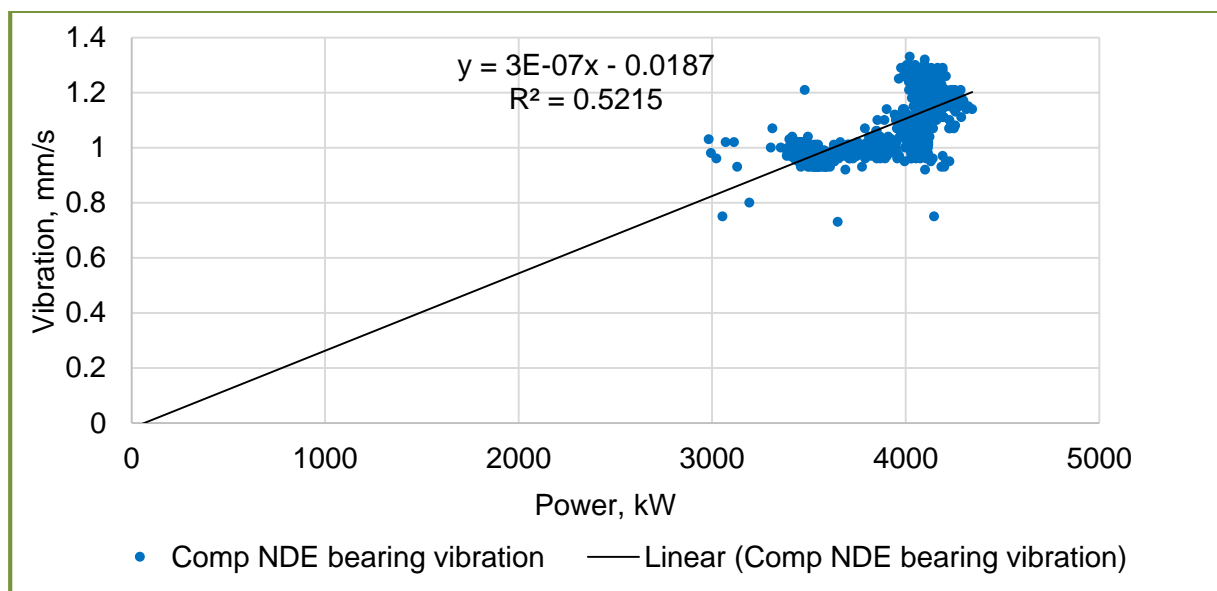


FIGURE 3-9 COMPRESSOR VIBRATION VERSUS POWER CONSUMPTION

Figure 3-9 shows the relationship of vibration versus the power. According to Devore & Farnum (2005) the correlation coefficient, $R = 0.722$, or coefficient of determination, $R^2 = 0.5213$ suggests a moderate positive relationship between the power and the vibration.

Another vibration-performance correlation example is shown in Figure 3-10. The NDE vibration is plotted versus the efficiency of the pump. The efficiency of the pump is calculated using the Equation 2-1 which is a function of the temperature and pressure increases over the pump (Murray, 1989; Beebe, 2004).

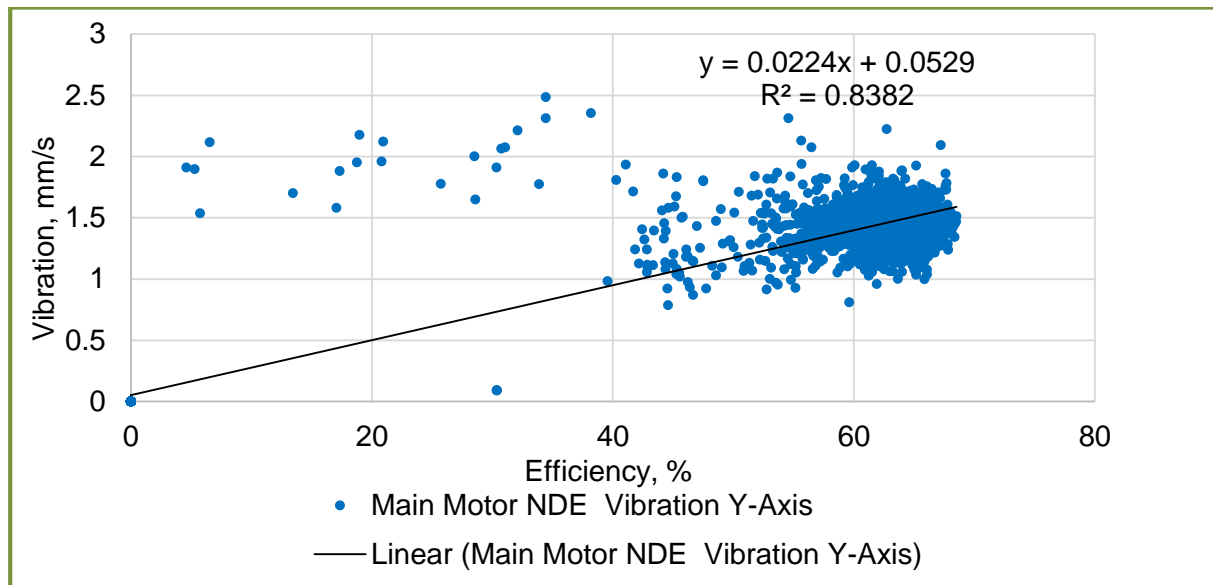


FIGURE 3-10 CORRELATION BETWEEN PUMP EFFICIENCY AND VIBRATION

Figure 3-10 shows the vibration plotted versus the efficiency. The data consists of 3327 data points. The high coefficient of correlation $R^2 = 0.84$ suggests a strong positive relationship (Devore & Farnum, 2005). The collected data points only show the machine under normal operating conditions.

Correlation is a measure of association, but association does not imply causation (Devore & Farnum, 2005). Factors such as the number of start-up and shutdown, cavitation can have an effect on the linearity of the data. No definitive conclusion is drawn from the correlation of the condition monitoring parameters and that the performance parameters.

3.3.3. MODEL TYPE

Baillie & Mathew (1996) recommend linear AR models for when data is freely available and if a simple system is desired. Schlechtingen & Santos (2010) found that AR models yield accurate results for modelling temperature of bearings in wind turbines. The large mass of the motor casing around the bearings cause a high autocorrelation of the bearing temperature signal (Schlechtingen & Santos, 2010). Assuming most large electrical equipment such as compressors, pumps and fans have similar heat dissipation rates, an AR model can be used to model the temperatures of the equipment. The performance of AR residual analysis with the temperatures of different types of equipment will be analysed in this study.

3.3.4. METHOD DEVELOPMENT

3.3.4.1. METHOD OVERVIEW

An overview of the condition monitoring method is given in Figure 3-11. The method development will follow the flowchart provided in Figure 3-11. The overview is based on the work of Ogidi *et al.* (2016) developed for the monitoring of the condition of wind turbines. This method is based on the real-time condition analysis. It prioritises the comparison of parameter data to set alarm and trip limits and employs the condition analysis method.

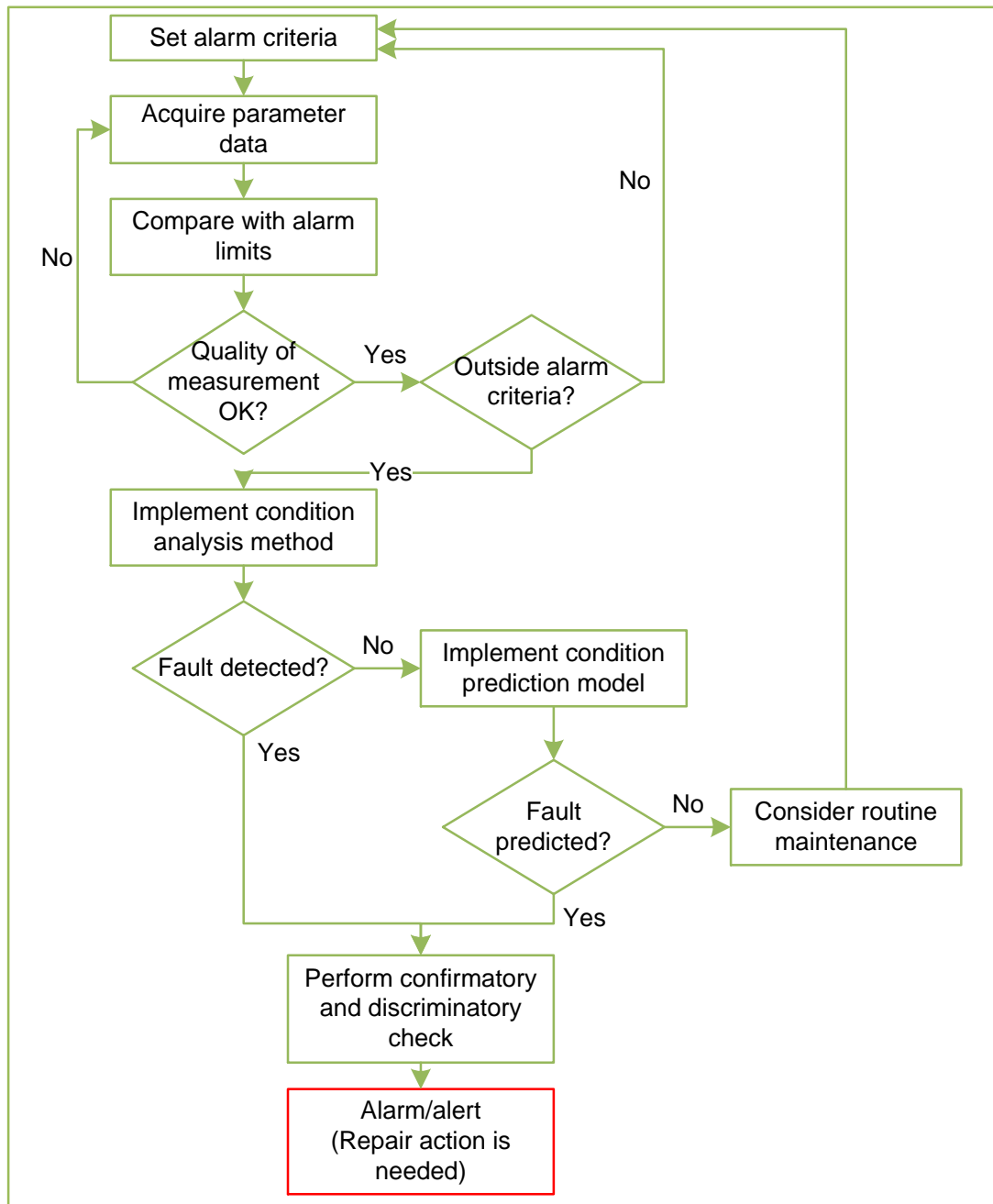


FIGURE 3-11 FLOWCHART FOR FAULT DETECTION AND CONDITION PREDICTION

3.3.4.2. TRIP AND ALARM LIMITS

Referring to the flowchart in Figure 3-11, the first step is to set alarm criteria for the pump. The alarm and criteria for a centrifugal pump on Mine A is given in Table 3-1. The pump trip values are added to Table 3-1 as a reference to show what is considered too high.

TABLE 3-1 ALARM AND TRIP LIMITS OF A CENTRIFUGAL PUMP

Instrument	Input	Alarm	Trip	Unit
<i>Motor NDE Bearing Temperature</i>	Analogue	76	80	°C
<i>Motor DE Bearing Temperature</i>	Analogue	76	80	°C
<i>Motor DE Bearing Vibration</i>	Analogue	4	8	mm/s
<i>Pump NDE Bearing Temperature</i>	Analogue	76	80	°C
<i>Pump DE Bearing Temperature</i>	Analogue	76	80	°C
<i>Pump DE Bearing Vibration</i>	Analogue	4	8	mm/s
<i>Pump Inlet Pressure</i>	Analogue	N/A	1 600	kPa
<i>Pump Outlet Pressure</i>	Analogue	N/A	16 000	kPa
<i>Motor Winding U Temperature</i>	Analogue	115	120	°C
<i>Motor Winding V Temperature</i>	Analogue	115	120	°C
<i>Motor Winding W Temperature</i>	Analogue	115	120	°C
<i>Impeller Displacement</i>	Digital	Manual Setup: 3 mm		Proximity
<i>Balance Disc Flow</i>	Analogue	40	45	l/s
<i>Motor Air Temperature</i>	Analogue	115	120	°C
<i>Motor Shaft Displacement</i>	Analogue	N/A	<2 >8	mm
<i>Column Flow</i>	Analogue	N/A		l/s

Table 3-1 shows the upper trip and alarm limits of the different measured parameters of the pumps in the example. After the alarm criteria has been set, the parameter data is compared to the alarm criteria for an instantaneous check; this check serves as face validation for the alarm criteria. Thereafter a filter is added to ensure that the quality of the data is acceptable.

If the parameter does not exceed the alarm criteria, then the condition is accepted. If the parameter exceeds the trip limit, a confirmatory and discriminatory check is recommended. When the alarm level is exceeded, the condition analysis and prediction model is implemented.

3.3.4.3. MODEL-BASED CONDITION PREDICTION SYSTEM

A flow chart of the AR condition prediction system is given in Figure 3-12. It is adapted from work done by Baillie & Mathew (1996). Baillie & Mathew (1996) illustrates the methodology of the AR model as seen in Figure 3-12.

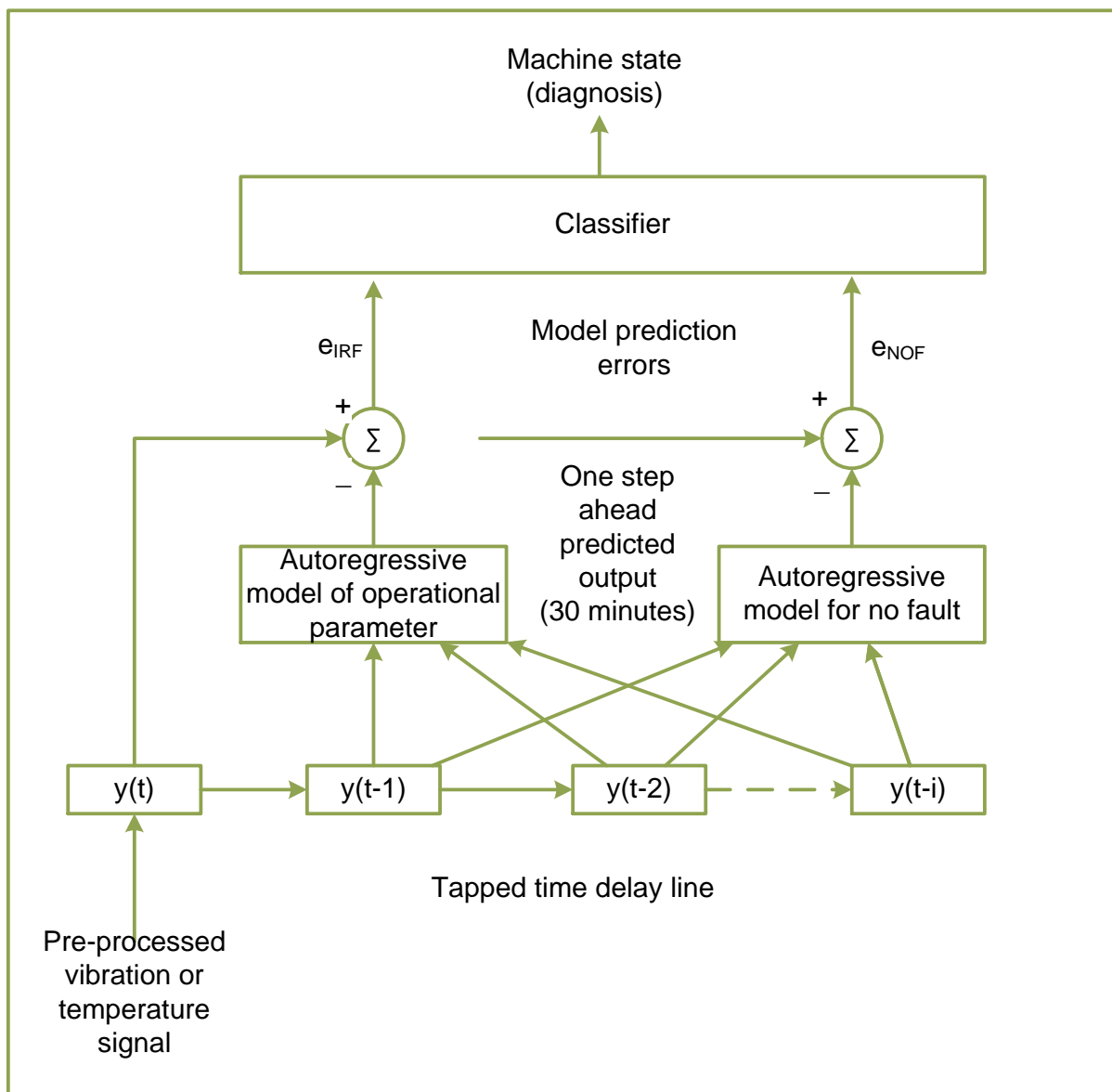


FIGURE 3-12 A MODEL-BASED CONDITION PREDICTION SYSTEM

Referring to Figure 3-12, the model-based prediction system shows how the machine diagnosis is determined. For a first order AR model, AR(1), only one previous data point, namely $y(t - 1)$, is considered. For a second order AR model, two previous data points are used, namely: $y(t - 1)$ and $y(t - 2)$, and so forth. Thus, if the AR model is updated in real-time, the $y(t - i)$ values have to be stored in memory and read to update the model to determine the future value.

Figure 3-12 shows that the residuals, or errors, e_{IRF} and e_{NOF} , are analysed in the classifier to make a machine diagnosis. The error behaviour for temperature is expected to be similar for machines with similar amount of mass around the probe, depending on how the probe is installed.

The AR model is applied in a dewatering pump case study. The AR model was fitted to data developed while the equipment was under normal operation conditions. The temperature of the NDE bearings was modelled for with data of the most reliable pump. A first, second and third order linear AR model was fitted to the temperature data. The three models are shown below:

$$\hat{y}(t) = 0.97 \cdot y(t - 1) + 1.54 \quad (3.1)$$

$$\hat{y}(t) = 1.30 \cdot y(t - 1) - 0.34 \cdot y(t - 2) + 2.06 \quad (3.2)$$

$$\hat{y}(t) = 1.33 \cdot y(t - 1) - 0.51 \cdot y(t - 2) + 0.14 \cdot y(t - 3) + 1.75 \quad (3.3)$$

The calculated AIC, RSS, MLE and the p-value for the AR(1), AR(2) and AR(3) models are given in Table 3-2.

TABLE 3-2 AUTOREGRESSIVE MODEL RESULTS ON CONTINUOUS DATA

	AIC	RSS	MLE	p-value
<i>AR(1)</i>	0.88	25683	12.9	1.50E-09
<i>AR(2)</i>	1.12	22875	11.5	1.23E-71
<i>AR(3)</i>	-1.54	86623	43.4	1.09E-14

From Table 3-2 it is observed that the p-values are small which means that the AR model is statistically significant. The AIC should be minimised to find the best fit. In this case the third order model has the lowest AIC, therefore the third order model is used to model the

temperatures. The actual temperature signal versus the predicted signal is plotted in Figure 3-13. The residuals are plotted Figure 3-14.

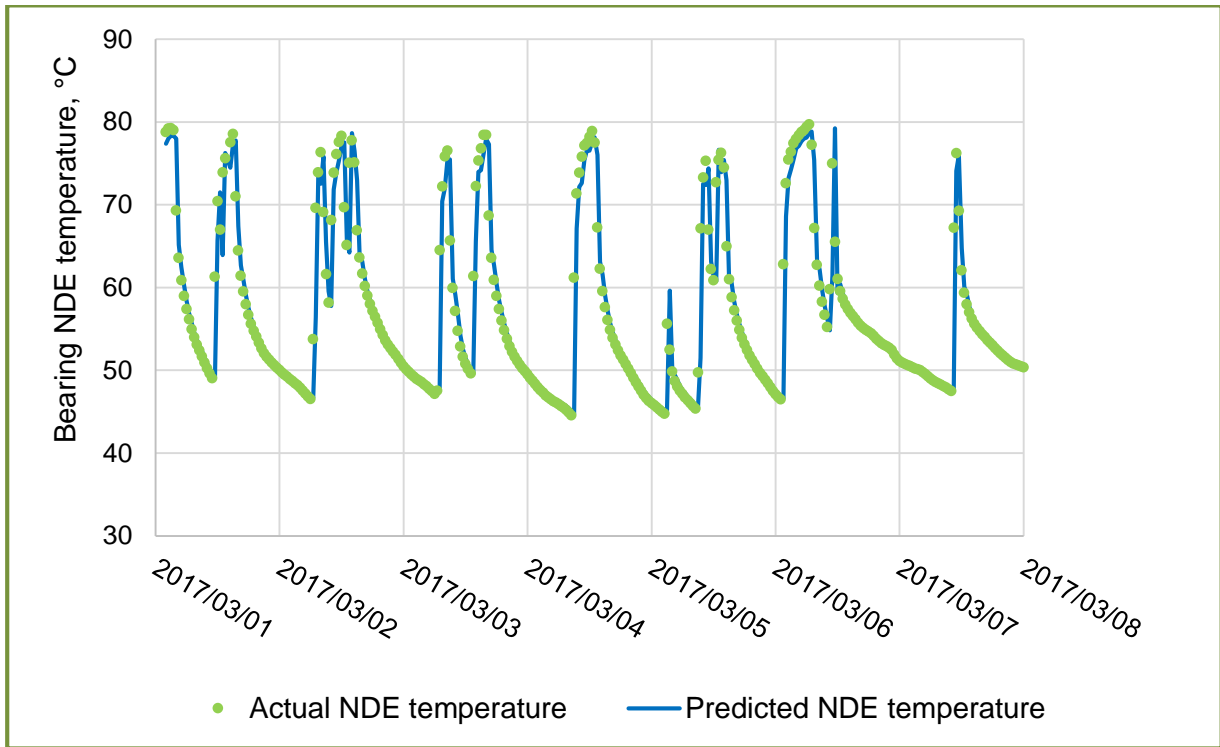


FIGURE 3-13 ACTUAL TEMPERATURE VERSUS AR(3) PREDICTED TEMPERATURE

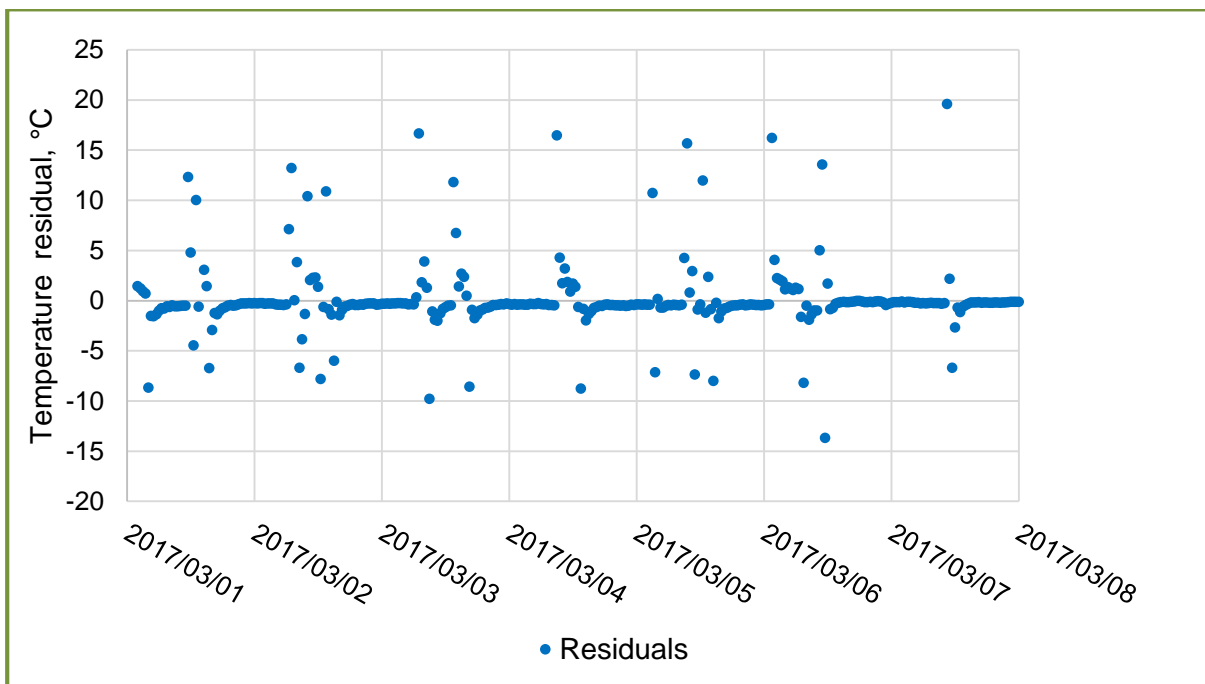


FIGURE 3-14 RESIDUALS OF THE AR MODEL

Referring to Figure 3-13, the AR model follows the trend of the actual temperature. The model's resulting statistics are shown in Table 3-3. Figure 3-14 shows the difference between the actual temperature and the predicted temperature. By comparing Figure 3-13 and Figure 3-14, it is seen that the outlier residuals correlate with the sudden drop and rise of temperatures.

TABLE 3-3 AR(3) REGRESSION STATISTICS OF UNFILTERED TEMPERATURE RESIDUALS

Multiple R	0.975
R^2	0.950
Adjusted R^2	0.950
Standard deviation	3.073
Root mean square error	9.430
Observations	2600

Referring to Table 3-3, the regression statistics is given. The regression model uses the data for the whole month of March, therefore the number of observations are 2600 and not 336 for a week's data as plotted in the figures. The next step is to plot the residuals on a control chart shown in Figure 3-15. If a disturbance occurs, it will be detected by the control chart.

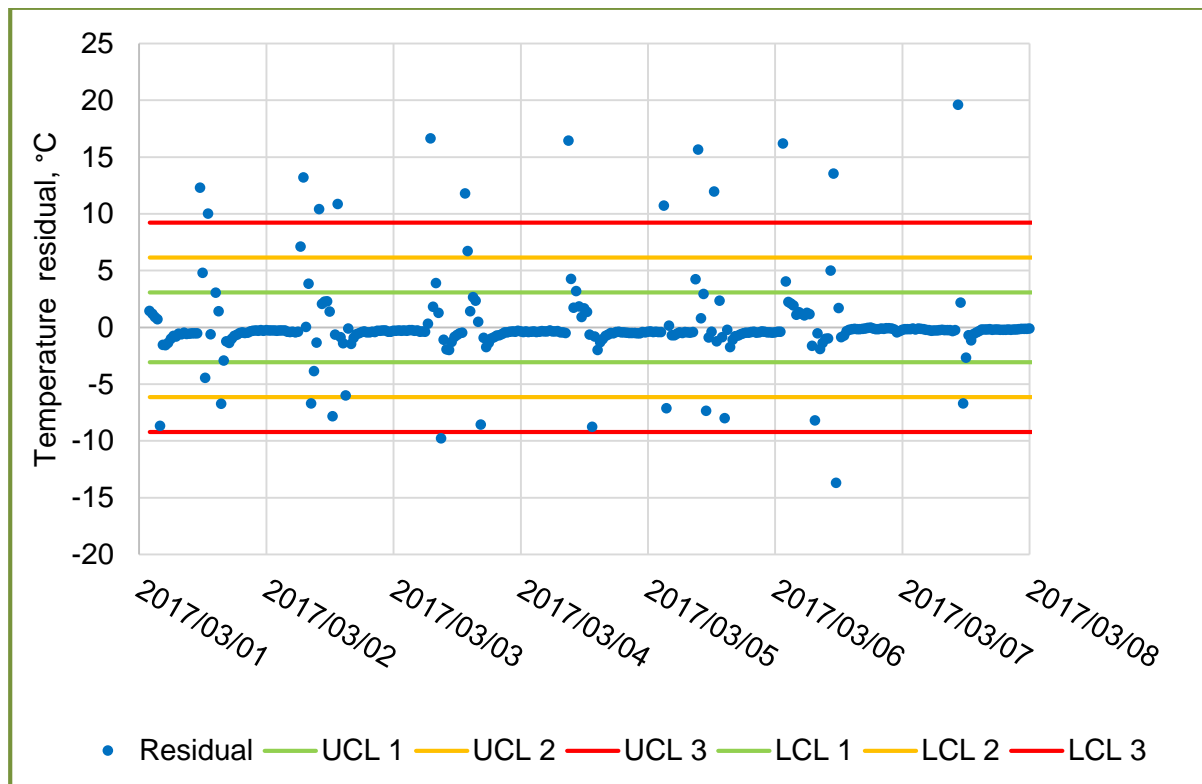


FIGURE 3-15 RESIDUAL DISTURBANCES WITH CONTROL LIMITS

Referring to Figure 3-15, the residuals are plotted with a Shewhart chart with three upper control limits (UCL) and three lower control limits (LCL). The UCLs are added to the chart to monitor the underestimated temperatures whereas the LCLs are added to monitor the overestimated temperatures. The UCLs and the LCLs are calculated using Equation 3.4 and Equation 3.5 respectively.

$$UCL\ i = \mu_{sample} + i \cdot \sigma_{sample} \quad (3.4)$$

and

$$LCL\ i = \mu_{sample} - i \cdot \sigma_{sample} \quad (3.5)$$

Where:

- $UCL\ i$ is the upper control limit of iteration i
- $LCL\ i$ is the lower control limit of iteration i
- i is the iteration number of the limit
- μ_{sample} is the sample mean
- σ_{sample} is the sample standard deviation

Control limits are usually set at three times above and below the standard deviation for the UCL and LCL respectively. If the residuals follow a normal distribution around the mean, the area bracketed by the control limits, UCL 3 and LCL 3, will on average contain 99.73% of all the plot points on the chart. Figure 3-15 shows many instances where the third upper control limit (UCL 3) is exceeded.

From the correlation observed by comparing Figure 3-13 and Figure 3-14, it is noted that the residual outliers are caused by the increase and decrease of temperature. The outliers can be reduced by filtering the bearing temperature the running status. The AR model is updated and trained using the running status filtered raw data. The equations for the AR(1), AR(2) and AR(3) are given in Equations 3.6, 3.7 and 3.8.

$$\hat{y}(t) = 0.65 \cdot y(t - 1) + 25.5 \quad (3.6)$$

$$\hat{y}(t) = 0.54 \cdot y(t - 1) - 0.16 \cdot y(t - 2) + 21.37 \quad (3.7)$$

$$\hat{y}(t) = 0.52 \cdot y(t - 1) + 0.072 \cdot y(t - 2) + 0.17 \cdot y(t - 3) + 17.92 \quad (3.8)$$

TABLE 3-4 AUTOREGRESSIVE MODEL RESULTS ON DISCONTINUOUS DATA

	AIC	RSS	MLE	p - value
AR(1)	-2.52	23269	70.9	1.35E-41
AR(2)	-2.52	23196	70.7	2.71E-03
AR(3)	-2.51	23123	70.5	2.41E-03

Referring to Table 3-4, the AIC for the models are similar. The p-values are small which means the models are significant. The AIC for the AR(1) models is the smallest, therefore the actual temperature is plotted together with the predicted temperature in Figure 3-16. The residuals are plotted in Figure 3-17 and the model statistics are given in Table 3-5.

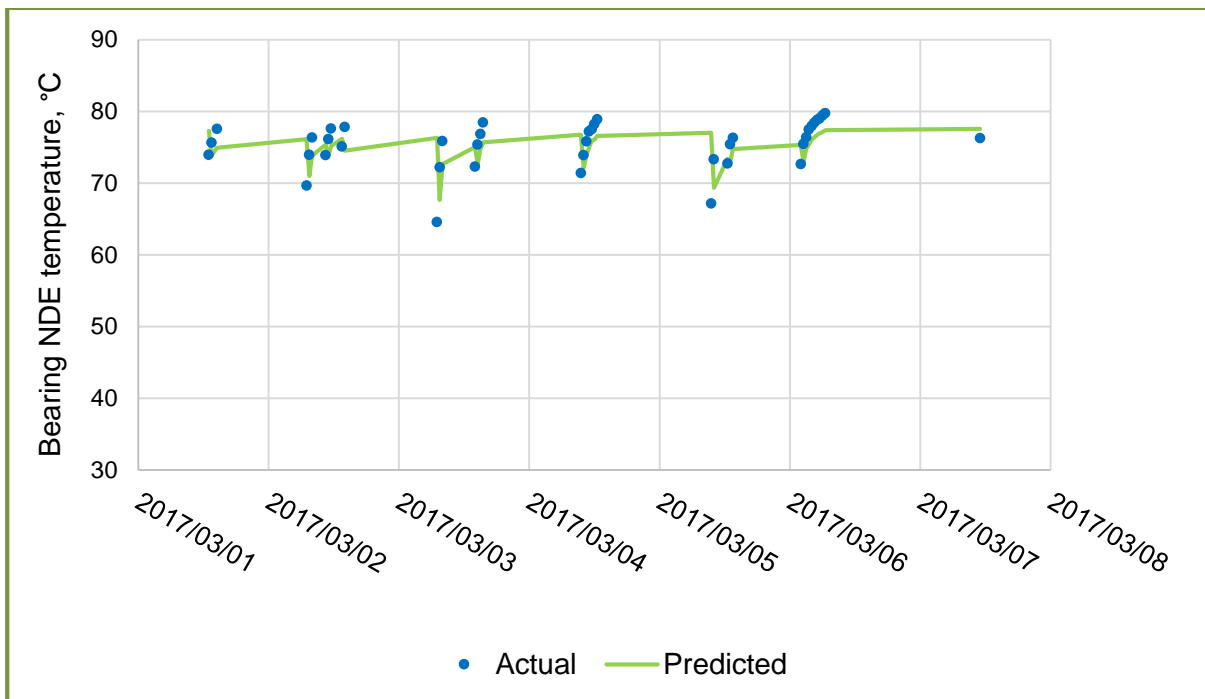


FIGURE 3-16 STATUS FILTERED, ACTUAL TEMPERATURE VERSUS AR(1) PREDICTED TEMPERATURE

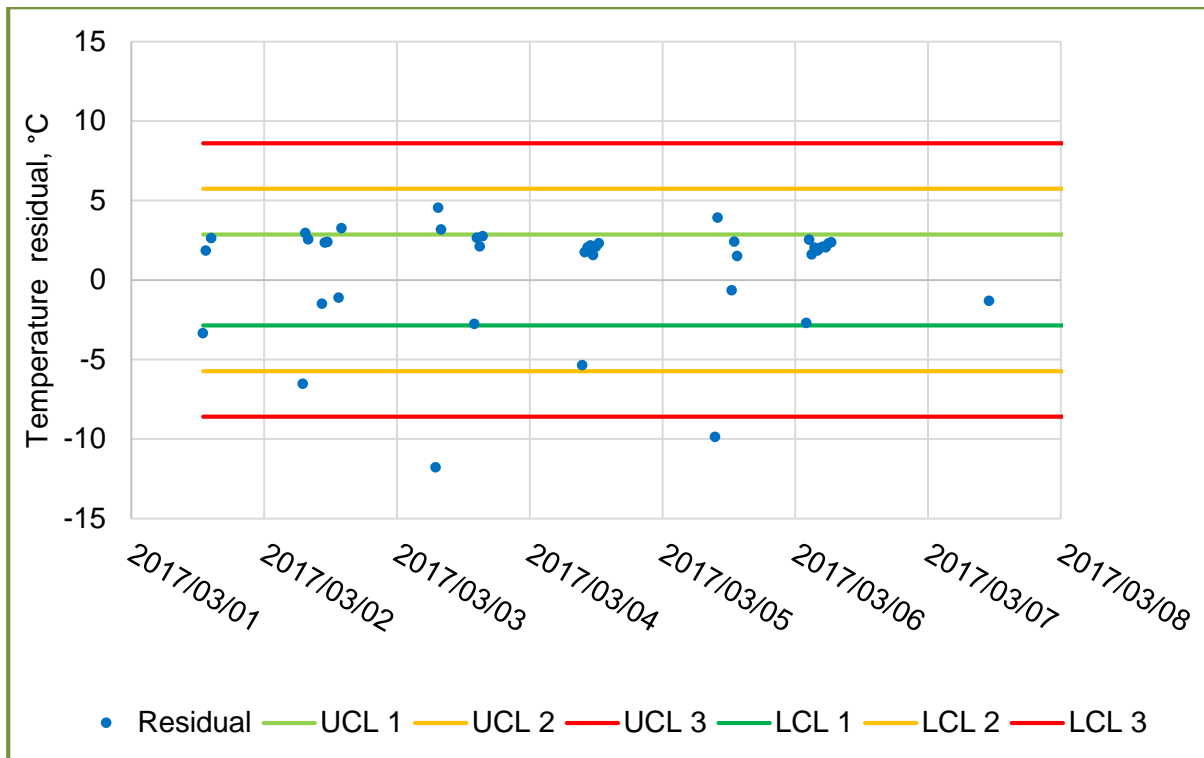


FIGURE 3-17 STATUS FILTERED, RESIDUAL DISTURBANCES

From Figure 3-16, it is observed that the predicted temperature follows the trend of the actual temperatures. From Figure 3-17, it is observed that the disturbances of the pump do not exceed UCL 2 or UCL 3.

TABLE 3-5 AR(1) REGRESSION STATISTICS OF STATUS FILTERED TEMPERATURE RESIDUALS

Multiple R	0.655
R^2	0.429
Adjusted R^2	0.427
Standard deviation	2.865
Root mean square error	8.16
Observations	328

By comparing Table 3-3 and Table 3-4, a clear difference between the filtered and unfiltered data is that there are only 328 data points in a month when the pump was running throughout the whole half-hour. For this specific pump, throughout the month of March, only 13% of the data is classified as operational data. The standard deviation of the filtered data ($\sigma_{filtered} = 2.865$) is less than that of the unfiltered data ($\sigma_{unfiltered} = 3.073$). The residuals of both cases are plotted on a normal distribution curve in Figure 3-18.

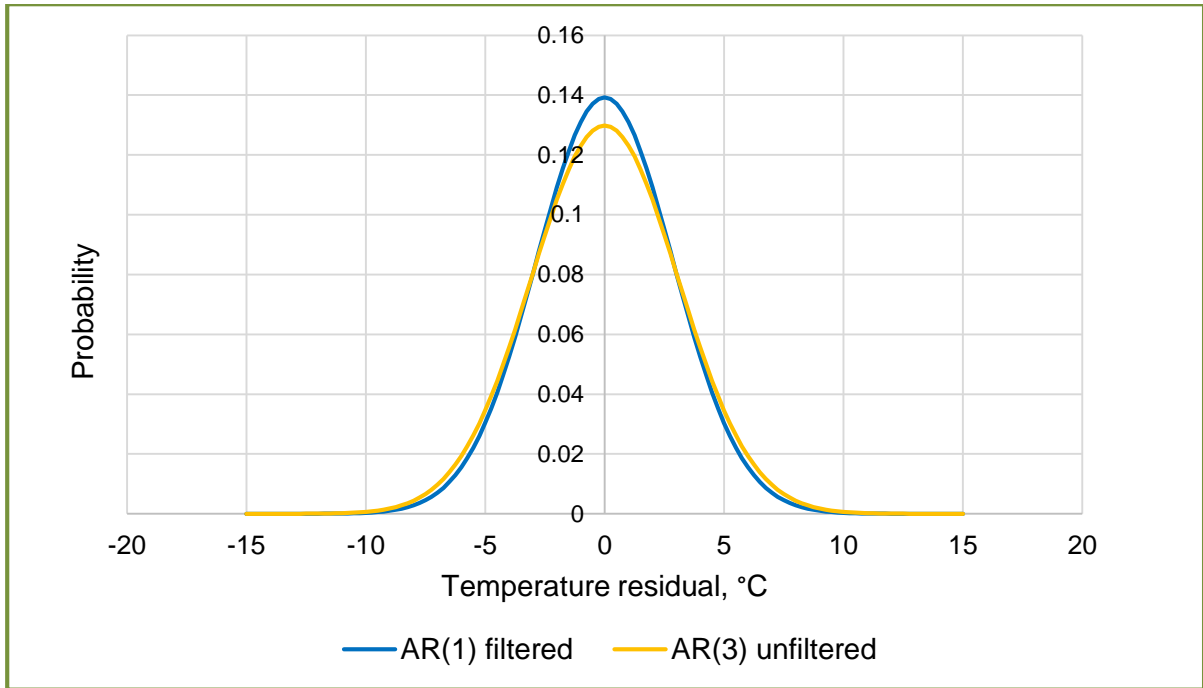


FIGURE 3-18 NORMAL DISTRIBUTION OF FILTERED AND UNFILTERED DATA

Figure 3-18 shows the normal distribution of both the filtered and unfiltered cases. Figure 3-18 validates that the residuals of both cases form an independent and identical distribution IID. The Figure 3-18 shows that the filtered data, which is predicted with the AR(1) model, gives a more accurate prediction than the unfiltered data which is predicted with the AR(3) model. Thus, in this case, the filtered data shows a better prediction of the data points.

3.4. MODEL VERIFICATION AND VALIDATION

To test the AR model methodology, AR models are fitted to different input signals which are presented in Figure 3-19 through to Figure 3-24. The best fit AR model will result in a more accurate natural disturbance detection; thus the signals are chosen to imitate probable temperature signals. Six different signals are included in the test they include:

- Linear function: to imitate a steady increase.
- Random function between two values: to simulate process noise.
- Sine function: to imitate usual variation.
- Combination of a two sine functions: to imitate usual variation in a slow process change.
- Linear random increase: To imitate a steady increase with process noise.
- Linear random increase with a simulated fault: To simulate a fault through noise.

The equations of the simulated signals are displayed on their respective figures.

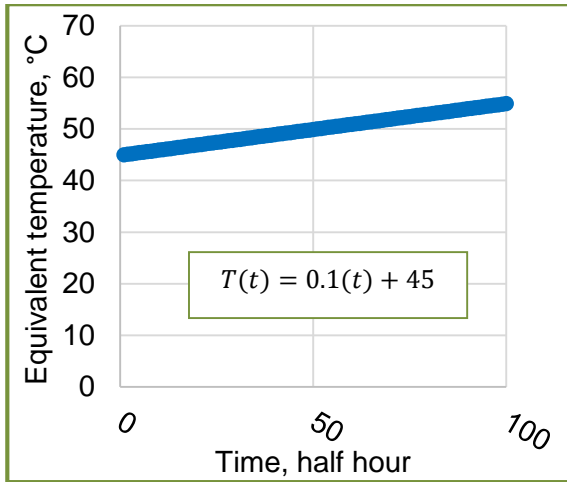


FIGURE 3-19 LINEAR FUNCTION

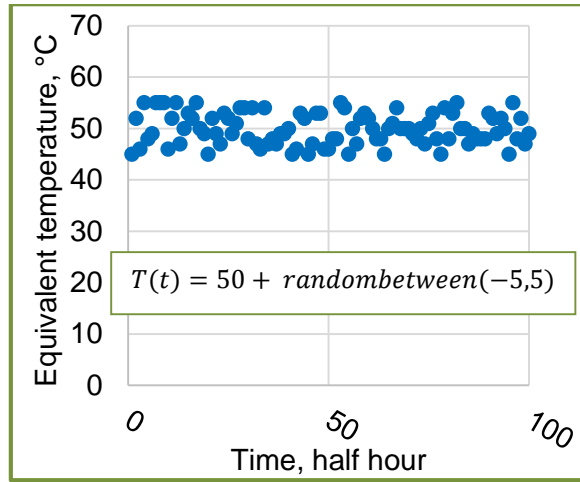


FIGURE 3-20 RANDOM BETWEEN FUNCTION

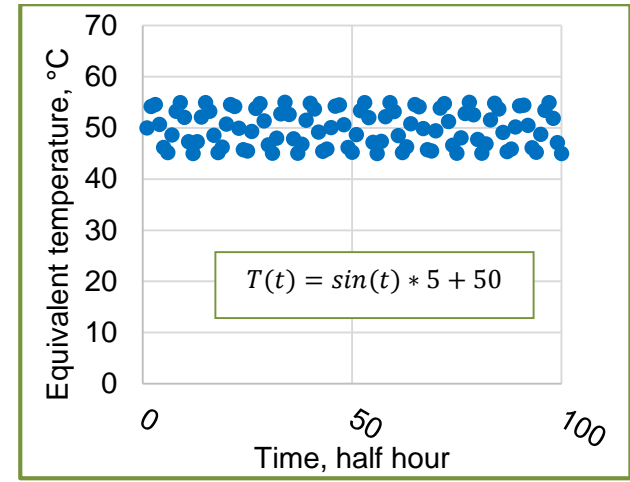


FIGURE 3-21 SINE FUNCTION

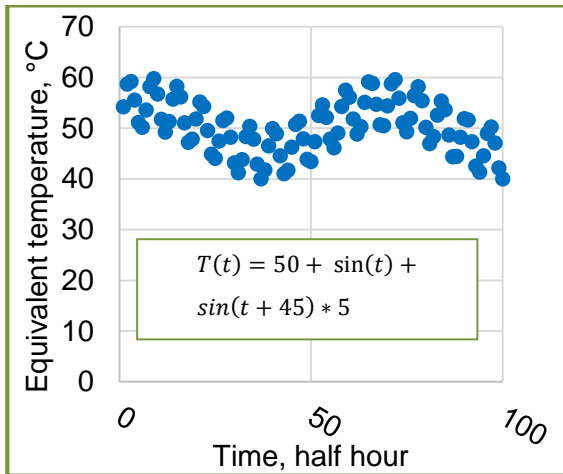


FIGURE 3-22 DOUBLE SINE FUNCTION

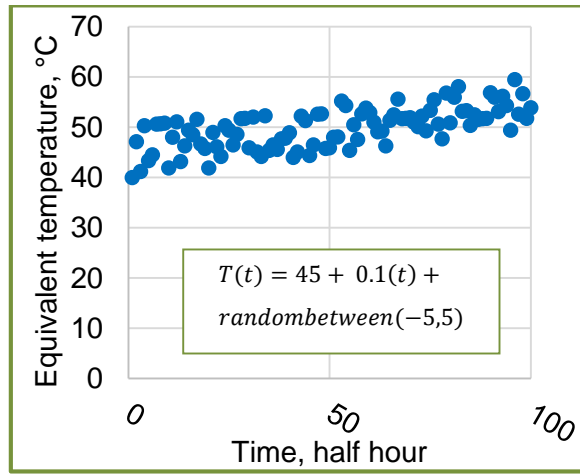


FIGURE 3-23 LINEAR AND RANDOM

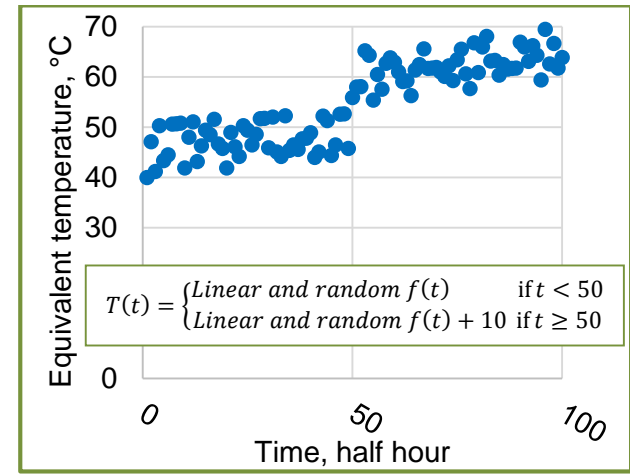


FIGURE 3-24 LINEAR, RANDOM WITH FAULT

Figure 3 19 to Figure 3 24 illustrates the simulated temperature signals AR(1), AR(2) and AR(3) models were fitted to all the equivalent temperature signals. The regression statistics for the models are given in Table 3-6.

TABLE 3-6 REGRESSION STATISTICS OF SIMULATED SIGNALS

Linear function								
	Multiple R	R ²	Adjusted R ²	Standard Error	RSS	MLE	AIC	p-value
AR(3)	1.000	1.000	0.979	~0	27720	282.85	-5.290	~0
AR(2)	1.000	1.000	0.990	~0	27720	282.85	-5.290	~0
AR(1)	1.000	1.000	1.000	~0	27720	282.85	-5.290	~0
Random between								
	Multiple R	R ²	Adjusted R ²	Standard Error	RSS	MLE	AIC	p-value
AR(3)	0.148	0.022	-0.009	3.019	31004	316.37	-5.514	0.8898462
AR(2)	0.148	0.022	0.001	3.003	31007	316.39	-5.514	0.1519779
AR(1)	0.019	0.000	-0.010	3.020	31024	316.57	-5.515	0.8512709
Sine function								
	Multiple R	R ²	Adjusted R ²	Standard Error	RSS	MLE	AIC	p-value
AR(3)	1.000	1.000	0.989	3.634E-15	30150	307.65	-5.458	~0
AR(2)	1.000	1.000	1.000	4.419E-15	30150	307.65	-5.458	~0
AR(1)	0.541	0.293	0.285	2.995	31011	316.44	-5.514	8.975E-09
Double sine function								
	Multiple R	R ²	Adjusted R ²	Standard Error	RSS	MLE	AIC	p-value
AR(3)	0.998	0.996	0.996	0.308	30163	307.78	-5.459	1.287E-81
AR(2)	0.906	0.822	0.818	2.167	30596	312.20	-5.487	2.386E-18
AR(1)	0.774	0.600	0.596	3.228	31150	317.86	-5.523	8.425E-21
Linear and random function								
	Multiple R	R ²	Adjusted R ²	Standard Error	RSS	MLE	AIC	p-value
AR(3)	0.494	0.244	0.220	3.419	31234	318.72	-5.529	0.0061
AR(2)	0.426	0.181	0.164	3.541	31328	319.67	-5.535	0.0647
AR(1)	0.389	0.151	0.142	3.586	31384	320.24	-5.538	7.71E-05
Random and fault function								
	Multiple R	R ²	Adjusted R ²	Standard Error	RSS	MLE	AIC	p-value
AR(3)	0.890	0.793	0.786	3.661	31400	682.62	-7.052	0.0002
AR(2)	0.871	0.759	0.754	3.928	31523	685.29	-7.060	0.0001
AR(1)	0.845	0.714	0.711	4.256	31644	687.91	-7.067	7.44E-28

Table 3-6 shows the multiple correlation coefficient (R), multiple coefficient of determination (R^2), adjusted R^2 , standard error (or standard deviation), RSS, MLE, AIC and p-values of the different signal's respective models.

Referring to Table 3-6, it is observed that the multiple coefficient of determination, R^2 , suggests a strong relationship between the predicted and actual temperatures in all cases where the random function was not used. The standard errors show that the AR model accurately predicts the linear and sine functions except for the random cases. A small p-value indicates a more statistically significant model. The p-values are small for the linear and sine functions, except for the random functions.

The sine function was accurately predicted with the AR(2) and AR(3) models. Since the AR(1) model only takes the previous step value into account, it is not an accurate prediction with this time interval. Ultimately, if the time interval is large enough and the data points are calculated using an average function, the resulting dataset will seem linear and an AR(1) model will be sufficiently predict the next value.

By following the developed method, the AR model order is chosen by selecting the model with the lowest AIC value. The results show that the order of the AR model is dependent on the type of signal and the degree of randomness.

3.5. CONCLUSION

It is possible, with the help of a Shewhart \bar{X} control chart, to detect mean and variance outliers of developed residual temperature signals. Thus, this fault detection method is feasible without having any additional information about the alarm limits. This makes the developed fault detection method generic and is expected to apply to other components of similar heat capacities.

Vibration is usually analysed in the frequency domain. With the half hourly data, the high frequency analysis is not possible, so a test was performed to analyse the correlation between vibration and performance. Previous studies show a relationship between performance parameters and vibration (Zhang *et al.*, 2014). No obvious correlation was found with the available data.

The ambient temperature of equipment has an effect on the overall machine temperature. A method to determine the ambient temperature of idling equipment is developed. By analysing the idling temperature, the cooling method of the equipment can be monitored without a supplementary ambient temperature measurement.

A running status filter was implemented to reduce the residual standard deviation which proved to be successful, herewith improving the accuracy of the AR model. The model-based fault detection method is implemented; the use of a filter should be justified. If the machine is constantly running, a filter is not required.

The condition monitoring method was developed and mainly consists of four parts: a static limit check, a best fit model choice, a displayed result and a dynamic limit check.

- The static limit check refers to the comparison of the input signal to alarm limits. If the alarm limits are exceeded, the event should be noted and reported in a table format.
- The best fit model choice consists of fitting different AR models to the data and picking one that best represents the data. The choice is made by minimising the AIC.
- The displayed result consists of a control chart of the parameter trend and the static alarm and trip limits. The residuals of the fitted models along with the upper and lower limits are given to detect any shifts.
- The dynamic limit checks refer to the comparison of the generated residuals to the UCLs and LCLs.

Maintenance and breakdown reports are to validate the condition prediction model. The reports can be difficult to obtain, and if there are reports available they do not necessarily contain the useful or relevant information. An example of such a log is given in Appendix E. The model is further tested and validated in Chapter 4 where the model is applied to different case studies.



**ALTERNATIVE METHOD FOR EQUIPMENT
CONDITION MONITORING ON SOUTH AFRICAN MINES**

CHAPTER 4

**EVALUATION OF THE ALTERNATIVE CONDITION MONITORING
METHOD (CASE STUDIES)**

4. EVALUATION OF THE ALTERNATIVE CONDITION MONITORING METHOD (CASE STUDIES)

4.1. INTRODUCTION

The focus of Chapter 4 is to evaluate the developed method. The model is implemented in two case studies and tested if a mean and variance shift can be detected with AR residual analysis. If such a shift is observed the method will identify the component as faulty.

The developed method is implemented on a multistage centrifugal pump of a dewatering system and multistage compressors. The implementation of the model on the dewatering system and compressed air section is discussed in Section 4.2 and Section 4.3 respectively. Section 3.4 discusses the method verification and validation. The results of the developed method are discussed and compared in Section 4.4.

4.2. CASE STUDY 1: DEWATERING SYSTEM

4.2.1. CASE STUDY OVERVIEW

This case study focuses on the detection of a large sudden change in a bearing temperature of a 1.8 MW multistage centrifugal pump. An excessive temperature on the NDE motor of the pump on level 66 of Mine A was identified and repaired. The maintenance report is attached in Appendix F.

In a period of eight days from 15 to 23 March 2017, twenty alarms were triggered with the company's implemented condition monitoring method. The method notifies responsible personnel if the parameter exceeds the alarm limit for more than five minutes.

The period where the alarm was triggered, before maintenance was done, is plotted Figure 4-1. The defective bearing temperature along with the alarm and trip limits are shown. The running status of the pump is included to indicate whether the pump is operational. The trip limit of the motor NDE was set at 80°C and the alarm level was set at 76°C.

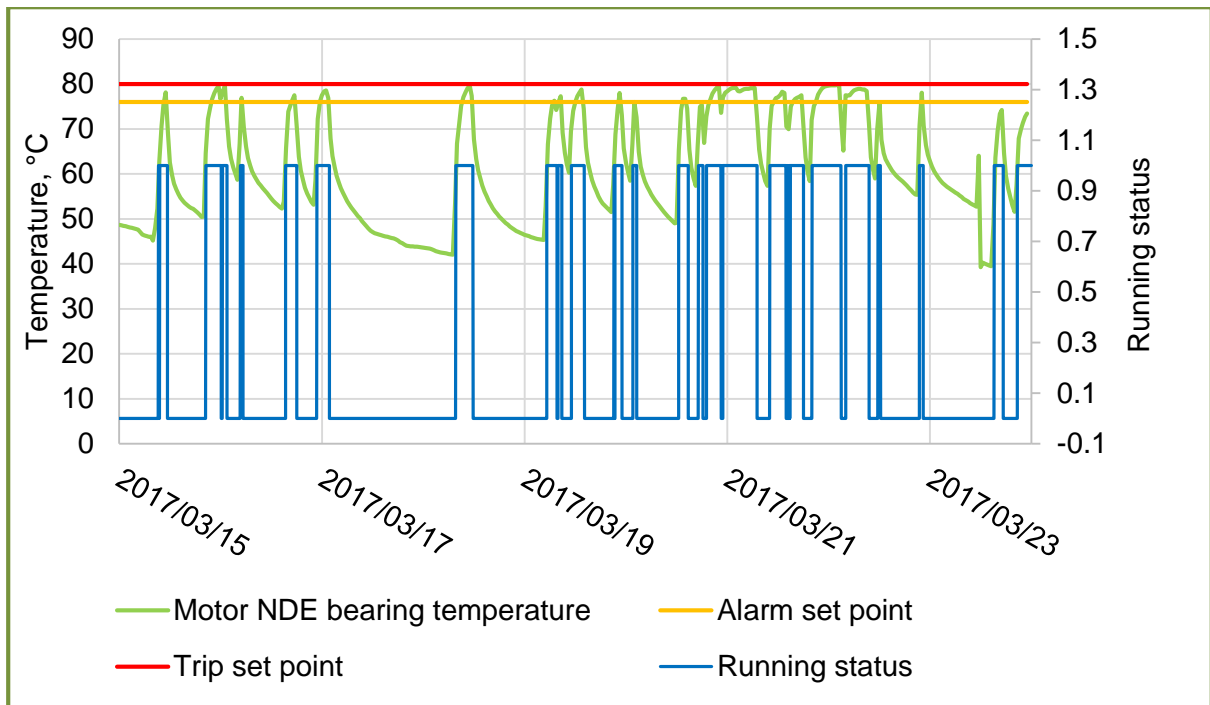


FIGURE 4-1 CASE STUDY 1: NDE BEARING TEMPERATURE BEFORE MAINTENANCE

The developed NDE motor bearing temperature and the pump running status is plotted of the primary and secondary y-axis respectively in Figure 4-1. The alarm and trip limits, 76°C and 80°C respectively, are also shown in Figure 4-1. Figure 4-1 shows that the motor bearing temperature exceeded the alarm limit numerous times during this period. The correlation of the running status and the temperature spikes which crosses the trip limits indicate that the pump had tripped due to the excessive temperatures.

The maintenance report, attached in Appendix F, states that the unit was isolated and locked out for the inspection upon arrival. The coupling and NDE bearing was opened for investigation. It was noted that the coupling gap was about 2 mm and the rotor thrust on the bearing. Before the maintenance, the pump was installed incorrectly and the motor alignment, coupling gap and magnetic centre was not determined correctly.

The problem was corrected by moving the motor away from the pump, removing and scraping the bearing thrust face, and installing the bearing back into position. Magnetic centre was established and the coupling gap set to 8 mm. Re-alignment was completed and the unit started. The bearing temperatures were then monitored on the motor and settled after an hour of operation at 63°C at both the motor bearings.

4.2.2. MODEL IMPLEMENTATION

The AIC was determined for first, second and third order models which were fitted to the unfiltered NDE bearing temperature signal. The AIC of the third order AR model was found to be the minimum as determined in Section 3.3.4.3 on the same dataset. The available temperature data before the maintenance period was used to construct a third order AR model. This period is shown in Figure 4-2. The AR(3) model is fitted to actual NDE bearing temperature in Figure 4-3.

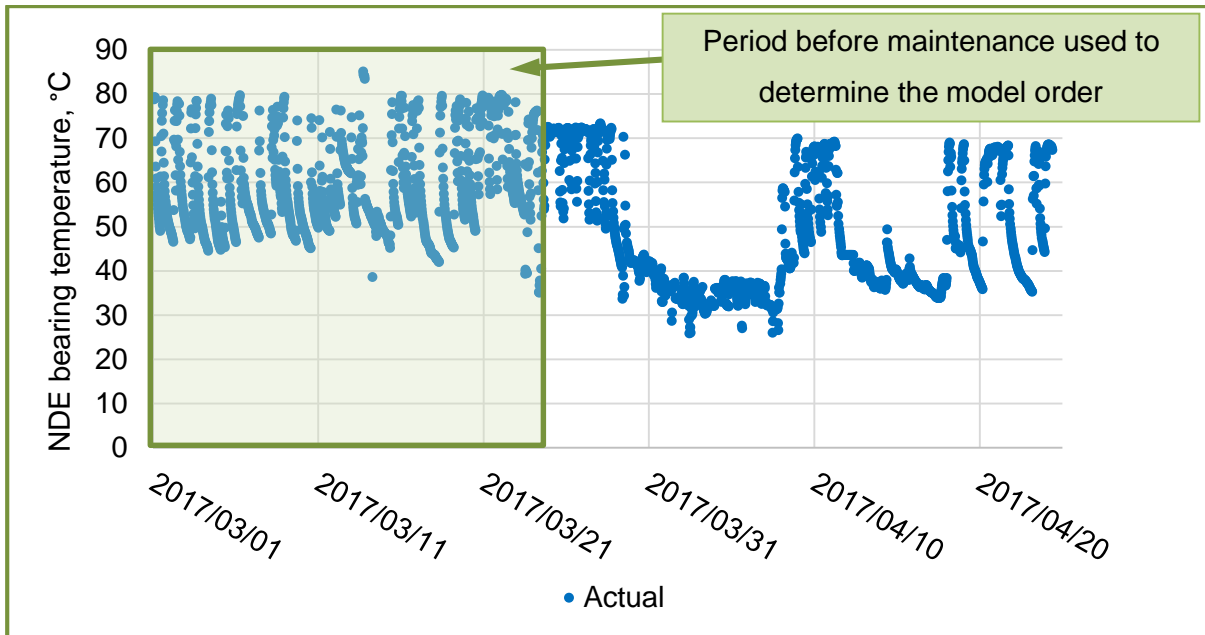


FIGURE 4-2 PERIOD USED TO DETERMINE THE AR(3) MODEL

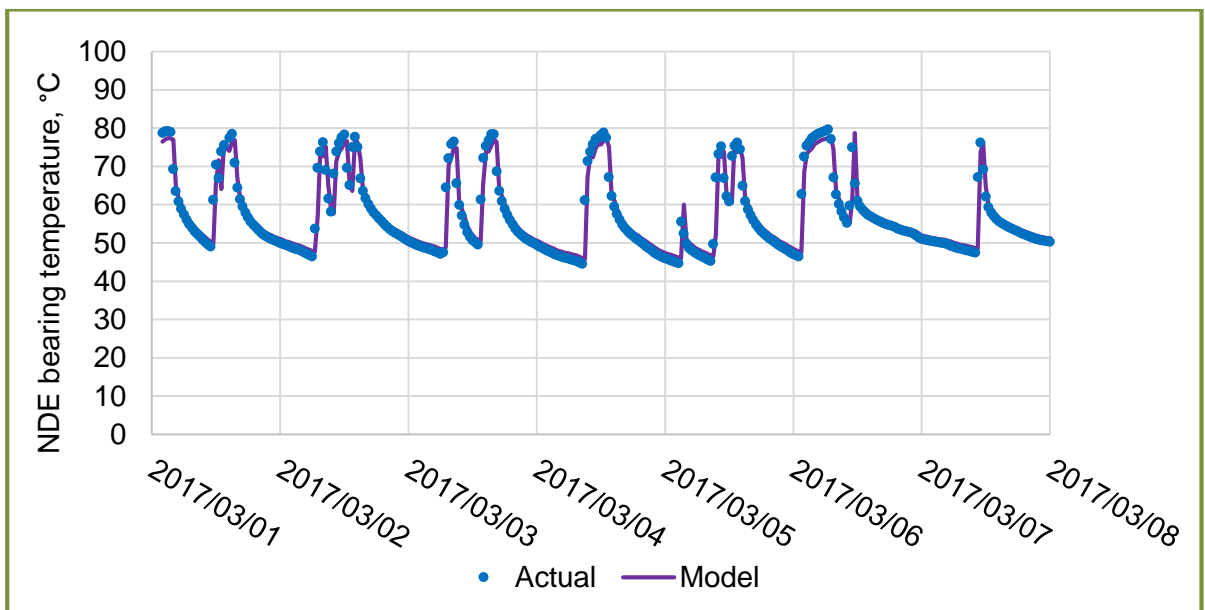


FIGURE 4-3 AR(3) MODEL FITTED TO THE TEMPERATURE BEFORE THE MAINTENANCE PERIOD.

Figure 4-2 shows the NDE bearing temperature during and after the maintenance period. The period before the maintenance was chosen to determine the AR model order. Figure 4-3 shows the fitted AR(3) model to the NDE bearing temperature. It is observed that the model's movement corresponds to the actual temperature signal. The fitted AR(3) model is shown in Equation 4.1 with the regression statistics in Table 4-1.

$$\hat{y}(t) = 0.20 \cdot y(t - 1) - 0.69 \cdot y(t - 2) + 1.43 \cdot y(t - 3) + 1.88 \quad (4.1)$$

TABLE 4-1 AR(3) REGRESSION STATISTICS AR(3) MODEL

Multiple R	0.934
R^2	0.872
Adjusted R^2	0.872
Standard deviation	3.815
Root mean square error	14.502
Observations	1098

Table 4-1 gives the regression statistics for the period before the maintenance. The coefficient of multiple determination (R^2), indicates a strong relationship between the model and the actual data points. The residuals for the period before and after the maintenance period is plotted in Figure 4-4.

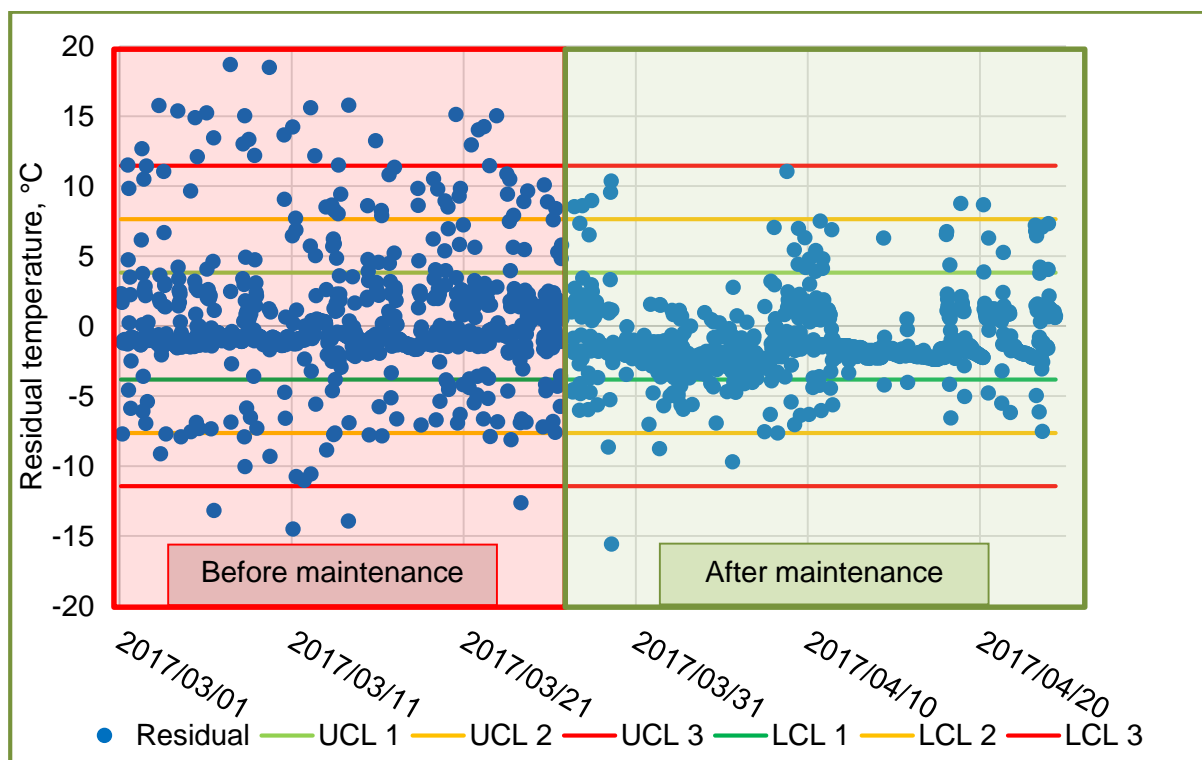


FIGURE 4-4 RESIDUALS BEFORE AND AFTER MAINTENANCE

Figure 4-4 shows the residuals of the AR(3) model along with the UCL and LCL. From Figure 4-4, it is clearly observed that the residuals of the model are more concentrated around the mean after the bearing temperatures have been maintained on 31 March 2017. Table 4-2 gives the residual distribution before and after maintenance periods.

TABLE 4-2 RESIDUAL DISTRIBUTION COMPARISON BEFORE AND AFTER MAINTENANCE

	Before maintenance 1 to 31 March 2017	After maintenance 9 to 24 April 2017
Above UCL 3	4%	0%
Above UCL 2	9%	0%
Above UCL 1	15%	4%
Below LCL 1	12%	3%
Below LCL 2	3%	0%
Below LCL 3	1%	0%

From Table 4-2 it is observed that there is a significant change in the percentage of data points exceeding the UCL and LCL. The data points are more concentrated around the mean; thus, a variance shift is observed.

4.2.3. DISCUSSION

In the modelling stage of the method development it was shown that the data used to train the model affects the accuracy of the prediction. In this case study, the AIC was minimised and thereby showed that the AR(3) model is the best prediction for the dataset. The dataset used to minimise the AR model contained the data before the maintenance was performed.

Even though the model was trained with the temperature before the maintenance, the model was able to detect the variance shift, shown in Table 4-2. This suggests that the model can be applied to already faulty equipment and still be able to detect mean and variance shifts. By observing the linear trend of the percentages exceeding the control limits of the AR residuals, it is possible to predict faults and estimate the failure date.

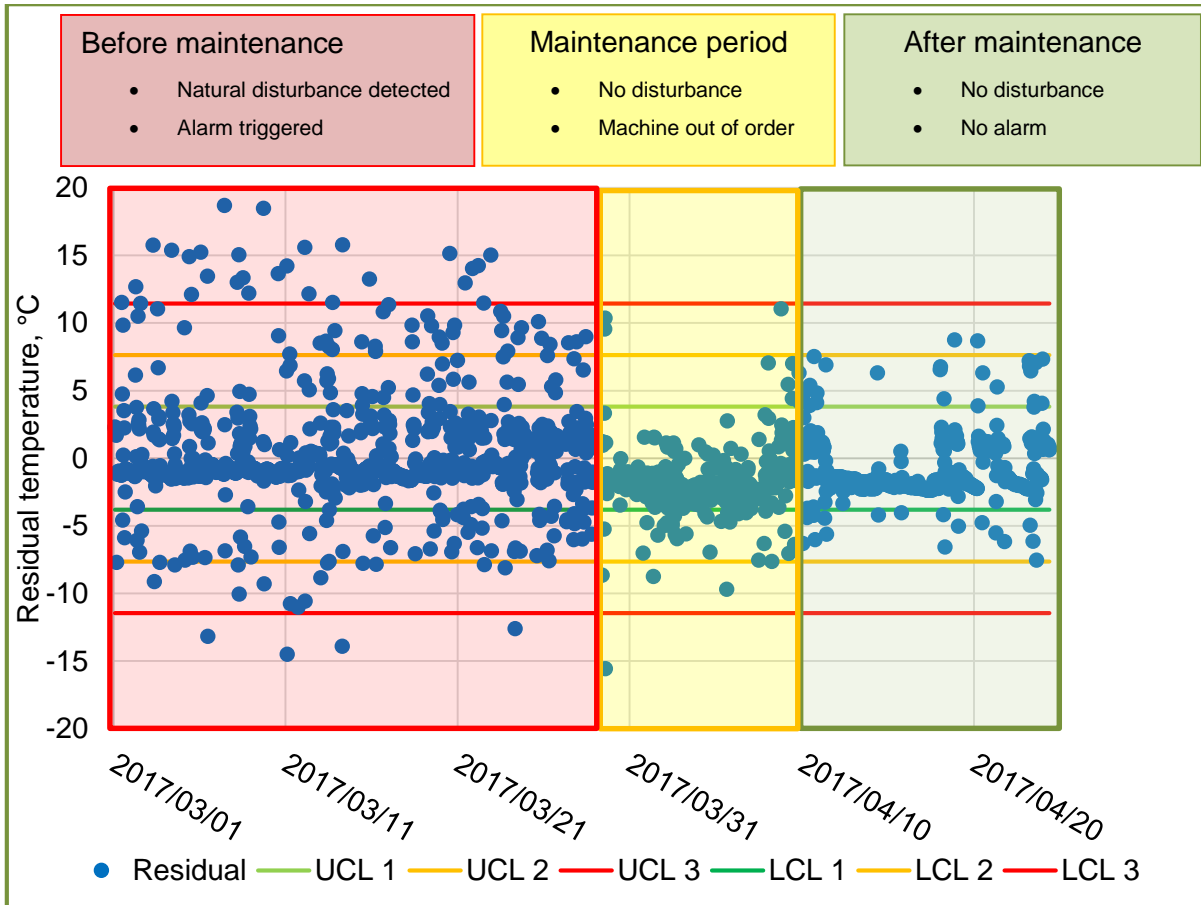


FIGURE 4-5 CASE STUDY 1: TEMPERATURE RESIDUALS BEFORE AND AFTER MAINTENANCE

Figure 4-5 illustrates how the model is able to detect faults. The control limits are specified to be static in Case Study 1, if dynamic control limits are implemented, the system can automatically update itself, and recognise even smaller changes specific to the system. A slow, continuous change is analysed in Case Study 2.

4.3. CASE STUDY 2: COMPRESSORS

4.3.1. CASE STUDY OVERVIEW

This case study determines if the method can detect a slow and continuous change. The AR model is implemented on the compressor system where the cooling system lost effectivity. The case study is performed on temperature signals of a 1.8 MW compressor that serves as a backup to increase the pressure if the compressed air demand is too high, hence the many start-ups and shutdowns.

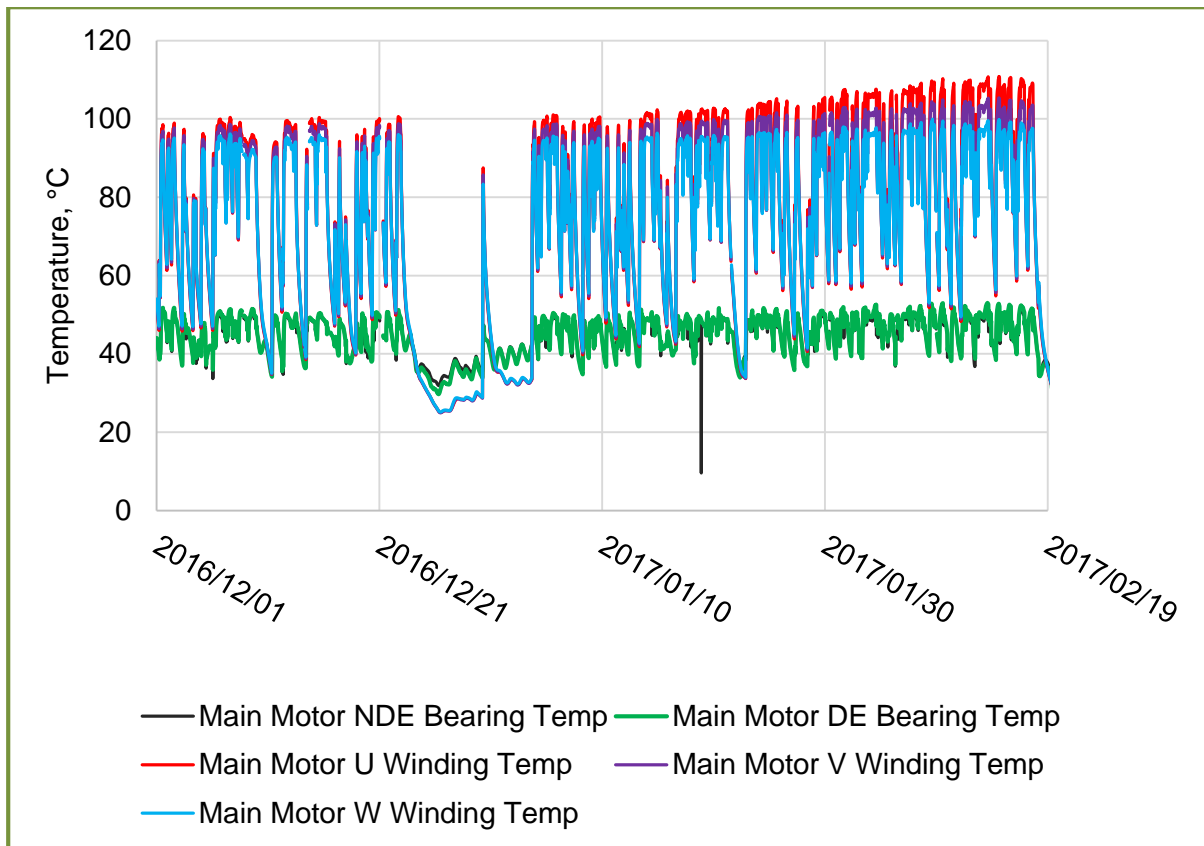


FIGURE 4-6 COMPRESSOR MOTOR BEARING AND WINDING TEMPERATURES

Figure 4-6 shows the rise of the motor temperatures along with the motor bearing temperature. The main motor winding temperature U, increased from a normal operating temperature of less than 100°C to 110°C.

4.3.2. MODEL IMPLEMENTATION

Evaluating the data shows 1% data loss throughout the observed period of 1 December 2016 to 28 February 2017. The lost data points were excluded in the model fit procedure. The whole sample period from 1 December 2017 to 28 February 2017 was used to construct the AR models. The results of the AR models are presented in Table 4-3.

TABLE 4-3 AUTOREGRESSIVE MODEL RESULTS

	AIC	RSS	MLE	p - value
<i>AR(1)</i>	-0.99	65777	33.0	~0
<i>AR(2)</i>	-0.86	61467	30.8	~0
<i>AR(3)</i>	-0.85	61413	30.8	0.037

Table 4-3 shows the AIC for the AR(1) model is the smallest, thus the AR(1) model is used to predict the winding temperature. The model is fitted to the actual temperature of the main motor winding temperature U and presented in Figure 4-7. The regression statistics for the model is given in Table 4-1.

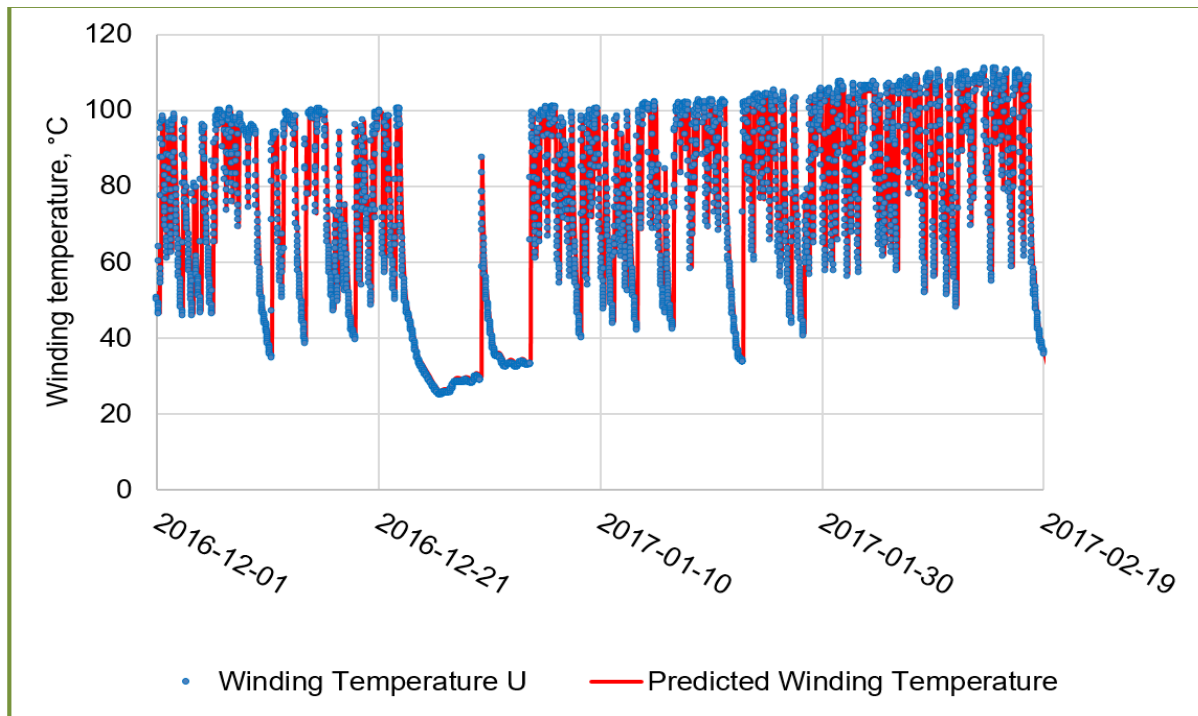


FIGURE 4-7 AR(1) MODEL RESULTS

TABLE 4-4 REGRESSION STATISTICS OF AR(1) MODEL

Multiple R	0.981
R^2	0.962
Adjusted R^2	0.962
Standard deviation	4.983
Root mean square error	0.487
Observations	4278

Table 4-4 shows that the AR(1) model's regression statistics. The multiple coefficient of determination, R^2 , suggests a strong correlation relationship between the model's prediction and the actual values. Comparing the regression statistics of both case studies shows that the AR(1) model in Case Study 1, $R^2 = 0.981$ is larger than that of the AR(3) model in Case Study 2, $R^2 = 0.934$.

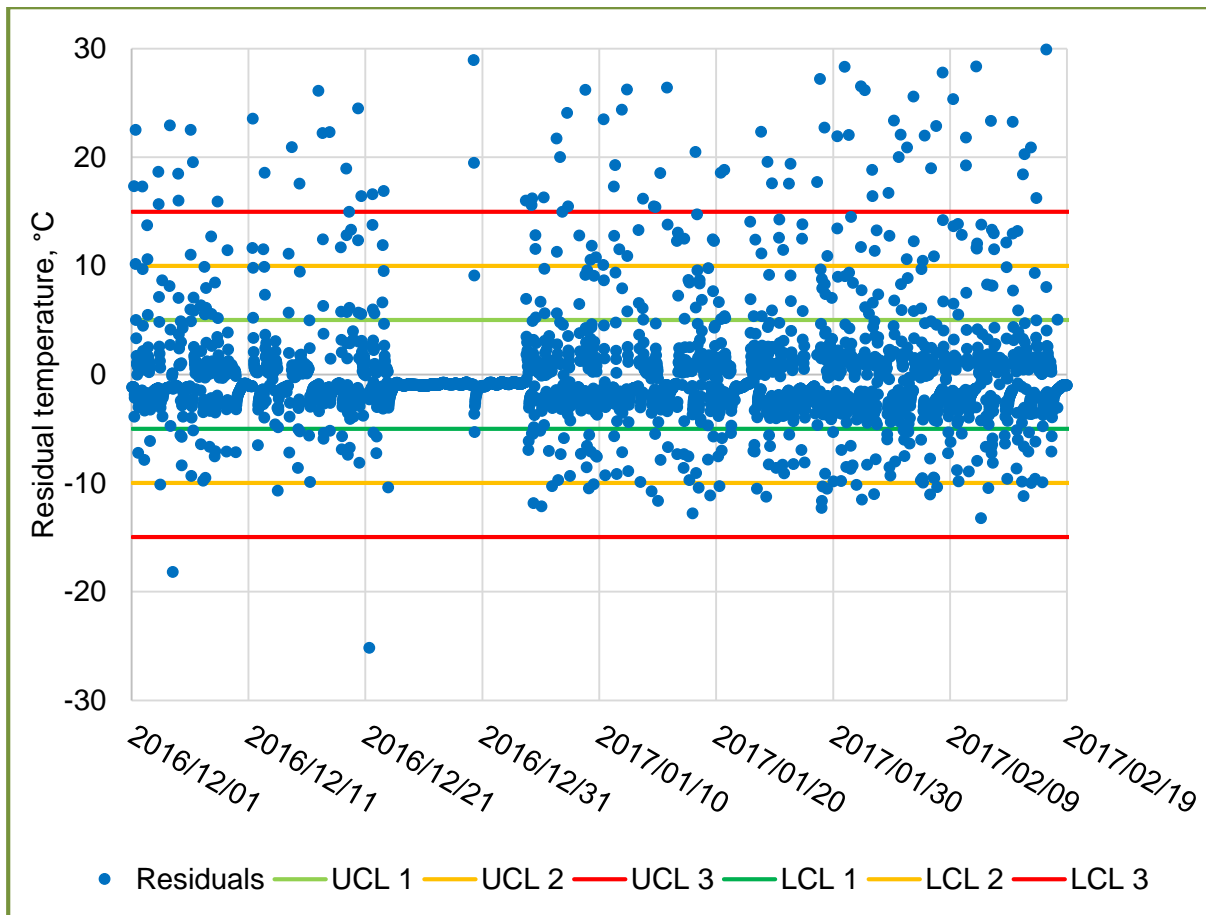


FIGURE 4-8 RESIDUALS WITH CONTROL LIMITS

Figure 4-8 shows the residuals of the AR(1) model. 2.7% of the residuals exceed the third UCL. Two data points from a sample of 4278 data points exceeds the third LCL. Table 4-5 shows the variance shift before and after the shutdown.

TABLE 4-5 RESIDUAL DISTRIBUTION COMPARISON BEFORE AND AFTER SHUTDOWN

	Before shutdown 1 to 25 December 2016	After shutdown 1 January to 19 February 2017
Above UCL 3	2%	3%
Above UCL 2	4%	5%
Above UCL 1	7%	8%
Below LCL 1	3%	5%
Below LCL 2	0%	1%
Below LCL 3	0%	0%

Table 4-5 shows that there is an increase in change in the percentage of data points exceeding the UCL and LCL. The data points spread out further around the mean; thus, a variance shift is observed. This means that the natural disturbance before the shutdown is less than the natural disturbance after the shutdown. Figure 4-9 is added to show the small mean residual change.

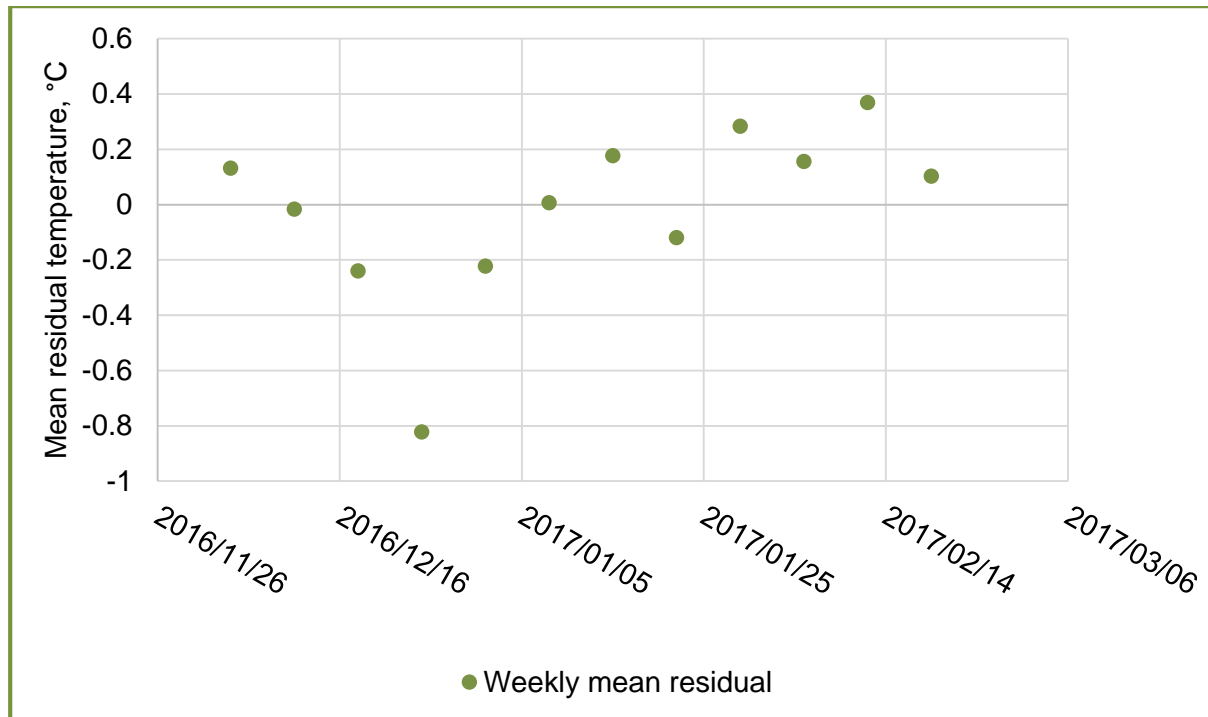


FIGURE 4-9 WEEKLY MEAN RESIDUAL

Figure 4-9 shows the weekly mean residual change, that fell to $\mu = -0.82\text{ }^{\circ}\text{C}$ during the shutdown. This means that the model overpredicted the temperature during the shutdown period. The mean shift of the shutdown is detected. A larger mean shift is observed after the shutdown reached a maximum of $\mu = 0.3\text{ }^{\circ}\text{C}$.

4.3.3. DISCUSSION

From the residual analysis, an increase in the variance is observed. The mean difference before and after the shutdown also showed an increase. The slow increase of the motor winding temperature residuals could not be observed from the control chart in Figure 4-8. The increase was observed by calculating the weekly average mean residuals, as shown in Figure 4-9.

The mean shift change suggests a disturbance in the system. The means shift analysis also detected the shutdown period, where the AR(1) model under predicts the temperatures. If the

mean shifts during a disturbance such as presented in Case Study 2, is benchmarked, a specific fault can be matched in future occurrences.

4.4. CONCLUSION

The temperature signal of a defected component was analysed in this chapter. The AR residual analysis has shown that it is able to detect a mean and variance shift. Guo *et al.*, (1998) states that the AR residuals represent the natural disturbance of the system. The results prove that the AR model can detect an unnatural disturbance, which suggests that a fault has occurred.

In Case Study 1, the model has shown the capability of detecting a variance shift in the operating temperature of the NDE bearing of the compressor motor. In Case Study 2, the model has shown the capability of detecting a small mean shift change in the operating temperature of a motor winding temperature.

The model is validated throughout the development and case studies, by implementing the model with historical data from real machines. Sargent (2012) defines historical data validation as one of the techniques used to validate a model. The data is shown on a control chart that graphically displays the model's output that validates the model's operational behaviour. The illustration of the control chart eases the face validation process of the analyst (Kleijnen, 1999).

The model is validated using the parameter variability technique by using two different types of changes to the inputs. Case Study 1 presented a large change in temperature after maintenance was performed on the pump, and Case Study 2 presented a small change over time. The model's behaviour was validated by using Case Study 1 and Case Study 2 as different subjects. The observed behaviour of the model was proven to detect a sudden change as well as a uniform change over time.

Using the model to predict the system's behaviour and comparing the model's forecast to the actual system behaviour can give an indication of the model's accuracy. The regression analysis shows the accuracy of the estimation. The calculated the multiple coefficient of determination, or R^2 , and the mean square error, or MSE, statistics used to validate models. In both case studies, the multiple coefficient of determination suggested a strong correlation.

Overall it was shown that temperature in thirty minute intervals shows high autocorrelation in large three-phase induction machines. A mean and variance shift alarm has to be developed for the specific equipment, setup and sample rate.



**ALTERNATIVE METHOD FOR EQUIPMENT
CONDITION MONITORING ON SOUTH AFRICAN MINES**

CHAPTER 5

CONCLUSION AND RECOMMENDATIONS

5. CONCLUSION

5.1. INTRODUCTION

Chapter 5 provides the summary and recommendations of the study. In the study, problems regarding condition monitoring in the South African mining industry and presented an alternative condition monitoring method. The method includes a model to analyse underlying information of available condition-indicative parameters.

5.2. SUMMARY

A need for a condition monitoring system that can operate automatically, analyse multiple systems, continuously evaluate the system while making use of existing infrastructure exists. This study proposed a method to turn an existing preventative maintenance strategy into a predictive maintenance strategy, with the aim to increase equipment availability and reduce maintenance costs.

The study has shown that the developed method can be implemented using the mines' existing infrastructure. Even with the constraint of half hourly sample rates, the system was able to detect the mean and variance shifts. Unfortunately, with the low sample rates, fault diagnosis is deemed not viable for in-depth vibration analysis. Vibration is preferably analysed in the frequency domain with high sample rates using Fourier spectral analysis. Since only half hourly averaged data is available, the analysis is restricted to the time-domain.

Literature has shown that AR models can accurately predict temperatures in cases where the measured component is surrounded by a large metal mass (Schlechtingen & Santos, 2010). South African mines make use of large electrical machines that showed adequate temperature autocorrelation to detect the natural disturbance in the system. AR residual analysis was chosen to be used as the condition prediction model.

The developed method mainly consists of four parts: a static limit check, a best fit model choice, a displayed result and a dynamic limit check.

- The static limit check refers to the comparison of the input signal to alarm limits. If the alarm limits are exceeded, the event should be noted and reported in a table format.
- The best fit model choice consists of fitting first, second and third order AR models to the data and selecting one that best represents the data. The choice is made by minimising the AIC.

- The displayed result consists of a parameter trend control chart of the and the static alarm and trip limits. The residuals of the fitted models along with the upper and lower limits are given to detect any significant signal shifts.
- The dynamic limit check refers to the comparison of the generated residuals to the UCL and LCL.

In Case Study 1, the model was trained on a machine in an unhealthy state and displayed an adequate fit to detect the mean and variance changes. A large variance shift was observed that indicated an unusual disturbance. In Case Study 2, the model was trained on a healthy machine and was also detecting the mean shift changes successfully.

An advantage of the proposed fault detection model is to detect changes that occur due to factors outside normal operation. With this model, faults can be detected within the specified alarm and trip limits. Another advantage is that the model can be applied generically to different machinery without additional information about the alarm or trip limits.

5.3. RECOMMENDATIONS

The recommendations for future studies are as follows:

- The extent of interchangeability of the method should be determined in future studies. Wang & Wong (2002) states that an AR model with the order p , $AR(p)$, built on a stationary process will be able to predict stationary processes that are of the same family. The extent of the statement should be tested to determine if the model only applies to similar equipment such as different sizes of pumps, or different models of the same size pump.
- The effect of the model training period should be examined. Future studies should determine if the AR model should be trained on healthy equipment, or to what extent the model will be accurate if it is trained using unhealthy equipment.
- Linear AR models with larger orders should be evaluated.
- Other AR analysis techniques such as ANNs and radial basis functions have to be evaluated and compared to linear regression models.
- By benchmarking the AR residuals for various types of equipment, the mean and variance shift trends can be compared to previous test results. Thereby, the fault detection probability can be increased.

REFERENCE LIST

- Amari, S. V. & McLaughlin, L. 2006. Cost-effective condition-based maintenance using markov decision processes. *Annual Reliability and Maintainability Symposium, 2006 (RAMS '06)*, 0(C):464–469. DOI: 10.1109/RAMS.2006.1677417.
- Ashlock, D. & Warren, A. 2015. The engineer's guide to signal conditioning. Available at: ftp://ftp.ni.com/evaluation/signal_conditioning/20712_Benefits_of_Integrated_SC_WP_HL.pdf.
- Baillie, D. C. & Mathew, J. 1996. A comparison of autoregressive modelling techniques for fault diagnosis of rolling bearings. *Mechanical Systems and Signal Processing*, 10(1):1–17.
- Bansal, D., Evans, D. J. & Jones, B. 2005. Application of a real-time predictive maintenance system to a production machine system. *International Journal of Machine Tools and Manufacture*, 45(10):1210–1221. DOI: 10.1016/j.ijmachtools.2004.11.029.
- Bauer, B., Gerop, B. & Seeliger, A. 1998. Condition monitoring and predictive maintenance in mining industry using vibration analysis for diagnosis of gear boxes. *International Federation of Automatic Control*.
- Baydar, N., Chen, Q. & Ball, A. 2002. Detection of incipient tooth defect in helical gears using multivariate statistics. *Mechanical Systems and Signal Processing*, 15(2):303–321.
- Beebe, R. S. 2004. Condition monitoring. DOI: 10.1049/tpe.1987.0113.
- Bloch, H. P. 1990. Root cause analysis of five costly centrifugal pump failures. *Seventh International Pump User Symposium*, 15–26. Available at: <http://turbolab.tamu.edu/proc/pumpproc/P7/P715-25.pdf>.
- Booth, C. & McDonald, J. . 1998. The use of artificial neural networks for condition monitoring of electrical power transformers. *Neurocomputing*, 23(1–3):97–109. DOI: 10.1016/S0925-2312(98)00064-2.
- Brodgesell, A., Lipták, B. G. & Eren, H. 2003. Safety and miscellaneous sensors. In Lipták, B. (ed.) *Instrument engineers' handbook: Process measurement and analysis*. 4th ed. CRC press, 1061–1076. Available at: <http://www.library.wisc.edu/selectedtocs/aa751x.pdf>.
- Campbell, J., Lilly, L. & Maddox, R. 1992. Gas conditioning and processing: The equipment

modules. *Gas Conditioning and Processing Vol. 2*, 162–165.

Chindondondo, B., Nyanga, L., Van der Merwe, A., Mupinga, T. & Mhlanga, S. 2014. Analysis of a time based and corrective maintenance system for a sugar producing company. In *Southern African Institute for Industrial Engineering*, 1–14.

Costinas, S. & Comanescu, G. 2004. Developing strategies for maintenance management of electrical substation equipment. In *The Fifth International World Energy System Conference*.

Crystal Instruments. 2017a. Condition monitoring systems. Available at: https://www.crystalinstruments.com/spider80x-machine-condition-monitoring-system?gclid=CjwKEAjjwvOzOBRDG95DXw43t8V0SJACAO8aHJ44WvdMI8YmKfcy_4hC7K_Hf0CQ8I4WuQbTAK8kSARoC-8Hw_wcB. Date of access: 12 April 2017.

Crystal Instruments. 2017b. Dynamic Signal Analyzers & Systems. Available at: <https://www.crystalinstruments.com/dynamic-signal-analyzers/>. Date of access: 15 October 2017.

Davies, A. 1998. Handbook of condition monitoring: Techniques and methodology. 1st ed. Chapman & Hall.

Devore, J. & Farnum, N. 2005. Applied statistics for engineers and scientists. 3rd ed. Cengage Learning.

Etchson, D. M. 2017. The impact of equipment reliability on human safety. *Production Technology*. Available at: <http://production-technology.org/the-impact-of-equipment-reliability-on-human-safety/#more-993>. Date of access: 20 October 2017.

Fugate, M., Sohn, H. & Farrar, C. 2001. Vibration-based damage detection using statistical process control. *Mechanical Systems and Signal Processing*, 15(4):707–721. DOI: 10.1006/mssp.2000.1323.

Gouws, R. 2007. Condition monitoring of active magnetic bearing systems. PhD Thesis. Potchefstroom: NWU.

Grimmelius, H. T. 1999. Three state-of-the-art methods for condition monitoring. *IEEE Transactions on Industrial Electronics*, 46(2):407–416. DOI: 10.1109/41.753780.

Guenel, A., Meshram, A. P., Bley, T., Klusch, M. & Schuetze, A. 2013. Statistical and semantic multisensor data evaluation for fluid condition monitoring in wind turbines. In *Proceedings of*

the 16th International Conference on Sensors and Measurement Technology (SENSOR). International Conference on Sensors and Measurement Technology (SENSOR-13), 16th, May 14-16, Nuremberg, Germany, 604–609. DOI: 10.5162/sensor2013/D8.1.

Guo, P., Infield, D. & Yang, X. 2012. Wind turbine generator condition monitoring using temperature trend analysis. *IEEE Transactions on Sustainable Energy*, 3(1):124–133.

Guo, R., Chen, A., Tseng, C., Fong, I., Yang, A., Lee, C., Wu, C., Lin, S., Huang, S., Lee, Y., Chang, S. & Lee, M. 1998. A real-time equipment monitoring and fault detection system. *Semiconductor Manufacturing Technology Workshop, 1998*, 111–121. DOI: 10.1109/SMTW.1998.722666.

Han, Y. & Song, Y. H. 2003. Condition monitoring techniques for electrical equipment: A literature survey. *IEEE Transactions on Power Delivery*, 18(1):4–13. DOI: 10.1109/TPWRD.2002.801425.

Harmony Gold Mining Company Limited. 2017. 2017 Results. Available at: <https://investor.ryanair.com/wp-content/uploads/2017/05/FY17-Results.pdf>.

ISO. 2009. ISO 10816-3. Mechanical vibration -- Evaluation of machine vibration by measurements on non-rotating parts -- Part 3: Industrial machines with nominal power above 15 kW and nominal speeds between 120 r/min and 15 000 r/min when measured in situ

Jardine, A. K. S., Lin, D. & Banjevic, D. 2006. A review on machinery diagnostics and prognostics implementing condition-based maintenance. *Mechanical Systems and Signal Processing*, 20(7):1483–1510. DOI: 10.1016/j.ymssp.2005.09.012.

Jasinski, S. M. 2017. Mineral commodities summaries, U.S. geological survey. DOI: <http://dx.doi.org/10.3133/70140094>.

Johansson, M. 2010. Effective process monitoring in underground mining. In *Fourth International Platinum Conference: Platinum In Transition 'Boom or Bust'*. Southern African Institute of Mining and Metallurgy, 223–230.

Jun, C. H. & Suh, S. H. 1999. Statistical tool breakage detection schemes based on vibration signals in NC milling. *International Journal of Machine Tools and Manufacture*, 39(11):1733–1746. DOI: 10.1016/S0890-6955(99)00028-0.

Karakurt, I., Aydin, G. & Aydiner, K. 2011. Mine ventilation air methane as a sustainable energy source. *Renewable and Sustainable Energy Reviews*. Elsevier Ltd, 15(2):1042–1049.

DOI: 10.1016/j.rser.2010.11.030.

Kleijnen, J. P. C. 1999. Validation of models : Statistical techniques and data availability. In *Proceedings of the 1999 Winter Simulation Conference*, 647–654. DOI: 10.1145/324138.324450.

Krauel, C. & Weishäupl, L. 2016. Multivariate approach for equipment health monitoring. *International Federation of Automatic Control-PapersOnLine*. Elsevier B.V., 49(12):716–720. DOI: 10.1016/j.ifacol.2016.07.858.

Kullaa, J. 2003. Damage detection of the Z24 bridge using control charts. *Mechanical Systems and Signal Processing*, 17(1):163–170. DOI: 10.1006/mssp.2002.1555.

Lonmin Plc. 2017. 2017 Interim Results. Available at: <https://www.lonmin.com/investors/reports-and-presentations>

Louit, D. M. & Knights, R. F. 2001. Simulation of initiatives to improve mine maintenance. *Mining Technology: Transactions of the Institutions of Mining and Metallurgy: Section A*, 110(1):47–58. DOI: <http://dx.doi.org/10.1179/mnt.2001.110.1.47>.

Marais, H., Schoor, G. Van, Uren, K. R., Schoor, V., Kenneth, R., Marais, H., Van, G., Schoor, V., Kenneth, R. & Uren, R. 2015. An energy-based approach to condition monitoring of industrial processes. *International Federation of Automatic Control*. Elsevier B.V., 48(21):772–777. DOI: 10.1016/j.ifacol.2015.09.620.

Mkema, R. 2011. Maintenance procedures and practices for underground mobile mining equipment. MEng Dissertation. Luleå: Luleå University of Technology.

Moubray, J. 1997. Reliability-centered maintenance. 2nd ed. Industrial Press Inc.

Munio, M. C. 2017. Predictive vs. Preventive: The debate and the future. *Plant Engineering*, 40–42.

Murray, B. G. 1989. Pump performance - Its application to condition monitoring. In *Proceedings of the First International Congress on Condition Monitoring and Diagnostic Engineering Management*, 183.

Nandi, S., Toliyat, H. A. & Li, X. 2005. Condition monitoring and fault diagnosis of electrical motors - A review. *IEEE Transactions on Energy Conversion*, 20(4):719–729. DOI: 10.1109/TEC.2005.847955.

Neale, M. J. & Woodley, B. J. 1975. Condition monitoring methods and economics. *Symposium of the Society of Environmental Engineers*.

Neingo, P. N. & Tholana, T. 2016. Trends in productivity in the South African gold mining industry, 6(November 2015):8–11.

Oberholzer, P. J. 2014. Best practices for automation and control of mine dewatering systems. MEng Dissertation. Potchefstroom: NWU.

Ogidi, O. O., Barendse, P. S. & Khan, M. A. 2016. Fault diagnosis and condition monitoring of axial-flux permanent magnet wind generators. *Electric Power Systems Research*. Elsevier B.V., 136:1–7. DOI: 10.1016/j.epsr.2016.01.018.

Page, E. S. 1954. Continuous inspection schemes. *Biometrika*, 41:100–114.

Prakash Kumar & Srivastava, R. 2014. Development of a condition based maintenance architecture for optimal maintainability of mine excavators. *IOSR Journal of Mechanical and Civil Engineering (IOSR-JMCE)*, 11(3):18–22. Available at: <http://www.iosrjournals.org/iosr-jmce/papers/vol11-issue3/Version-5/C011351822.pdf>.

Rall, D., Lipták, B. G., Moore, W. L. & Adler, B. 2003. Temperature measurement. In Lipták, B. G. (ed.) *Engineers' handbook: Process measurement and analysis*. 4th ed, 565–708.

Reynolds, M. R., Amin, R. W. & Arnold, J. C. 1990. CUSUM charts with variable sampling intervals. *Technometrics*, 32(4):371. DOI: 10.2307/1270114.

Reynolds, M. R. & Lu, C.-W. 1997. Control charts for monitoring processes with autocorrelated data. *Proceedings of the 2nd World Congress of Nonlinear Analysts*, 30:4059–4067.

Rockwell Automation 2017a. Condition monitoring. Available at: <http://ab.rockwellautomation.com/Condition-Monitoring>. Date of access: 12 April 2017.

Rockwell Automation 2017b. Emonitor condition monitoring software. Available at: <http://ab.rockwellautomation.com/Condition-Monitoring/9309-Emonitor-Software>.

Sargent, R. G. 2012. Verification and validation of simulation models. *Nature Publishing Group*, 7(1):12–24. DOI: 10.1057/jos.2012.20.

Schlechtingen, M. & Santos, I. F. 2010. Comparative analysis of neural network and

regression based condition monitoring approaches for wind turbine fault detection. *Mechanical Systems and Signal Processing*, 25(5):1849–1875.

Schneider Electric Software. 2016. Historian Concepts Guide. Available at: <https://www.logic-control.com/datasheets/1/Historian/HistorianConcepts.pdf>.

Shafiee, M., Finkelstein, M. & Bérenguer, C. 2015. An opportunistic condition-based maintenance policy for offshore wind turbine blades subjected to degradation and environmental shocks. *Reliability Engineering and System Safety*, 142:463–471. DOI: 10.1016/j.ress.2015.05.001.

Sherwin, D. J. & Al-Najjar, B. 1999. Practical models for condition monitoring inspection intervals. *Journal of Quality in Maintenance Engineering*, 5(3):203–222.

Siemens South Africa 2009. Planning and monitoring preventive, condition-based, reactive maintenance activities. Available at: http://www.siemens.co.za/en/news_press/news2009/may_06_2009_7.htm.

Sitayeb, F. B., Guebli, S. A., Bessadi, Y., Varnier, C. & Zerhouni, N. 2011. Joint scheduling of jobs and preventive maintenance operations in the flowshop sequencing problem: A resolution with sequential and integrated strategies. *International Journal of Manufacturing Research*, 6(1):30–48. DOI: 10.1504/IJMR.2011.037912.

SKF 2017. SKF Online Motor Analysis System - NetEP software. Available at: <http://www.skf.com/group/products/condition-monitoring/surveillance-systems/on-line-systems/motor-performance-monitoring-netep/skf-motor-condition-surveyor/index.html>. Date of access: 27 October 2017.

Statistics South Africa. 2015. The decreasing importance of gold mining in South Africa. Available at: <http://www.statssa.gov.za/?p=4252>. Date of access: 25 February 2017.

Statistics South Africa. 2016. Quarterly employment statistics. Available at: <http://www.statssa.gov.za/?p=10136>

Stephenson, D. 1983. Distribution of water in deep gold mines in South Africa. *International Journal of Mine Water*, 2(2):21–30. DOI: 10.1007/BF02504560.

Sullivan, P. G., Pugh, R., Melendex, P. A. & Hunt, D. W. 2010. Types of maintenance programs. *Operations & Maintenance Best Practices*, 1–9. Available at: http://www1.eere.energy.gov/femp/pdfs/omguide_complete.pdf.

TAS Online 2017. Remote monitoring. Available at: <http://www.tasonline.co.za/remotemonitoring.htm>. Date of access: 16 May 2017.

Tavner, P. J. 2008. Review of condition monitoring of rotating electrical machines. *IET Electric Power Applications*. DOI: 10.1049/iet-epa:20070280.

Večeř, P., Kreidl, M. & Šmíd, R. 2005. Condition indicators for gearbox condition monitoring systems. *Acta Polytechnica*, 45(6):35–43.

Wang, T., Chu, F., Han, Q. & Kong, Y. 2017. Compound faults detection in gearbox via meshing resonance and spectral kurtosis methods. *Journal of Sound and Vibration*, 392:367–381. DOI: 10.1016/j.jsv.2016.12.041.

Wang, W. & Wong, A. K. 2002. Autoregressive model-based gear fault diagnosis. *Journal of Vibration and Acoustics*, 124(2):172. DOI: 10.1115/1.1456905.

Wasif, H., Brown, D., Aboutaleb, A. & Axel-berg, L. 2012. Condition monitoring system for process industries A business approach. In *IEEE Symposium on Industrial Electronics and Applications*, 251–256.

WearCheck. 2017. Reliability solutions. Available at: <http://www.wearcheck.co.za/reliability-solutions>. Date of access: 27 October 2017.

Wessels, W. R. 2003. Cost-optimized scheduled maintenance interval for reliability-centered maintenance. *Annual Reliability and Maintainability Symposium, 2003.*, 412–416. DOI: 10.1109/RAMS.2003.1182024.

Wiggelinkhuizen, E., Verbruggen, T., Braam, H., Xiang, J., Scheffler, D., Becker, E., Christensen, A., Tipluica, M., Norton, E. & Giebel, G. 2007. CONMOW: Condition monitoring for offshore wind farms. In *Proceedings of the 2007 EWEA European Wind Energy Conference*. Milan, 7–10. Available at: <http://www.ecn.nl/publications/PdfFetch.aspx?nr=ECN-M--07-037>.

Wilson, J. W. & Taylor, J. G. 1975. The mechanization of haulage drilling in the gold mines of Anglo American Corporation. *Journal of the Southern African Institute of Mining and Metallurgy*, 75(January):151–162.

Yang, W., Court, R. & Jiang, J. 2013. Wind turbine condition monitoring by the approach of SCADA data analysis. *Renewable Energy*. Elsevier Ltd, 53:365–376. DOI: 10.1016/j.renene.2012.11.030.

- Yang, W., Tavner, P. J., Crabtree, C. J., Feng, Y. & Qui, Y. 2014. Wind turbine condition monitoring: Technical & commercial challenges. *Wind Energy*, 17(5):673–693.
- Yates, M. 2002. Pump performance monitoring complements condition. *World Pumps*, (May):36–38.
- Zhang, N., Yang, M., Gao, B. & Li, Z. 2014. Vibration characteristics induced by cavitation a centrifugal pump with slope volute, 2015:1–10. DOI: 10.1155/2014/936218.
- Zhang, S., Mathew, J., Ma, L., Sun, Y. & Mathew, A. D. 2004. Statistical condition monitoring based on vibration signals. *Proceedings of VETOMAC-3 & ACSIM-2004*, 2004:1238–1243. Available at: <http://eprints.qut.edu.au/13310/1/13310.pdf>.
- Zhou, W., Habetler, T. G. & Harley, R. G. 2007. Bearing condition monitoring methods for electric machines: A general review. *2007 IEEE International Symposium on Diagnostics for Electric Machines, Power Electronics and Drives*, 3–6. DOI: 10.1109/DEMPED.2007.4393062.

Appendix A SYMPTOMS OR PARAMETERS THAT ARE RELEVANT TO PUMPS

<i>Fault</i>	<i>Fluid Leakage</i>	<i>Length / dimensions</i>	<i>Power</i>	<i>Head, Pressure</i>	<i>Flow</i>	<i>Speed</i>	<i>Vibration</i>	<i>Temperature</i>	<i>Time to coast down</i>	<i>Wear debris in oil</i>	<i>Oil Leakage</i>
<i>Damaged impeller</i>		S	S	S	S	S	S	S	S		
<i>Damaged external seals</i>	S	S		S		S	S				
<i>Eroded casing</i>		S									
<i>Worn sealing rings</i>			S	S	S						
<i>Eccentric impeller</i>			S	S		S	S	S	S		
<i>Bearing damage</i>		S	S			S	S	S	S	S	S
<i>Bearing wear</i>		S					S	S	S	S	
<i>Mounting fault</i>							S	S			
<i>Unbalance</i>							S				
<i>Misalignment</i>		S					S				

S: Symptoms that may occur, or parameter change with fault, according to pump design

FIGURE A-1 SYMPTOMS OR PARAMETERS THAT ARE RELEVANT TO PUMPS
(BEEBE, 2004)

Appendix B THE INDICATORS OF MACHINE AND COMPONENT DETERIORATION

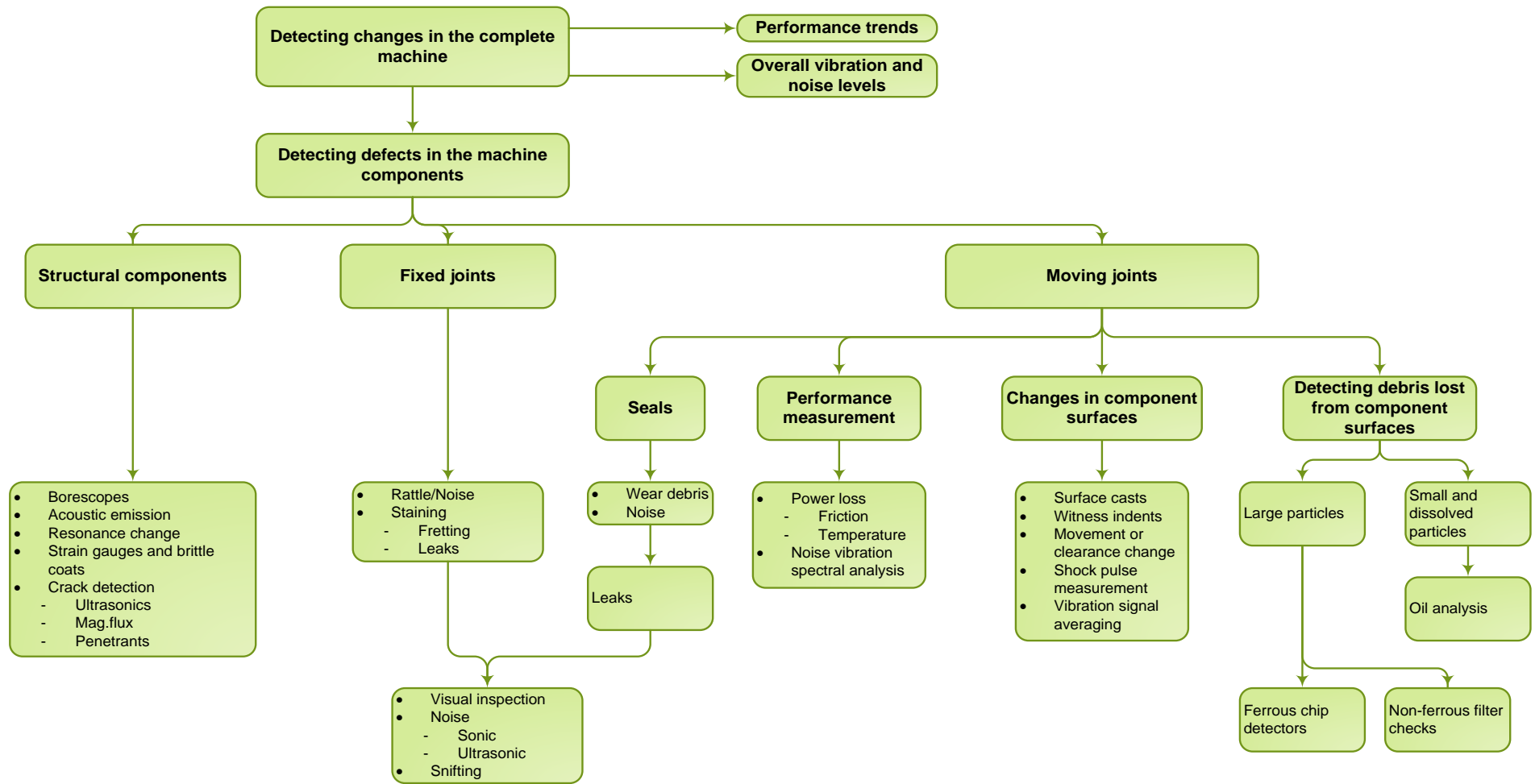


FIGURE B-1 THE INDICATIONS OF COMPONENT DETERIORATION (NEALE & WOODLEY, 1975)

Appendix C REGRESSION ANALYSIS

The statistical calculations in the study were using the equations presented in Appendix C. Figure C-1 provides a supplementary illustration of how the actual and modelled values are used to determine the explained and unexplained variance.

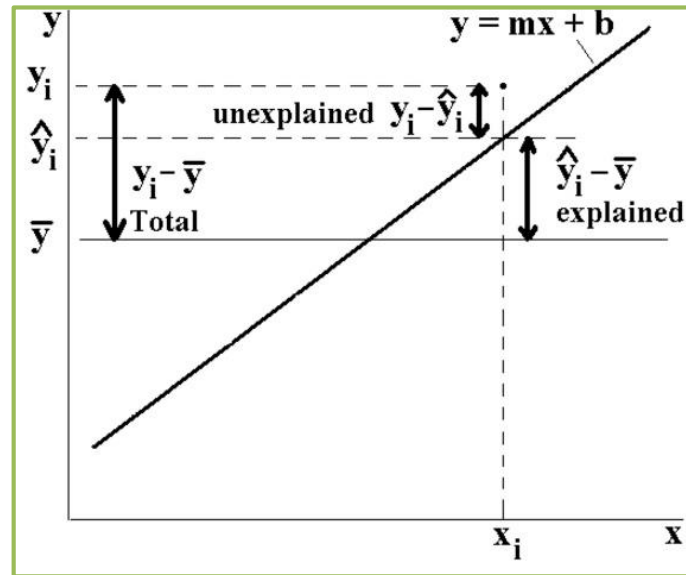


FIGURE C-1 MODELLED DATA STATISTICS

The MSE is calculated using Equation C.1

$$MSE = \frac{1}{n} \sum_{i=1}^n (y_i - \hat{y}_i)^2 \quad (C.1)$$

Where:

- n is the number of observations
- y_i is the actual value for data point i
- \hat{y}_i is the predicted or fitted value

The residuals or EV are calculated using Equation C.2

$$EV = y_i - \hat{y}_i \quad (C.2)$$

Where:

- y_i is the actual value for data point i
- \hat{y}_i is the predicted or fitted value

The mean MAE is calculated using Equation C.3.

$$MAE = \sum_{i=1}^n |\hat{y}_i - \bar{y}| \quad (C.3)$$

Where:

- \bar{y} is the value returned by the model
- \hat{y}_i is the actual value for data point i

The variance (σ^2) is calculated using Equation C.4.

$$\sigma^2 = \sum \frac{(X - \mu)^2}{N} \quad (C.4)$$

Where:

- X is the measured quantity variable
- μ is the mean of the sample
- N is the number of terms in the distribution

The standard deviation, σ , is the positive square root of the variance, σ^2 .

For the analysis of the AR model, a different set of regression statistics are used.

The coefficient of multiple determination, R^2 , is calculated with Equation C.5.

$$R^2 = 1 - \frac{SSResid}{SSTo} \quad (C.5)$$

Where:

- $SSResid$ is the sum of the squared residuals
- $SSTo$ the total sum of squares defined in Equation C.6

$$SSTo = \sum (y_i - \bar{y})^2 \quad (C.6)$$

The adjusted R^2 for multiple regression is calculated with Equation C.7.

$$adjusted R^2 = 1 - \frac{SSResid/[n - (k + 1)]}{SSTo/(n - 1)} = 1 - \left[\frac{n - 1}{n - (k + 1)} \frac{SSResid}{SSTo} \right] \quad (C.7)$$

Appendix D VIBRATION INSTRUMENT SPECIFICATIONS

ST5484E Seismic Velocity 4-20 mA Transmitter

Datasheet

OVERVIEW

The ST5484E is a self-contained seismic velocity transmitter that incorporates a piezoelectric accelerometer, signal integrator, RMS peak detector, and a 4-20 mA signal conditioner into a single package. It can be mounted directly on a machine case or bearing housing without intervening signal conditioning equipment. The amplitude of the integrated acceleration (velocity) signal is converted to a proportional 4-20 mA signal compatible with industrial process control instrumentation such as PLCs, DCSs, and SCADA systems that can provide trending and/or alarming capabilities for a simplified vibration monitoring strategy.

When the flying lead or terminal block connector options are chosen, the transmitter does not need a separate environmental housing and can directly accept conduit. To reduce installed cost, it can be used with barriers for intrinsically safe installations, or wired directly to explosion-proof conduit fittings for explosion-proof installations.



Need A Local Display?

When continuous, local indication of vibration levels is required at the transmitter, the Metrix ST5491E provides these capabilities. Its sensing and transmitter elements are similar to the ST5484E, but it includes a convenient 2½ digit LCD display in an integral conduit elbow and is rated for use in temperatures from -10°C to +70°C. Refer to Metrix datasheet 1004598 for ordering information and detailed specifications.



Flying Leads
(Option D=0, 1, 5, or 6) (2-wire shown; 4-wire also available)



4-Pin Terminal Block
(Option D=3)



2-Pin Terminal Block
(Option D=2)



2-Pin MIL Connector
(Option D=4)



Why Measure Velocity?

Acceleration and displacement levels are heavily influenced by the frequencies at which the vibration is occurring, while velocity levels are much less influenced. Thus, although acceleration, velocity, and displacement measurements are inter-related mathematically, seismic velocity measurements tend to be more consistent over a wide range of frequencies than either displacement or acceleration. Consequently, broadband (sometimes called "overall" or "unfiltered") velocity measurements are appropriate for monitoring many machines as a reliable indicator of damaging vibratory energy, with the notable exception of machines with fluid-film bearings, which are usually better addressed by shaft-observing proximity probes.

Casing displacement is not a practical measurement to make directly and is typically just an integrated seismic velocity measurement. As such, the primary decision when selecting a seismic sensor will usually be whether to measure casing velocity or casing acceleration. As noted above, casing velocity will often be more appropriate because it tends to be a more reliable indicator of damaging vibratory energy over a broad frequency spectrum for low- to medium-speed machinery.





NOTE: For machines with fluid-film bearings, shaft-observing proximity probes will provide more effective vibration measurements than seismic transducers due to the rotor dynamics of the machine and the attenuation of vibratory energy through a fluid-film boundary. Accordingly, Metrix recommends and provides proximity probes and associated 4-20 mA transmitters or monitoring systems for such applications.

For machines with rolling element bearings and running above 6,000 rpm, and/or where impulsive casing vibration occurs, acceleration may be a better measurement. In such situations, it is recommended that you consult with a Metrix sales professional who can review your application and assist with selection of the proper transducer type and associated transmitter or monitoring system.

FEATURES

- **RFI/EMI Immunity** – Enhanced circuit design and installation techniques aggressively filter out noise from common sources such as handheld radios
- **Excellent Moisture Resistance** – The 2-pin MIL connector version is hermetically sealed to provide an IP67-rated enclosure. Flying lead and terminal block versions are fully potted and rated to IP66 when installed with optional IEC conduit elbow
- **Hazardous Area Approvals** – North American (CSA), Brazilian (INMETRO), and European (ATEX & IEC) approvals available
- **Dynamic Signal Availability** – 2-wire versions provide a 4-20 mA velocity-proportional signal for easy connection to PLCs, DCSs, and other plant control systems. Optional 4-wire versions¹ also provide the raw acceleration signal (100 mV/g) for use with vibration data collectors and analyzers
- **Variety of Connection Options** – Flying leads, terminal block, and MIL-type connectors available
- **Conduit-Ready²** – Terminal block and flying lead options have conduit threads on top of sensor. No special housings are required for connection of conduit
- **Rugged, Industrial Design** – Robust construction offers outstanding durability; built-in base and housing strain protection helps ensure that over-torquing sensor-to-machine and sensor-to-conduit connections won't damage internals or body
- **High- and Low-Pass Filter Options** – The ST5484E can be ordered with a wide variety of low- and high-pass filter options to precisely tailor the band over which vibration is measured
- **Polarity-Independent Wiring** – Metrix patented IPT[®] technology allows loop power to be connected without regard to voltage polarity, reducing field wiring errors and ensuring that the raw acceleration output⁴ is not phase inverted
- **Multiple Mounting Options** – Integral and removable mounting stud options available in both metric and English thread sizes; flat base mounting adapters are also available
- **Loop-Powered** – Runs on nominal 24 V_{DC} power supplied by the 4-20 mA current loop
- **Wide Supply Voltage Range** – Accepts loop power voltages from 11 to 29.6 V_{DC} (intrinsically safe) or 30.0 V_{DC} (explosion proof & non-incendive)

- **RMS Amplitude Detection** – Measures Root Mean Square (RMS) vibration amplitude. Options available for True RMS or scaled RMS (RMS x V₂) for “derived peak”
- **Numerous Full Scale Ranges** – The full scale ranges provided in option AAA reflect frequently-ordered ranges; however, many others (too numerous to list) are also available. Consult factory for applications requiring other full scale ranges

Notes:

1. Dynamic raw acceleration signal available with 4-wire versions only (ordering options D=1 and D=3).
2. Metrix recommends flexible (rather than solid) conduit when possible. Solid conduit can introduce preload forces on the sensor and alter the vibration response of the sensor.

SPECIFICATIONS

All specifications are at +25°C (+77°F) and +24 V_{DC} supply voltage unless otherwise noted.

Inputs	
Supply Voltage (see also note under max loop resistance)	11 – 29.6 V _{DC} (24 V _{DC} nominal) (intrinsically safe); 11 – 30 V _{DC} (24 V _{DC} nominal) (explosion proof and non-incendive); Metrix patented IPT [®] independent polarity diode bridge circuit allows voltage to be connected without regard to polarity
Circuit-to-Case Isolation	500 Vrms
Outputs	
4-20 mA	Proportional to velocity full scale range (4mA = 0 vibration, 20mA = full scale vibration)
Maximum 4-20 mA loop resistance	R _L = 50 x (V _S – 11) Ω where V _S = Supply voltage at transmitter terminals. NOTE: For every 50 Ω of resistance in the 4-20 mA loop, 1 V _{DC} above the minimum supply voltage (11 V _{DC}) must be available at the transmitter terminals. For example, 12 V _{DC} at the transmitter terminals will allow a 50 Ω loop resistance; 30 V _{DC} at the transmitter terminals will allow a 950 Ω loop resistance. For intrinsically safe applications, the use of a passive zener barrier will incur a voltage drop of approximately 8.1 volts at the barrier, and the loop supply voltage is limited to 26 V _{DC} . Thus, with passive barriers and a 26 V _{DC} supply, the maximum available voltage at the transmitter will be 17.9 V _{DC} and the corresponding maximum loop resistance will be 345 Ω.
Dynamic Signal	100 mV/g (10.2 mV / m/s ²) acceleration, filtered to same frequency band as proportional velocity (see ordering options E & F)



Dynamic Signal Output Impedance	10 kΩ NOTES: 1. The dynamic signal output is short-circuit protected by means of a 10 kΩ resistor, resulting in a relatively large output impedance. Many data collectors and analyzers have relatively low input impedances (100 kΩ or less) which will load this dynamic output and attenuate the signal by 10% or more. Refer to Table 1 for the dB and percentage attenuation for various load impedances. 2. Because the ST5484E is a loop-powered device with low operating power, the dynamic signal output requires a buffer amplifier for cable runs in excess of 16 feet (5 meters). Longer cable runs will also introduce distributed cable capacitance that acts as a low-pass filter, attenuating high-frequency signal content. In such situations, consult the factory for assistance selecting an appropriate low-capacitance cable.
Recommended Minimum Load Impedance (Zload) for Dynamic Signal Connection	500 kΩ (see also note 1 above)
Signal Processing	
Frequency Response (+/- 3dB passband)	2 Hz – 1500 Hz (standard) 2 Hz – 2000 Hz (optional)
Optional High-Pass Filter Corner	5, 10, 20, 50, 100, or 200 Hz (must be specified at time of ordering)
High-Pass Roll-Off	12 dB / octave
Optional Low-Pass Filter Corner	230, 250, 350, 450, 500, or 1000 Hz (must be specified at time of ordering)
Low-pass Roll-Off	12 dB / octave
Accuracy	± 2.5% (within passband) ± 4% (at corner frequencies)
Maximum Full Scale	5.0 in / sec (others by request)
Minimum Full Scale	0.5 in / sec (others by request)
Full Scale Range Units	• in / sec (standard) • mm / sec (available by request)
Amplitude Detection	True RMS detector; full scale may be ordered with True RMS units or scaled RMS (RMS x √2) for "derived peak" measurements See ordering option AAA.

Physical	
Operating Temperature	-40°C to +100°C (-40°F to +212°F)
Weight	0.9 lbs (0.36 kg)
Dimensions	Refer to Figures 1 and 2 on page 8
Sensitive Axis	Same as mounting stud axis
Axis Orientation	Any
Enclosure Material	• 303 stainless steel (standard) • 316L stainless steel (optional)
Enclosure Rating	MIL-Style Connector (option D=4): • IP67 and NEMA 4X Flying Leads and Terminal Block Connectors (option D=4): • IP66 when used with the following conduit elbows: 8200-001-IEC, 8200-002-IEC, 8200-003-IEC, 8200-008-IEC, 8200-009-IEC • No Rating* when used with the following conduit elbows: 8200-001, 8200-002, 8200-003, 8200-005, 8200-006, 8200-008, 8200-009, 8200-010, 8200-101, 8200-103, 8200-108 * NOTE: IP and NEMA ratings pending; refer to table on page 6.
Connector Types	• Flying Leads (2- and 4-wire) • MIL-C-5015 (2-wire only) • Terminal Block (2- and 4-wire)
Humidity	• 95%, non-condensing (flying lead and terminal block versions) • 100% condensing (MIL-style connector)
Approvals	
CE Mark	• Yes
Hazardous Areas	• CSA • ATEX • IECEx • INMETRO • GOST (consult factory) (refer to ordering option C)
Recommended IS Barriers	
Passive (Zener Type)	MTL 7787+ or equal
Active (Zener Type)	MTL 7706 or equal
Active (Galvanic Type)	MTL 5541 or equal
ST5484E Entity Parameters	• Vmax: 29.6 V _{DC} (intrinsically safe) • Vmax: 30 V _{DC} (explosion proof and non-incendive) • Imax: 100 mA



ORDERING INFORMATION

AAA - B C D - E F
ST5484E-□□□-□□□□□□

AAA			Full Scale Range ¹
	1	2	1.0 in/sec (25.4 mm/s) peak ²
	1	2	0.5 in/sec (12.7 mm/s) peak ²
	1	2	2.0 in/sec (50.8 mm/s) peak ²
	1	2	5.0 in/sec (127 mm/s) peak ²
	1	2	0.8 in/sec (20.3 mm/s) peak ²
	1	3	3.0 in/sec (76.2 mm/s) peak ²
	1	5	1.0 in/sec (25.4 mm/s) true RMS
	1	5	0.5 in/sec (12.7 mm/s) true RMS
	1	5	2.0 in/sec (50.8 mm/s) true RMS
	1	5	5.0 in/sec (127 mm/s) true RMS
	1	5	0.8 in/sec (20.3 mm/s) true RMS
	1	6	3.0 in/sec (76.2 mm/s) true RMS

B		Housing Material & Stud Size ¹
	0	303 SS housing, 1/4" NPT stud
	1	303 SS housing, 1/2" NPT stud
	2	303 SS housing, 3/8 x 24 UNF – 1/2" stud
	3	303 SS housing, 1/2 x 20 UNF – 1/2" stud
	4	303 SS housing, M8 x 1.0 – 12 stud
	5	303 SS housing, M10 x 1.25 – 12 stud
	6	303 SS housing, 3/8 x 20 UNC – 1/2" stud
	7	303 SS housing, 1/4 x 28 UNF – 1/2" stud
	8	303 SS housing, M8 x 1.25 – 12 stud
	9	303 SS housing, 3/8 x 16 UNC – 1/2" stud
	10	316 SS housing, 1/4" NPT stud
	11	316 SS housing, 1/2" NPT stud
	12	316 SS housing, 3/8 x 24 UNF – 1/2" stud
	13	316 SS housing, 1/2 x 20 UNF – 1/2" stud
	14	316 SS housing, M8 x 1.0 – 12 stud
	15	316 SS housing, M10 x 1.25 – 12 stud
	16	316 SS housing, 3/8 x 20 UNC – 1/2" stud
	17	316 SS housing, 1/4 x 28 UNF – 1/2" stud
	18	316 SS housing, M8 x 1.25 – 12 stud
	19	316 SS housing, 3/8 x 16 UNC – 1/2" stud
	20	303 SS housing, 1/2 x 13 UNC – 1/2" stud
	30	316 SS housing, 1/2 x 13 UNC – 1/2" stud

C		Hazardous Area Certification ^{3,4,5}
	0	No Hazardous Approval Area
	1	CSA US/C, Class I, Div 2, Grps A-D (non-incendive)
	2	CSA US/C, Class I, Div 1, Grps B-D and Class II, Div 1, Grps E-G (explosion proof)
	3	ATEX, EEx ia IIC T4 Ga (intrinsically safe)
	4	CSA US/C, Class I, Div 1, Grps A-D (intrinsically safe)
	5	INMETRO, Ex ia IIC T4 Ga (intrinsically safe)
	6	INMETRO, Ex d IIC T4 Gb (explosion proof)
	7	IECEX, Ex ia IIC T4 Ga (intrinsically safe)
	8	ATEX/IECEX, Ex d IIC T4 Gb (explosion proof)

D		Connection Type ³
	0	24" Flying Leads, 2-wire; (4-20 mA output only)
	1	24" Flying Leads, 4-wire; (4-20 mA output and dynamic raw acceleration signal)
	2	Terminal Block, 2-wire ⁶ ; (4-20 mA output only)
	3	Terminal Block, 4-wire ⁶ ; (4-20 mA output and dynamic raw acceleration signal)
	4	2-Pin MIL-Style (MIL-C-5015); (4-20 mA output only)
	5	72" Flying Leads, 2-wire; (4-20 mA output only)
	6	72" Flying Leads, 4-wire; (4-20 mA output and dynamic raw acceleration signal)

E		High-Pass Filter
	0	2 Hz (standard)
	1	5 Hz
	2	10 Hz
	3	20 Hz
	4	50 Hz
	5	100 Hz
	6	200 Hz ⁷
	X	Custom (consult factory) ⁷

F		Low-Pass Filter
	0	1500 Hz (standard)
	1	500 Hz
	2	1000 Hz



	3	2000 Hz
	4	250 Hz ⁷
	5	230 Hz ⁷
	6	350 Hz ⁷
	7	450 Hz
	X	Custom (consult factory) ⁷

NOTES:

1. Smaller-diameter mounting studs are not able to withstand sustained ambient vibration levels above 2.0 in/sec. Consult Table 2 for allowable combinations of A and B options.
2. The ST5484E uses an RMS amplitude detection circuit. Full scale ranges in peak units use scaled RMS (i.e., RMS x $\sqrt{2}$). The "derived peak" measurements will equal true peak only under the special case of a pure sinusoid, not complex vibration signals.
3. Hazardous Area Certifications are not compatible with all connection types. Consult Table 3 for allowable combinations of C & D options.
4. Some approvals require intrinsic safety barriers, others require Explosion-Proof wiring practices. Refer to Table 4.
5. ATEX/IECEX/INMETRO Ex d (flameproof) approvals (ordering option C=8 or C=6) require conduit elbow 8200-AAA-IEC, sold separately.
6. It may be difficult to connect wires to terminal blocks with the optional 8200 conduit elbow attached. It is suggested that wires be routed through conduit elbow, then landed on terminals, and then conduit elbow secured. Use of union adapter 8201 may be required. Refer to the Accessories section of this document.
7. High- and Low-Pass filter corners for standard filters must be separated by at least one octave (low-pass frequency must be at least twice the high-pass frequency). All combinations are allowed except E = 6 and F = 4, 5, or 6. Custom filters with closer separation and/or different roll-offs may be available in some instances. Consult the factory if custom filters are required.

Data Collector / Analyzer Load Impedance (Z_{load})	Dynamic Signal Voltage Attenuation (dB)	Dynamic Signal Voltage Attenuation (%)
10 M Ω	0.01 dB	0.1%
5 M Ω	0.02 dB	0.2%
2 M Ω	0.04 dB	0.5%
1 M Ω	0.09 dB	1%
500 k Ω	0.18 dB	2%
200 k Ω	0.43 dB	5%
100 k Ω	0.84 dB	9%
50 k Ω	1.61 dB	17%
20 k Ω	3.57 dB	33%
10 k Ω	6.10 dB	50%

Full Scale Range AAA =	Allowable B options (Mounting Stud Sizes)
121, 122, 123, 126, 151, 152, 153, 156	All (no restrictions)
124 and 154	0, 1, 3, 10, 11, 13
132 and 162	0, 1, 2, 3, 5, 9, 10, 11, 12, 13, 15, 19

D \ C	0	1	2	3	4	5	6	7	8
0	Y	Y	Y	N	N	N	Y	N	Y
1	Y	Y	Y	N	N	N	Y	N	Y
2	Y	Y	N	Y	Y	Y	N	Y	N
3	Y	Y	N	Y	Y	Y	N	Y	N
4	Y	Y	N	Y	Y	Y	N	Y	N
5	Y	Y	Y	N	N	N	N	N	N
6	Y	Y	Y	N	N	N	N	N	N

C	Agency	Approved Areas	I.S. Barriers Required	Explosion-Proof Wiring Required	I.S. Barriers or XP Wiring Not Required
1	CSA US/C	Class I, Div 2, Groups A-D (non-incendive)			•
2	CSA US/C	Class I, Div 1, Groups B-D; Class II, Div 1, Groups E-G (explosion proof)		•	
3	ATEX	Ex ia IIC T4 Ga (intrinsically safe)	•		
4	CSA	Class I, Div 1, Groups A-D (intrinsically safe)	•		
5	INMETRO	Ex ia IIC T4 Ga (intrinsically safe)	•		
6	INMETRO	Ex d IIC T4 Gb (explosion proof)		•	
7	IECEX	Ex ia IIC T4 Ga (intrinsically safe)	•		
8	ATEX / IECEX	Ex d IIC T4 Gb (explosion proof)		•	



ACCESSORIES - ELBOWS

Conduit elbows are used with flying lead and terminal block versions of the ST5484E transmitter. They are not compatible with MIL-connector versions of the transmitter. A variety of available configurations accommodate English and metric conduit thread sizes, hazardous area approvals, materials of construction, and IP ratings. Most may also be purchased with or without terminal blocks under the cap. Note that not all configurations are available with hazardous area approvals or IP ratings. Consult the ordering information below.



Stainless steel elbows
(models AAA=005 and 006 only)



Copper-free aluminum elbows
(all models except
AAA=005 and 006)

ELBOWS									
A	A	A	B ^{2,5}	Conduit Fitting Size	Terminal Block	Coating	Approvals	IP Rating (Elbow)	Material
0	0	1		3/4" NPT	No	Powder	CSA/UL ¹	NEMA4	Copper-free aluminum
0	0	1	IEC	3/4" NPT	No	Powder	ATEX/IECEX ^{3,4}	IP66	Copper-free aluminum
0	0	2		1/2" NPT	4-position	Powder	CSA/UL ¹	NEMA4	Copper-free aluminum
0	0	2	IEC	1/2" NPT	4-position	Powder	ATEX/IECEX ^{3,4}	IP66	Copper-free aluminum
0	0	3		1/2" NPT	No	Powder	CSA/UL ¹	NEMA4	Copper-free aluminum
0	0	3	IEC	1/2" NPT	No	Powder	ATEX/IECEX ^{3,4}	IP66	Copper-free aluminum
0	0	5		1/2" NPT	No	None	None	None	303 stainless steel
0	0	6		1/2" NPT	4-position	None	None	None	303 stainless steel
0	0	8		M20 x 1.5 metric	No	Powder	CSA/UL ¹	NEMA4	Copper-free aluminum
0	0	8	IEC	M20 x 1.5 metric	No	Powder	ATEX/IECEX ^{3,4}	IP66	Copper-free aluminum
0	0	9		M20 x 1.5 metric	4-position	Powder	CSA/UL ¹	NEMA4	Copper-free aluminum
0	0	9	IEC	M20 x 1.5 metric	4-position	Powder	ATEX/IECEX ^{3,4}	IP66	Copper-free aluminum
0	1	0		3/4" NPT	4-position	Powder	CSA/UL ¹	NEMA4	Copper-free aluminum
1	0	1		3/4" NPT	No	Powder + clear epoxy	CSA/UL ¹	NEMA4	Copper-free aluminum
1	0	3		1/2" NPT	No	Powder + clear epoxy	CSA/UL ¹	NEMA4	Copper-free aluminum
1	0	8		M20 x 1.5 metric	No	Powder + clear epoxy	CSA/UL ¹	NEMA4	Copper-free aluminum

NOTES:








- CSA approved through manufacturer (not Metrix) for the following areas:
Class I, Div. 1 (Grps C & D)
Class II, Div. 1 (Grps E, F & G)
Class III
- B=IEC is only available for AAA=001, 002, 003, 008, and 009 at this time
- ATEX approved through manufacturer (not Metrix), (B=IEC)
ITS09ATEX16417U
Ex II2G, Ex d IIC
- IECEX approved through manufacturer (not Metrix)
IECEXITS09.0024U
Ex d IIC
- Elbow 8200-AAA-IEC is required for ST5484E installations meeting ATEX/IECEX/INMETRO Ex d (flameproof) hazardous area certifications

UL approved through manufacturer (not Metrix) for the following areas:






- Class I; Div. 1 (Grps. B, C, D)
Class II; Div. 1 (Grps. E, F, G)



ACCESSORIES - CABLES

	Part Number	Description
 <p>NOTE: Dielectric grease must be applied on the rubber boot connector to prevent moisture ingress.</p>	8978-111-XXXX	<p>2-pin MIL Splash-Proof (IP66) Cable Assembly Used with 2-pin MIL style connector. Cable-to-sensor connection made by means of tight friction fit between cable molded boot and sensor - does not use threads. Connector is fully potted to provide IP66 seal against moisture ingress. 6.4mm (0.25") diameter polyurethane jacketed cable encapsulates a single twisted pair of conductors and shield.</p> <p>XXX.X = cable length in meters (example: 0035= 3.5 m) Min. cable length: 0.5m (XXXX=0005) Max. cable length: 999.5m (XXXX=9995) Note: Must be ordered in increments of 0.5m</p>
	8978-211-XXXX	<p>2-pin MIL Cable Assembly Similar to 8978-111 but without splash-proof boot and without IP66 rating; identical constraints on XXXX ordering options.</p>
	8978-200-0000	<p>2-pin MIL Connector Assembly Similar to 8978-211 but without cable (connector can be disassembled for field installation of cable)</p>
	8978-311-XXXX	<p>2-pin MIL Submersible (IP67) Cable Assembly Similar to 8978-111 but uses overmolded screw-type connector for IP67 rating. 4.9mm (0.19") diameter polyurethane jacketed cable encapsulates a single twisted pair of 20 AWG conductors and shield. Gold plated contacts, Stainless steel 316L Nut.</p> <p>XXX.X = cable length in meters (example: 0050= 5.0 m) NOTE: only 5m, 10m, and 20m lengths available at this time. 5m length stock std; other length may incur longer lead times.</p>
	9334-111-XXXX-YYYY	<p>2-pin MIL Splash-Proof (IP66) Cable Assembly With Armor Used with 2-pin MIL-style connector. Connector is fully potted and provided with integral molded boot to provide IP66 seal against moisture ingress. 7.1mm (0.28") diameter 304 stainless steel armor encapsulates a single twisted pair of conductors and shield.</p>
 <p>NOTE: Dielectric grease must be applied on the rubber boot connector to prevent moisture ingress.</p>	9334-211-XXXX-YYYY	<p>2-pin MIL Armored Cable Assembly Similar to 9334-111 but without splash-proof boot and without IP66 rating; identical constraints on XXXX and YYYY ordering options.</p> <p>XXX.X = armor length in meters (example: 0035= 3.5 m) Min. armor length: 0.5m Max. armor length: 60m Must be ordered in 0.5m increments</p> <p>YYYY = cable length in meters Min. cable length: 1.0 Max: 999.5m Must be ordered in 0.5 m increments; NOTE: cable length must exceed armor length by at least 0.5 m.</p>
	8169-75-002-XXX	<p>2-wire Cable Assembly Designed for installations where conduit will not be used to protect field wiring. Fitting mates directly to all 8200 elbows with 3/4" NPT reducers. Cable is 2-conductor (20 AWG) twisted, shielded pair in PVC jacket. Cable grip included for strain relief. Material: zinc-plated steel</p> <p>XXX= length in feet (example: 010=10 feet) Min. cable length: 1 foot (001) Max. cable length: 999 feet (999)</p>



	8201-001	Conduit Union Fits between ST5484E and 8200 conduit elbow when there is not enough room to rotate the elbow. Suitable for Class I, Div 1 (Grps A,B,C,D) and Class II, Div 1 (Grps E,F,G) hazardous areas. Material: zinc-plated steel
	7084-001	Flange Mount Adapter Adapts ½" NPT mounting stud on ST5484E to 3-hole flat-base pattern. Hole pattern is three equally spaced 0.26" diameter holes on 1.5" diameter circle. Adapter is 2" diameter x 0.75" thick. Material: 303 stainless steel
	7084-002	Flange Mount Adapter Same as 7084-001 except center hole adapts ¼" NPT stud on the 5484E.
	7084-005	Flange Mount Adapter Same as 7084-001 except center hole adapts ¼ x 24 UNF stud on the 5484E.
	8253-002	½" NPT to ¼" NPT Reducer Bushing Adapts ¼" NPT stud on ST5484E (B=0) to ½" NPT mounting hole. Material: 303 stainless steel
	93818-004	Cable Grip Strain Relief Fitting Used primarily with 8978 cable assemblies where cable enters junction box. ¼" NPT male thread to cable grip. Fits cable diameters from 0.156" to 0.25". Complete with sealing ring and locknut. Hot dip / mechanically galvanized finish. Suitable for NEMA 4 junction boxes.
	93818-018	Cable Grip Strain Relief Fitting Similar to 93818-004, but fits larger cable diameters from 0.4" to 0.5", such as customer-supplied cables used with terminal block versions of ST5484E (D = 2 or 3).

OUTLINE DIAGRAMS

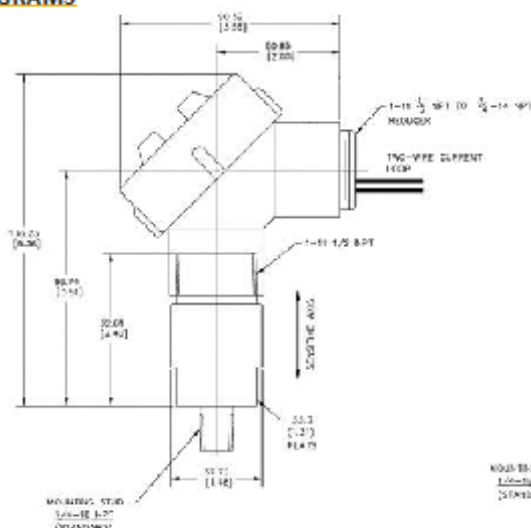


Figure 1: Outline dimensions of the ST5484E (all versions except MIL-Style Connector). Dimensions in mm [inches]. Optional* 8200-001 conduit elbow shown installed.

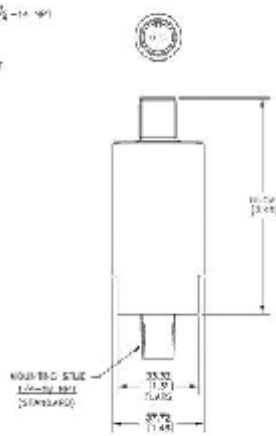



Figure 2: Outline dimensions of the ST5484E-XXX-XX4-XX (MIL-Style Connector). Dimensions in mm [inches].

* NOTE: 8200-AAA-IEC elbow is mandatory for ATEX/IECEX/INMETRO Ex d (flameproof) approved installations.



WIRING CONNECTIONS

Table 5 – Wiring Connection Legend		
Connector Type	Dynamic Signal Connections	Power Connections
MIL-C-5015	Not Available	<p>24 V_{DC} power may be connected to all ST5484E models without regard to polarity. Sensor uses IPT® independent polarity diode bridge circuit that will always orient voltage correctly inside sensor, regardless of polarity externally.</p> <p>NOTE: Although the ST5484E allows polarity in either direction, installations using I.S. barriers will need to observe correct polarity at the barrier input side. However, the barrier output side (i.e., sensor connection) may be wired without regard to polarity.</p>
2-wire flying leads	Not Available	
2-wire terminal block	Not Available	
4-wire flying leads	Red: Power + Blue: Power - White: Dynamic Signal - Black: Dynamic Signal +	
4-wire terminal block	 <p>NOTE: ND – SYMBOLS ARE NOT ON LABEL</p>	

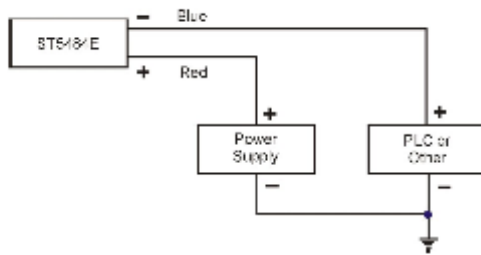


Figure 3: Typical installation for a single ST5484E seismic vibration transmitter.

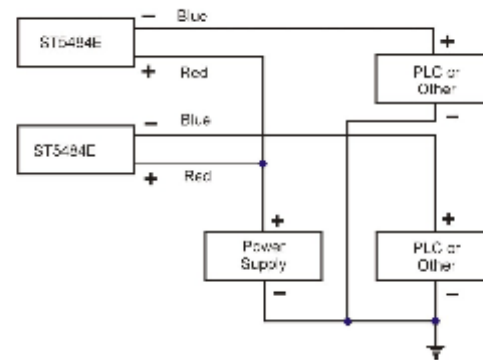


Figure 4: Typical installation for multiple ST5484E seismic vibration transmitters.

ADDITIONAL DOCUMENTATION

Description	Metrix Document Number
Manual	M9162
Installation Drawing – Hazardous Area with I.S. Barriers (CSA)	9426
Installation Drawing – Hazardous Area with I.S. Barriers (CENELEC)	9278
Installation Drawing – Div 2 / Zone 2	1086105

Trademarks used herein are the property of their respective owners.
 Data and specifications subject to change without notice.
 © 2014 Metrix Instrument Co., L.P.



Appendix E MONTHLY FEEDBACK REPORT

A list of all the equipment breakdowns, trips and related problems during the month of April 2017 are presented in the Table E-1 below:

TABLE E-1 MONTHLY FEEDBACK REPORT

Date	Report time	Equip description	Breakdown	Remarks	Root cause
01 April 2017	01h34	Winch	55E 108x/c P2 Center g/winch tripped	Informed n/s Elect Anna,	Tripped
01 April 2017	00h50	Winch	69D/L 78x/c P15 G/winch tripped		Tripped
01 April 2017	02h39	Pump	45L Pump5 tripped	Call Warren. Reset O/L condition	
02 April 2017	22h25	Winch	66E 78x/c P15 winch trip	Informed n/s Elect Robert to check.	Tripped
03 April 2017	23h54	Winch	55w 91x/c P15 G/winch trip	informed n/s Elect Anna.03h00 cable need 50mtr.	Cable damage
03 April 2017	02h22	Winch	57w 91x/c P3 g/winch starter o/o/o	Morning shift to check.	Starter
03 April 2017	01h32	Winch	55E 104x/c P5A G/winch trip		Tripped
03 April 2017	11h02	Compressor	Comp no.3 tripped	Inform Anton - wait for shutdown and start again at 11h25	
04 April 2017	22h03	Winch	55w 91x/c P15 G/winch stop/start button o/o/o	informed n/s Elect Anna.	Starter
04 April 2017	00h53	Winch	55E 107x/c sect 113 center g/winch trip		Tripped
05 April 2017	19h44	Winch	55E 107x/c c/gully winch cable damaged	Call out Agnes -	Cable damage
05 April 2017	03h20	Winch	55w 91x/c P17 G/box tripped		Gully box tripped
05 April 2017	18h10	Pump	66L 2nd dirty water dam overflow pump no.2 flow = 0L/s	Call out Simon - closed water to dam - report at 20h00 overflow running into tip - inform Curt	
05 April 2017	17h55	Pump	Surf supply pump tripped	Call out Kobus - reset and start at 18h24	
06 April 2017	01h25	Winch	66E 78x/c sect114 P19 g/winch keep on tripping	morning shift will check	Tripped
06 April 2017	23h14	Winch	55E 108x/c P6 C,g/winch tripped	wait for n/s Elect Anna to call.	Tripped
07 April 2017	23h06	Winch	57w1 126x/c center g/winch cable damage	Call s/by Elect Bonang.at 23h30 Pina report back c/g.winch is okay,informed F/man,& Elect.	Cable damage
07 April 2017	22h17	Winch	73L 82x/c race winch no power	Nandipha confirm that winch is okay	Tripped

08 April 2017	22h40	Winch	69D/L 77x/c P11 G/winch no power	Informed n/s Elect Felix,00h41 restor power.	Tripped
08 April 2017	04h52	Pump	45L Pumps tripped,and 66L Pumps tripped	informed Neo,Ben-Running at 08h00	
08 April 2017	04h52	Pump	45L Pumps tripped,and 66L Pumps tripped	informed Neo,Ben-Running at 08h00	
10 April 2017	23h35	Fan	75L HLG South fan tripped	Call s/by Elect Nandipha.F/n is off informed F/man.	
11 April 2017	23h53	Fan	71L 102x/c Fan tripped	ask n/s Elect Felix to reset,	
12 April 2017	21h03	Winch	57w 91x/c P3A Center g/winch starter button o/o/o	Ask Elect to check.	Starter
14 April 2017	02h16	Winder	East winder tripped DC breaker when he tried to move	Call out Bertus - running	
15 April 2017	09h45	Pump	66 pump no1 motor NDE vibration high	Call out Thabo	
17 April 2017	22h31	Winch	52E 104x/c slusher winch fail to start	Report to Anna - report back at 01h22 that it is running	Tripped
18 April 2017	09h30	Pump	66 & 72 dams overflowing due to rx2 pump faulty	Informed Jona,Fred,Curt& Bernard	
18 April 2017	00h42	Fan	55W 89x/c B/reef 45kW fan tripped	Anna went to 52E 104x/c - got report at 03h21 at 52L station	
19 April 2017	02h11	Winch	Sub 71L 93x/c c/g winch has no power	Inform Thomas that he will have to go get elect at 69L elect shop (phones are not working)	Tripped
19 April 2017	02h17	Fan	Sub 69L 77x/c T/way fan tripped	Inform Felix at 02h25 - reset mini sub - report back at 04h31	
20 April 2017	04h30	Winch	69 77 slusher winch no power	Morning shift to check	Tripped
21 April 2017	22h35	Fan	55E 104E fan tripped	Morning shift to check	
22 April 2017	01h00	Winch	52E 104x/c center gully winch cable damaged	Morning shift to check	Cable damage
22 April 2017	01h38	Winch	66 78 P19 winch trips	Morning shift to check	Tripped
23 April 2017	01h00	Winch	57w3 90 P4 g/winch tripped	Informed Mabusela-In order at 02h25	Tripped
23 April 2017	00h05	Winch	71 93 center gully winch tripped	Informed Ncobile,Filix-	Tripped
23 April 2017	23h50	Fan	57w 87 B/Reef fan tripped	Informed Mabusela-In order at 01h25	Tripped
24 April 2017	22h25	Winch	57w3 91 raise winch tripped	Informed Mabusela-Reported back at 00h30 that the cable was damaged-in order	Cable damage
24 April 2017	15h57	Pump	Sub 78L dirty water dam pump no.1 of set 2, tripped	Call out Johan and inform Eldrid - restart pumps	Tripped

26 April 2017	23h25	Winch	57w3 90x/c P4 g/winch doesn't start	Informed Mabusela-reported back at 01h45 that the drums are not turning	Pinion gear
26 April 2017	03h50	Winch	55E 104x/c P3 g/winch pin gear loose	Morning shift to check	Pinion Gear
26 April 2017	05h00	Winch	55E 108 center gully raise winch trips	Morning shift to check	Tripped
27 April 2017	22h35	Winch	55w 91x/c P21 face winch no current	Informed Anna-reported back at 02h40 motor needs to be replaced due to no fan	Motor
27 April 2017	01h55	Winch	57W 91x/c P7 face winch no current		Tripped
27 April 2017	11h42	Winch	57W3 90x/c mac winch keeps tripping	Coenie will send somebody to fix -	Tripped
27 April 2017	21h25	Winch	55E 108x/c P2 winch tripped	Informed Anna-In order at 01h00	Tripped
27 April 2017	22h55	Winch	57w 91 wide raise g/winch tripped	Informed Timothy-In order at 01h40	Tripped
27 April 2017	00h10	Winch	71 77x/c P1A g/winch tripped	Informed Hennie	Tripped
28 April 2017	23h00	Winch	71E 102x/c center gully no current	Informed Hennie-In order at 04h40	Gully box tripped

Appendix F CASE STUDY 1: MAINTENANCE REPORT

MAINTENANCE REPORT

CONDITION MONITORING

28 March 2017



CONFIDENTIAL

HVAC International (Pty) Ltd. holds copyright of this document and owns all intellectual property mentioned or described herein.

EXECUTIVE DIRECTORS: EH Mathews (Chairman), M Kleingeld (CEO), SM Jiyana (Projects support)
TML Setiloane (Marketing & Strategy)
INDEPENDENT NON EXECUTIVE DIRECTOR: KM Nassiep
DISTRIBUTOR: OSIMS and MTB





List of figures

Figure 1: 66 L pump 5 temperatures on 15 March 2017	5
Figure 2: 66 L pump 5 temperatures on 16 March 2017	5
Figure 3 66 L pump 5 power consumption on 15 March 2017.....	6
Figure 4: 66 L pump 5 power consumption on 16 March 2017	6
Figure 5: Figure 2: 66 L pump 5 temperatures on 26 March 2017	7
Figure 6: 66 L pump 5 power consumption on 26 March 2017	8

Confidential





Table of contents

List of figures	2
Nomenclature	3
Report verification	3
1 Introduction	4
2 Identification	4
3 Notification	7
4 Investigation outcome	7
5 Conclusion	8

Confidential





Nomenclature

NDE Non-Drive End

Report verification

This report was compiled and checked by:

Author:	_____	Supervisor:	_____
Signed:	_____	Signed:	_____
Date:	_____	Date:	_____

Confidential





1 Introduction

HVAC International was contracted by Harmony to do condition monitoring on the major equipment on [REDACTED]. As part of the condition monitoring effort, excessive temperatures on the Non-Drive End (NDE) of pump 5 on level 66 was identified. This report summarises the identification, notification and corrective action that was taken on pump 5.

2 Identification

Alarms are set up to automatically trigger when temperatures and vibrations exceed specified limits that are based on the trip limit of each individual piece of equipment. For pump 5 on level 66, the trip limit on the NDE temperature is 80°C. Based on this trip limit the alarm limit was set at 76°C.

To trigger the alarm, the NDE temperature needs to exceed the alarm limit for more than 5 minutes. These alarms are then sent to [REDACTED] and [REDACTED] via SMS, and to HVAC International via email. HVAC International also has systems in place to notify them of systematic deterioration of equipment. Should it be picked up that the state of equipment is deteriorating and might fail soon, mine personnel are notified as well.

From 15 March to 23 March 2017, 20 alarms were triggered by high NDE temperatures on pump 5 on level 66. HVAC International investigated the temperatures during this period which can be seen in Figure 1 and Figure 2.

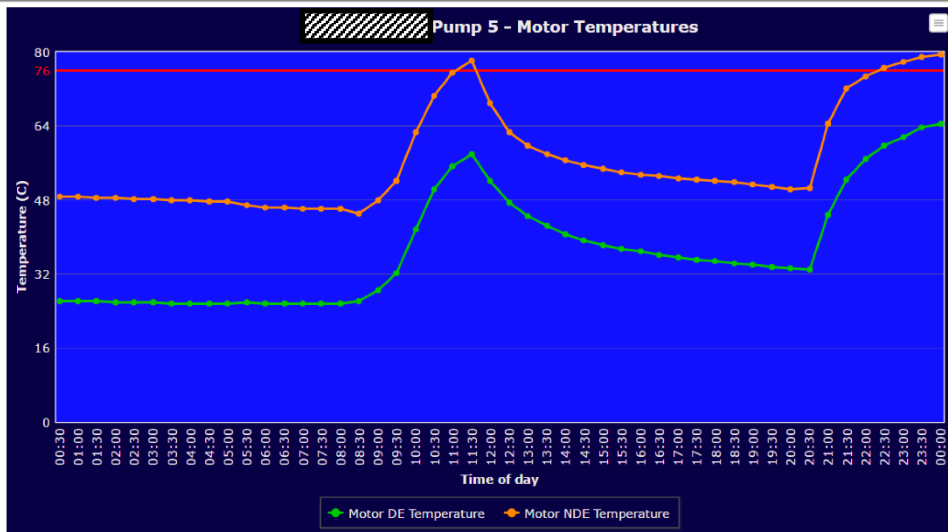


Figure 1: 66 L pump 5 temperatures on 15 March 2017

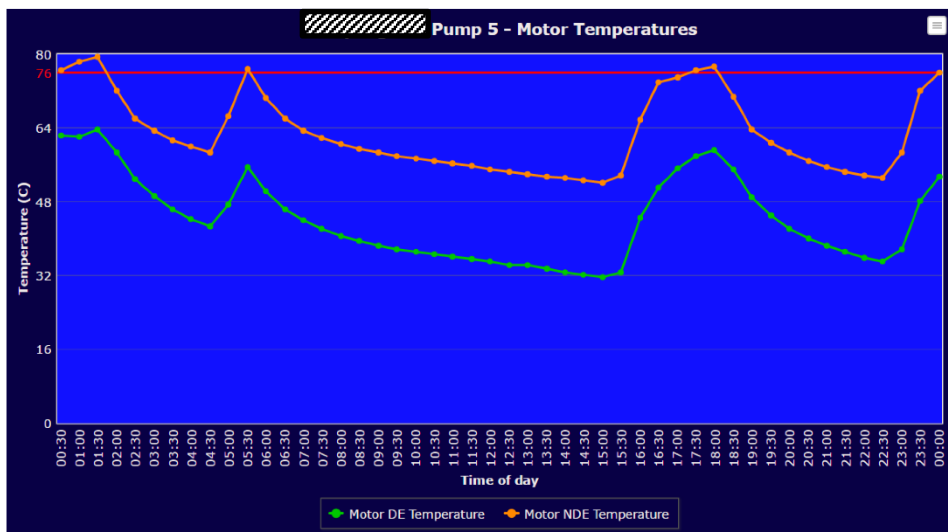


Figure 2: 66 L pump 5 temperatures on 16 March 2017

The corresponding power profiles can be seen in Figure 3 and Figure 4.

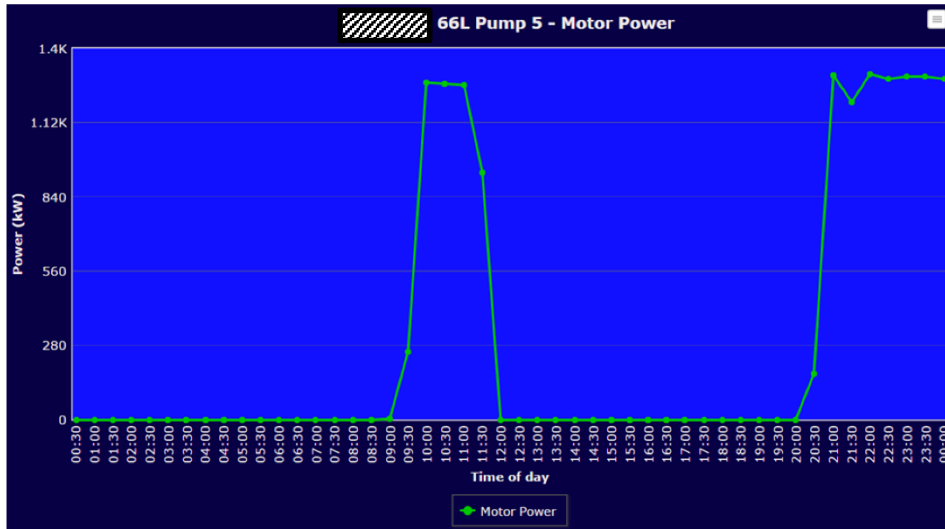


Figure 3 66 L pump 5 power consumption on 15 March 2017

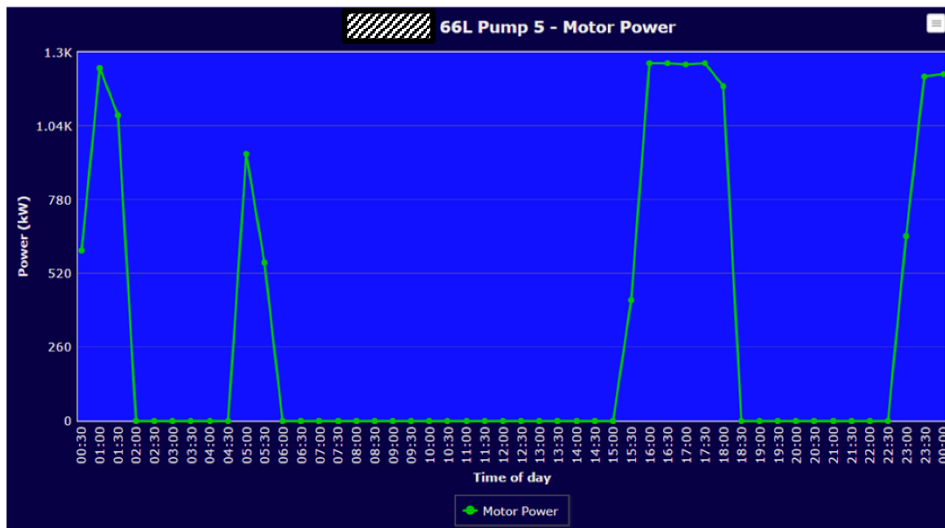


Figure 4: 66 L pump 5 power consumption on 16 March 2017

From these figures it can be seen that the temperature increases drastically when the pumps are switched on, as expected. The temperature continues increasing until it reaches 80°C and trips the pump. Note that the temperatures displayed are half hourly averages and depending on when the measurement is taken, will be close to 80°C.

3 Notification

HVAC International analysed the data from Management Toolbox and determined that pump 5 needs maintenance and notified Bernhard Lindner and Danie Steenkamp on 22 March 2017. Tshepong then promptly actioned this notification and investigated the temperatures on the pump on 24 March 2017.

4 Investigation outcome

On arrival at the pump station the unit was isolated and locked out for the inspection. The coupling and NDE bearing was opened for investigation and it was noted that the coupling gap was about 2mm and the rotor thrust on the bearing. The pump was installed incorrectly and the motor alignment, coupling gap and magnetic centre was not determined correctly.

The problem was corrected by moving the motor away from the pump, removing and scraping the bearing thrust face and installing the bearing back into position. Magnetic centre was established and the coupling gap set to 8mm. Re-alignment was completed and the unit started. The bearing temperatures were then monitored on the motor and settled after an hour of operation at 63°C at both the motor bearings. The temperatures for 26 March 2017 can be seen in Figure 5.

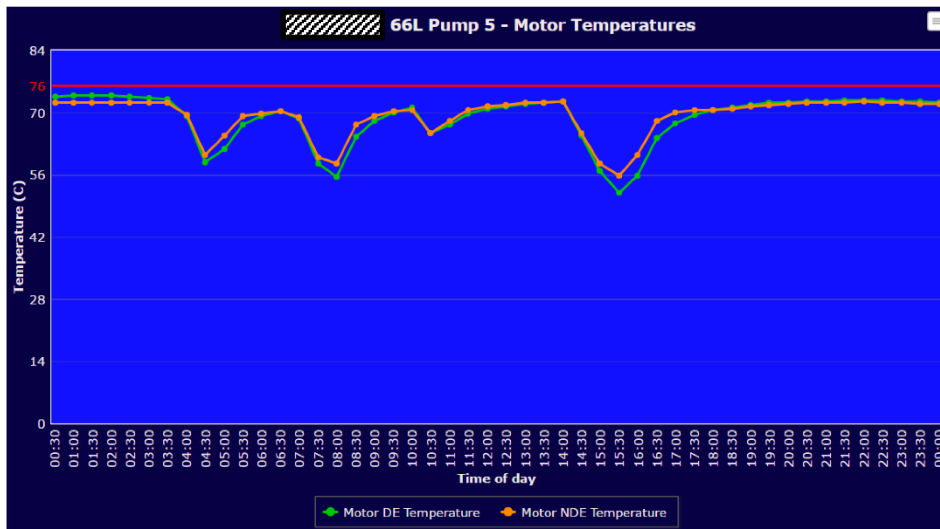


Figure 5: Figure 2: 66 L pump 5 temperatures on 26 March 2017

From this figure it is evident that the NDE temperature of the pump reduced considerably. Before the pump was fixed, the pump used to operate for a few hours, until it tripped at 80°C. After the intervention, the pump temperatures increased to 72°C where it stabilised. The corresponding power profile for 26 March 2017 can also be seen in Figure 6.

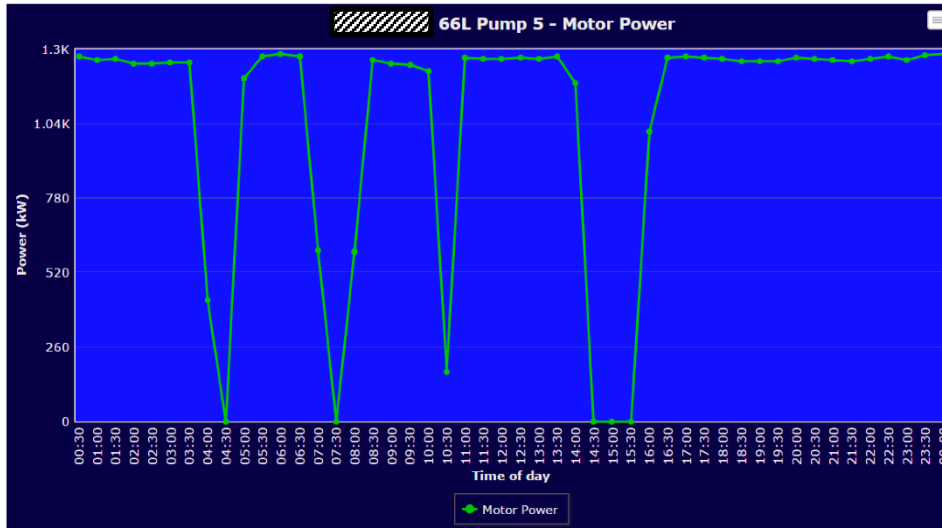


Figure 6: 66 L pump 5 power consumption on 26 March 2017

From this figure it is evident that the pump can operate for longer periods. Since the pump also stopped tripping on high NDE temperatures, the pump can also be stopped and started to accommodate for water demand.

5 Conclusion

By monitoring the pump condition and prompt response from the site personnel, the pump operation was restored to original design specifications. This will ensure efficient operation and extend the lifetime of the pump for years to come.